BACTERIAL OXIDATION OF ARSENITE AT HOT CREEK: CHARACTERIZATION OF BIOFILM COMMUNITIES AND ISOLATION OF NOVEL BACTERIA ASSOCIATED WITH *AQUATIC MACROPHYTES*

Thesis by

Tina M. Salmassi

In Partial Fulfillment of the Requirements

For the Degree of

Doctor of Philosophy

California Institute of Technology

Pasadena, California

2001

(Defended May 15, 2001)

Acknowledgments

Full circle. At last, I write the beginning. My feelings are of exhilaration and the exhaustion I felt only one month ago is gone.

Foremost I would like to thank my advisor, Janet Hering, for her guidance and encouragement during my undergraduate and graduate career. I know that the experiences over the last few years at Caltech would be non-existent without Janet's initial mentoring and faith in my abilities. For this opportunity I am most grateful. I thank Dianne Newman, my second advisor, for taking me into her laboratory family and making me feel at home, always. Dianne's kind, supportive words and expertise have been invaluable during the last year. I thank Ken Nealson, my third advisor for his assistance in getting me started in microbiology. As an engineer venturing into the realm of the near invisible, Ken's energy and ideas were very insightful. I am grateful to Jared Leadbetter for his commitment to this project and for helping me learn so much about phylogeny. Even now it is hard to believe that I made it through what seem like millions of sequences. It was possible only because of Jared's help and encouraging words.

Two of the last five summers I have spent in other laboratories. One of the most unforgettable experiences of my life was the MBL Microbial Diversity Course in Woods Hole. I would like to thank Abigail Salyers, Ed Leadbetter, Kurt Hanselmann, Tom Schmidt, and Scott Dawson as well as all the other staff members and fellow students of the 1999 class for the opportunity, the experience, and the memories. I write this now, mostly for myself, to always remember how enjoyable science can be in such a setting. I learned something every moment of my time there while in the field, in the lab, dining

and conversing with brilliant, brilliant, brilliant people, playing games and reading into the late hours of the night. I would like to thank Dr. Norman Pace and his group, particularly Jeff Walker and John Spears for hosting me during the summer of 2000. Yet another unforgettable summer, this time in Boulder... caving and cloning. Being a member of Norm's group, even for a short period, was a great honor.

I thank the many students I have interacted with while at UCLA and Caltech, beginning with those students who have graduated. Jennifer Wilkie was my first heroine and introduced me to Hot Creek. The gentleness of Penny Kneebone and Tatiana Piatina was a pleasure to experience, truly two of the most graceful people I have known. Within Janet's group, I also thank Dan Giammar for being my inspiration while I was writing and Jennie Stephens for the trips to Hot Creek and for being so good at everything and so cool all the time. I thank everyone in Dianne's lab for great times and good music: Chi-Ching, Mariu, Laura, Bruce, Doug, Michelle, Davin, Loretta, Tanya, Chad, Anthea and Lea... I hope I remembered everyone! In Ken's lab I'd like to thank Venkat for helping me with AOL15 and Brian Lanoil for assistance with phylogenetic trees. I'd also like to acknowledge Dr. Masataka Satomi for the DNA-DNA hybridization studies for AOL15 and Dr. Steve Lindow for identifying the plants at Hot Creek. And, before I forget, thank you NSF for the funding.

Thanks to Dr. Hoffmann and members of his research group (AJ, Nathan, WKC, Tim, Fok, Jeff, Bill and Chris) for making Keck an exciting place to work and socialize. I would also like to acknowledge Fran, Linda, and Irene for being so nice and patient with all the forms and account numbers and for the candy. Furthermore, I feel lucky to have shared the experiences of these past five years with my fellow classmates David,

Catherine, Yael, and Dan. Math problems will never be as fun as they were with you guys. I would particularly like to thank Yael for her friendship... you are one of the most beautiful and genuine people I've ever met. And what would Mrs. Shooblowski be without Mr. Shooblowski... thank you Yaniv for the computer and graphics help and for the good times with Netflix and Napster.

A owe a huge thanks to the residence life office and Fleming house. I'll miss it all, even the cold pitchers of water. Wow, graduate school is just full of unforgettable experiences. I've got a bit of space, so here's my favorite story and most vivid memory. First year at Fleming House. The night after picks. Red jerseys, everywhere, crowded into the lounge. Never in my life have I experienced 100 people looking, sounding, and acting like a million, like one, all at the same time. Rolls in... and the next thing I remember, silhouettes of Scurves on the rooftops, the smoke, the fire, the spray, and water. Rolls in...

Finally, I want to thank my family. My Mom, Floria, my step-Dad Hrand, my new family, Edik, Seda, and Annie Khachikian. The rest of my family and friends, in LA, Germany, Iran, and New York... thank you. It's so nice to have such good people with whom to share one's time and yummy food.

And in the end, there is Crist. No language I speak has words that are appropriate to use here, so I'm afraid this might sound silly or confusing. Merci pimpy jan... I know my life is extraordinary because of my relationship with you...there's only one of you out there in the world and I was lucky enough to find you... right under my nose, in Chemistry class, at UCLA. I love you, Crist, thanks for everything. Hamov jan. Seeroon us... flip the page, let's get on with the rest of our lives.

Abstract

Hot Creek, a tributary of the Owens River in the Long Valley Caldera in California, contains naturally elevated concentrations of arsenic as a result of geothermal activity. This site is of particular interest because of its substantial impact on the quality of the drinking water supply for the City of Los Angeles.

Previous studies revealed a rapid *in situ* oxidation of arsenite in Hot Creek. In this work, bacterial oxidation of arsenite is viewed from the perspective of cultivation-based studies (focusing on pure cultures of arsenite oxidizers) and molecular technique-based studies (surveying the community under ambient conditions).

The cultivation-based techniques yielded four new arsenite oxidizers. One isolate, *Agrobacterium albertimagni* strain AOL15, is an α-proteobacterium that was isolated using an enrichment-based isolation technique with arsenite concentrations much higher than ambient levels. Values of the kinetic parameters K_s (3.4 ± 2.2 μM) and V_{max} ($1.81 \pm 0.58 \times 10^{-12}$ μmole·cell^{-1}·min^{-1}) were determined for AOL15. The K_s is near the ambient concentration of arsenite in Hot Creek. However, molecular-based techniques suggested that AOL15 is not a significant member of the biofilm associated with submerged macrophytes.

The other three oxidizers, YED1-18, YED6-4, and YED6-21, all β-proteobacteria of the genus *Hydrogenophaga*, were isolated from solid media. Molecular techniques suggested that β-proteobacteria are important members of the macrophyte surface community. In the molecular survey, one sequence from Clone #44 (partial) was found to be 99.6% identical to YED6-21. This result, coupled with the isolation of the

Hydrogenophaga oxidizers from a million-fold dilution of a suspension of cells from the macrophyte surface, suggests that the *Hydrogenophaga* are significant members of this community and may be the dominant arsenite oxidizers.

The densities of total and oxidizer cells associated with the submerged macrophytes in Hot Creek were estimated using most probable number (MPN) analysis. The normalized MPN values were 1.4×10^9 total cells/g dry wt. plant and 3.3×10^8 oxidizer cells/g dry wt. plant. These estimates suggest that the oxidizers constitute a significant fraction (on average 24%) of the overall biofilm community.

Table of Contents

List of Figures

List of Tables

Chapter One

INTRODUCTION

1.1 Introduction and Motivation

The distribution of arsenic in natural waters (particularly systems that influence or contribute to drinking water supplies) is of major concern. The concentration of arsenic in drinking water has been regulated at 50 μg/L (or 0.67 μM) since 1942. A Maximum Contaminant Level (MCL) of 10 μg/L (or 0.14 μM) was promulgated in January 2001 but the effective date of this rule was later delayed until February 2002 (EPA, 2001). These reevaluations of the arsenic standard have been motivated by epidemiological studies suggesting potential cancer and chronic toxicity risks associated with the consumption of drinking water containing 50 μg/L (or 0.67 μM) arsenic (Pontius et al. 1994).

The redox speciation of arsenic controls its mobility, toxicity, and removal efficiency during treatment. Generally speaking, the reduced inorganic form of arsenic, arsenite, is the more mobile, the more (acutely) toxic, and the more difficult form to treat by most water treatment technologies (Chen et al. 1999). Thus, from a regulatory perspective it is important to understand the speciation and distribution of arsenic in drinking water systems.

The Los Angeles Aqueduct system supplies up to 75% of the drinking water for the City of Los Angeles. The water delivered to the Los Angeles Aqueduct Filtration

Plant contains elevated concentrations of arsenic due to geothermal inputs at Hot Creek, a tributary of the Owens River. For several years now, our research group has been studying Hot Creek and the downstream reservoir, Lake Crowley, to understand the redox chemistry of arsenic in this system.

Past studies at Hot Creek demonstrated rapid *in situ* oxidation of inorganic arsenic within a 1200 m reach of the creek downstream of the major inputs. Furthermore, these studies suggested that microorganisms attached to the surface of aquatic macrophytes in the creek were responsible for the oxidation. Based on these first observations, the bacterial cells (shown in Figure 1.1) associated with the macrophytes has been studied in depth to characterize the attached microbial community and to isolate arsenite-oxidizing bacteria from this community.

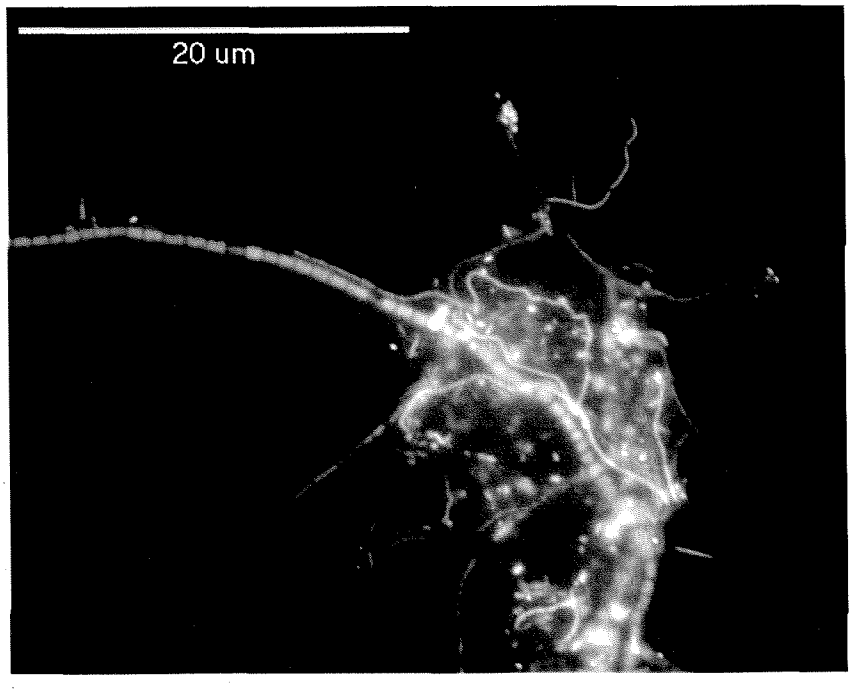

Figure 1.1: DAPI stained image of the attached bacterial communities shaken off aquatic macrophytes of Hot Creek.

1.2 Scope and Objectives

Motivated by the observations of microbially mediated arsenite oxidation at Hot Creek, this project addresses the following objectives and questions.

(1) Characterization of the attached microbial community. Molecular techniques were used to survey the microorganisms present in the biofilm community and classical techniques were applied to measure cell densities. Several questions were addressed in this study. What is the make-up of the community and are there any dominant microorganisms present? Once the community structure is better understood, can dominant members be visualized by microscopy or cultivated and purified under laboratory conditions? What is the cell density of the community associated with the macrophytes and what portion of this biomass contributes to the observed overall arsenite oxidation?

(2) Isolation and characterization of arsenite-oxidizing bacteria. Enrichment and isolation experiments were performed both before and after the molecular characterization of the biofilm community, and addressed the following questions. Could the better understanding of the community make-up and information on ambient environmental conditions be exploited to isolate some of the biofilm arsenite oxidizers for study under laboratory conditions in pure culture? What types of arsenite oxidizers can be isolated and how significant is their role in the community? Can the physiological role of oxidation (e.g., detoxification or energy generation for

autotrophic growth) be elucidated? What are the kinetic constants for the oxidation of arsenite in pure culture conditions?

(3) Relating field and laboratory observations of the kinetics of arsenite oxidation. If molecular and cultivation tools can be used to understand the biofilm under more controlled laboratory conditions, what comparisons can be made between the field and laboratory observations? Can the activity of arsenite oxidation under field conditions be quantified with respect to the cell densities and how do the kinetics under these conditions relate to other known abiotic and biologically mediated oxidation rates? Finally, what understanding is gained from this study about arsenite oxidation at Hot Creek?

These topics are addressed in the seven chapters (including this introduction) of this thesis. The biogeochemistry of arsenic and the bacterial oxidation of arsenite have been well documented in the literature. Chapter 2 presents an overview of these findings as well as a brief description of the molecular techniques that were utilized in this work. Chapter 3 describes the first arsenite oxidizer isolated for this project, *Agrobacterium albertimagni* strain AOL15, including an in-depth characterization of this strain and the kinetic parameters for its oxidation of arsenite. The use of molecular techniques to survey the overall community structure and diversity without cultivation techniques is presented in Chapter 4. The understanding of these microorganisms, gained in Chapters 3 and 4, is applied in Chapter 5, which describes the isolation of new arsenite oxidizers under conditions designed to target microorganisms with more significant roles in the natural community. These studies are linked back to the field in Chapter 6, which

attempts to describe the abundance and activity of arsenite oxidizers on the surface of aquatic macrophytes at Hot Creek. The conclusions of this work are presented in Chapter 7.

Chapter Two

BACKGROUND

2.1 Geomicrobiological Arsenic Cycling and Transformations

2.1.1 Arsenic Occurrence and Speciation in Surface Freshwater Environments

Arsenic, a metalloid of group VA of the periodic table, is ubiquitous in the Earth's soils, sediments, waters, and atmosphere, and in biological matter. Elevated concentrations of arsenic in aquatic systems can originate from natural or anthropogenic sources. Natural inputs of arsenic result from geothermal activity or the weathering of minerals while anthropogenic inputs result from mining activities or the manufacture and use of arsenic pesticides (Cullen and Reimer 1989). These inputs can cause significant variations in the arsenic concentration of freshwaters. For example, some European and North and South American rivers have arsenic concentrations ranging from 0.1-75 μg/L (or 0.001-1 μM) and an average of 2.3 μg/L (or 0.03 μM) has been reported for 16 California and Florida rivers. Geothermal activity results in arsenic concentrations of 1275 μg/L (or 17 μM) in Old Faithful in Yellowstone National Park, 200 μg/L (or 2.6 μM) in Hot Creek, and 1000 μg/L (or 13.3 μM) in the hot springs at Hot Creek (Eccles 1976).

Under the redox conditions of natural systems, arsenic can be present and stable in several oxidation states: +V (arsenate), +III (arsenite), 0 (arsenic), and -III (arsine)

(Ferguson and Gavis 1972). Arsenite can occur in oxic waters as a metastable species because of the slow kinetics of arsenite oxidation by oxygen. In surface freshwaters, the dominant inorganic forms of arsenic are the oxidized arsenic acid species $H_2AsO_4^-$ and $HAsO_4^{2-}$ at the pH of natural waters and the more reduced arsenous acid species H_3AsO_3 (Ferguson and Gavis 1972). Figure 2.1 is a pe-pH diagram of the aqueous inorganic species. The $Fe(OH)_3$(amorph,s)/Fe^{2+} and MnO_2(s)/Mn^{2+} couple are also included for comparison. From the position of the lines for the Mn- and Fe-oxides, it can be expected that these oxides should oxidize arsenite (in the entire pH range for Mn and more specifically in the lower pH range for Fe). Further discussion on abiotic oxidation of arsenite by these oxides is discussed later (see section 2.1.2).

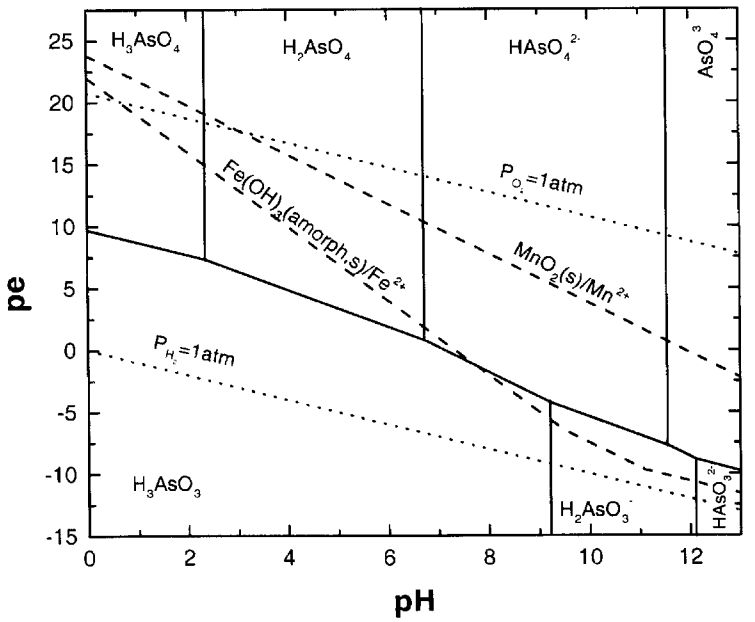

Figure 2.1: pe-pH diagram for dissolved inorganic arsenic species. $[Fe]_T$ and $[Mn]_T$ are each at 2 $\times 10^{-6}$ M. The $Fe(OH)_3$(amorph, s)/Fe^{2+} and MnO_2(s)/Mn^{2+} redox couples are also presented in a much simplified form. The hydrolysis species for Fe(II) were taken into consideration (at pH<9.5, dissolved Fe(II) at Fe^{2+}; at 11.1<pH<9.5, dissolved Fe(II) as $FeOH^+$; at pH>11.1, dissolved Fe(II) as $Fe(OH)_{2(aq)}$. Constants from Vink (1996) and Morel and Hering (1993). Dotted lines are upper and lower limits for natural waters based on the O_2/H_2O and H_2O/H_2 couples.

The organic forms of arsenic, monomethylarsonic acid [MMAA(V)], monomethylarsonous acid [MMAA(III)], dimethylarsinic acid [DMAA(V)], and dimethylarsinous acid [DMAA(III)], are less prevalent than the dissolved inorganic forms in natural waters. There are, however, some reports of aquatic systems where methylated species make an important contribution to the total dissolved arsenic concentration. One such case is Lake Biwa in Japan where DMAA(V) was found to be the dominant form of dissolved arsenic during the summer season (Sohrin and Matsui 1997). Methylated species are also relevant with respect to microbial transformations of arsenic species (Cullen and Reimer 1989, and Newman et al. 1998).

2.1.2 Arsenic Cycling

Arsenic is subject to various transformations that are of significance to its mobility and bioavailablity, including oxidation, reduction, and methylation. Physical and chemical processes such as adsorption, desorption, precipitation, and dissolution can control the concentrations of dissolved arsenic in freshwaters. In such processes, arsenate can co-precipitate with or adsorb onto hydrous iron oxides, aluminum hydoxides, and clays whereas arsenite co-precipitates with or adsorbs onto iron oxides or metal sulfides. Arsenic bound in these solid forms can then be re-released to a water column through microbial action. Additionally, arsenic can accumulate in the biota and thus be deposited or buried (Ferguson and Gavis 1972). Microorganisms can provide physical surfaces for the catalysis of chemical reactions or can directly be responsible for the oxidation,

reduction, or methylation of arsenic species (Figure 2.2). Some of these transformations will be discussed in greater detail in the following section.

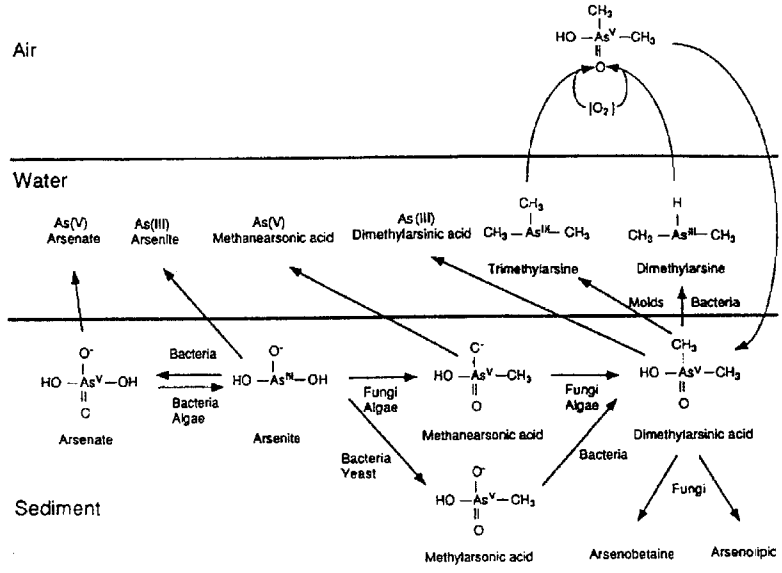

Figure 2.2: Arsenic cycling and microbial transformations (Cervantes et al. 1994).

Abiotic oxidation of arsenite has also been documented. Johnson and Pilson report data resulting in calculated half lives ranging from several months to one year for the oxygenation of arsenite in seawater (Johnson and Pilson 1975). In a series of studies with manganese and its oxides, Oscarson et al. report rate constants of 0.267 h^{-1} for the oxidation of arsenite by birnessite; 0.189 hr^{-1} by cryptomelane, 0.44×10^{-3} hr^{-1} by pyrolusite (Oscarson et al. 1981; Oscarson et al. 1983a,b). Compared to these oxidation rates by manganese oxides, Eary and Schramke report very slow rates for the oxygenation of arsenite with half lives ranging from one to three years in freshwater systems (Eary and Schramke 1990). Recently studies with H_2O_2 have reported half lives of 56 and 107 days (under different pH conditions) for arsenite oxidation (Pettine et al

1999; Pettine and Millero 2000). However, none of these reports of abiotic oxidation are as rapid as the rates of biological oxidations of arsenite, with half lives ranging from 0.3 hours (Wilkie and Hering 1998) to 13 hours (Scudlark and Johnson 1982).

2.1.3 Microbial Transformations of Arsenic

Microorganisms catalyze many transformations of arsenic species including oxidation (the focus of this project), reduction, and methylation reactions. Bacterial oxidation of arsenite was first reported in 1918 with an isolate from cattle-dipping fluids containing arsenic, provisionally referred to as *Bacillus arsenoxydans* (Green 1918). Green's bacterium was lost and the next report of bacterial oxidation of arsenite was not until 1949, when 15 strains capable of arsenite-oxidation were isolated from cattle-dipping fluids (Turner 1949). Since these studies, there have been a number of other organisms isolated from a variety of locations including soils, sewage, gold mines, and mine waters. Information on these arsenite oxidizers, including the sites from which these species were isolated, the concentrations of arsenic in experiments, and the Michaelis-Menten coefficients (K_m and V_{max}) for oxidation, is presented in Table 2.1.

Notable results from these studies include the isolation, from a gold-arsenic deposit, of the bacterium *Pseudomonas arsenitoxidans*, which is capable of chemolithoautotrophic growth where the oxidation of arsenite served as the sole energy source (Ilyaletdinov and Abdrashitova 1981). Previously, it had been suggested that this oxidation could be coupled to the production of energy for bacteria but no such ability had been observed or reported (Osborne and Ehrlich 1976).

Table 2.1: Summary of arsenite oxidizers.

Microorganism	Isolation Environment	Ambient [As]	Experimental [As], (mM)	K_m (μM)	V_{max}	Ref.
Bacillus arsenoxydans	cattle-dipping fluids	NR	20-100	NR	NR	1
Pseudomonas arsenoxydans, Xanthomonas arsenoxydans, Achromobacter arsenoxydans	cattle-dipping fluids	NR	20-100	450[†]	100 µM/mg N/hr 31 µM/mg dry wt./hr	2-5
Soil Consortium	soils	NR	2.5-40	NR	NR	6
Alcaligenes faecalis	raw sewage	NR	10-20	450[†] 2[‡]	0.05 µmol/mg protein/min	7
Alcaligenes strain	soil	NR	0.24-2.4	1540[†]	6.7 µl O_2/min (ca. 10^{10} cells)	8
Pseudomonas arsenitoxidans	mine water	NR	13.3-26.7	NR	NR	9
Seawater consortium	coastal seawater	< 70 nM	0.0013	70-144[†]	3.6-9.2 µM/hr	10
As1 – As6	mine water	27-173 µM	0.67-6.7	NR	NR	11
Sulfolobus acidocaldarius	---*	NA	1	NR	NR	12
Alcaligenes faecalis purified enzyme	---*	NA	0.20	NR	0.023 µmole/mg protein/min	13
ULPAs1	contaminated water	0.47 mmol/kg dry wt.	1.33	NR	NR	14
NT-25, NT-26	gold mine arsenopyrite rock	NR	5-10	NR	NR	15
Agrobacterium albertimagni strain AOL15	macrophyte surfaces	2.7 µM	0.002-5	3.4 ± 1.1[†]	$(1.81 \pm 0.58)\times10^{-12}$ µmol/cell/min 0.043 ± 0.017 µmol/mg protein/min	**

* previously isolated bacterium, [†]whole cells, [‡]cell extracts, **this study, NR = not reported, NA = not applicable; (1)Green 1918; (2)Turner 1949; (3)Turner 1954;(4)Turner & Legge 1954; (5)Legge 1954; (6)Quastel & Scholenfiled 1953; (7)Phillips & Taylor 1976; (8)Osborne & Erhlich 1976; (9)Ilyaletdinov & Abdrashitova 1982; (10)Scudlark & Johnson 1982; (11)Wakao 1988; (12)Sehlin & Lindstron 1992; (13)Anderson 1992; (14)Weeger 1999; (15)Santini 2000

More recently, a fast growing (doubling time 7.6 hr) arsenite-oxidizing chemolithoautotroph, strain NT-26, was isolated from another gold mine environment

(Santini et al. 2000). Other interesting results include the first report and isolation of acidophilic bacterial strains capable of oxidizing arsenite (Wakao et al. 1988). These organisms were isolated from acid mine waters from the Matsuo sulfur-pyrite mine in Japan and classified as acidophilic, aerobic, gram-negative rods growing optimally in the 3-4 pH range. There was also a report of an extremely thermophilic and acidophilic microorganism, the archaebacterium *Sulfolobus acidocaldarius* strain BC grown at 65°C and pH 2, that both oxidized and reduced arsenic (Sehlin and Lindstrom 1992). Additionally, there are reports of bacterial oxidation of the arsenic minerals orpiment, arsenopyrite, and enargite by members of the *Thiobacillus-Ferrobacillus* group of bacteria (Ehrlich 1963, Ehrlich 1964) where bacterial action was reported to enhance the oxidative dissolution of these minerals. There are also reports of indirect oxidation of arsenite where bacteria serve as the surface for oxidation (Mandl and Vyskovshy 1994) and still other reports of chemical oxidation of arsenite by ferric iron produced by bacterial oxidation of iron (Mandl et al. 1992).

Some explanations for the observed oxidation include (1) an inducible detoxification mechanism, (2) the substitution of arsenite in a system for enzymatic oxidation of some other substrate, (3) chemolithoautotrophy, and (4) co-oxidation, where arsenite oxidation is incidental in the presence of other energy-yielding substrates during cellular metabolism (Scudlark and Johnson 1982). The proposed model for arsenite oxidation involves the transfer of electrons from arsenite oxidase (purified from *Alcaligenes faecalis*) to azurin or cytochrome c (Figure 2.3).

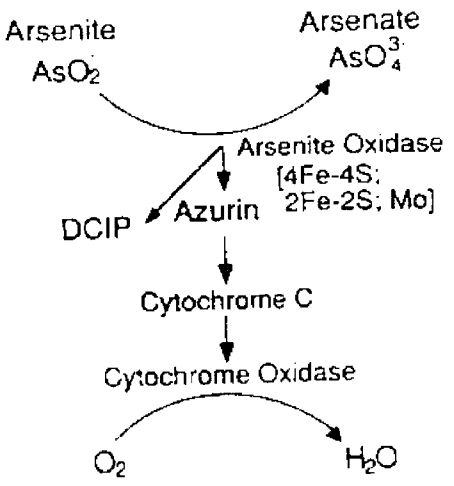

Figure 2.3: Electron flow and arsenite oxidase (Cervantes et al. 1994). Note: The artificial electron acceptor, DCIP, can replace azurin in this model.

Microorganisms are also known to reduce arsenate. From the cattle-dipping fluids where the first arsenite oxidizer was described, there is also report of arsenate reduction (Green 1918). Several microorganisms are described in the literature for their ability to reduce arsenate (Cullen and Reimer 1989; Ehrlich 1996; Newman et al. 1998). Some of these reports describe bacteria that are able to harvest the energy from reduction for growth (Ahmann 1994; Newman et al. 1997a,b; Newman et al. 1998; Blum et al. 1998). Finally, microbial methylation has also been studied, particularly in phytoplankton and methanogenic bacteria although non-methanogenic bacteria with this ability have also been described. The methylation of arsenic species is thought to be a mechanism for detoxification (as reviewed by Cullen and Reimer 1989; Tamaki and Frankenberger 1992; Maeda 1994).

2.1.4 Arsenic Toxicity

The chronic toxicity and regulation of arsenic are usually discussed in terms of human exposure and health risks. The major determinant of the level of acute toxicity of the different species of arsenic is the oxidation state (Tamaki and Frankenberger 1992). The toxicity of arsenite results from its affinity for sulfhydryl groups; various enzymes are inactivated when arsenite binds to the cysteine residues of these proteins (Ferguson and Gavis 1971; Summers and Silver 1978). Arsenate toxicity occurs because arsenate is an analogue for inorganic phosphate and causes interference when it substitutes for phosphate in membrane transport systems (Summers and Silver 1978). In general, toxicity in bacteria refers to those levels that result in an inhibition or disruption in the normal metabolic functions or growth of the cell. In the extreme case, the toxic effects of a compound result in a breakdown in cellular activity and cell death. Different bacteria have different levels of tolerance for toxic compounds. As an example, the bacterium AOL15 is able to grow in the presence of 500 μM arsenite, although cell yields are lower than when the culture is grown in the absence of arsenite. However, at these same levels (500 μM) the growth of the (phylogentically) closely related bacterium *Blastobacter aggregatus* is completely inhibited. This variation in tolerance depends on the resistance mechanism present in the different strains.

2.1.5 Arsenic Resistance in Bacteria

To survive exposure to arsenic, bacteria have developed and evolved several resistance mechanisms. The most common mechanism involves an efflux pump where the toxic component is removed or pumped out of the cell by a transport system. Enzymatic transformations of toxic components to less toxic or transportable forms are another significant mechanism for resistance and detoxification (Silver 1996). The genes for arsenic resistance, which includes both of the above mentioned mechanisms, can be located on the bacterial chromosome or on plasmids in both gram-negative and gram-positive bacteria (Rosen 1996). These genes are essentially the same varying only in the number of genes and in the details of their functions (Silver and Phung 1996; Silver 1998). To date, seven operons for arsenic resistance, called ars operons, have been sequenced (Figure 2.4). These sequences include the genes for resistance located on the chromosome of the gram-positive *Bacillus subtillis*, the pSX267 plasmid from the gram-positive *Staphylococcus xylosus*, the pI258 plasmid of the gram-positive *Staphylococcus aureus*, the chromosome of the gram-negative *Escherichia coli*, the R773 plasmid of *E. coli*, the R46 plasmid of *E. coli*, and the Yop plasmid from *Yersinia* (Figure 2.4) (Silver 1998).

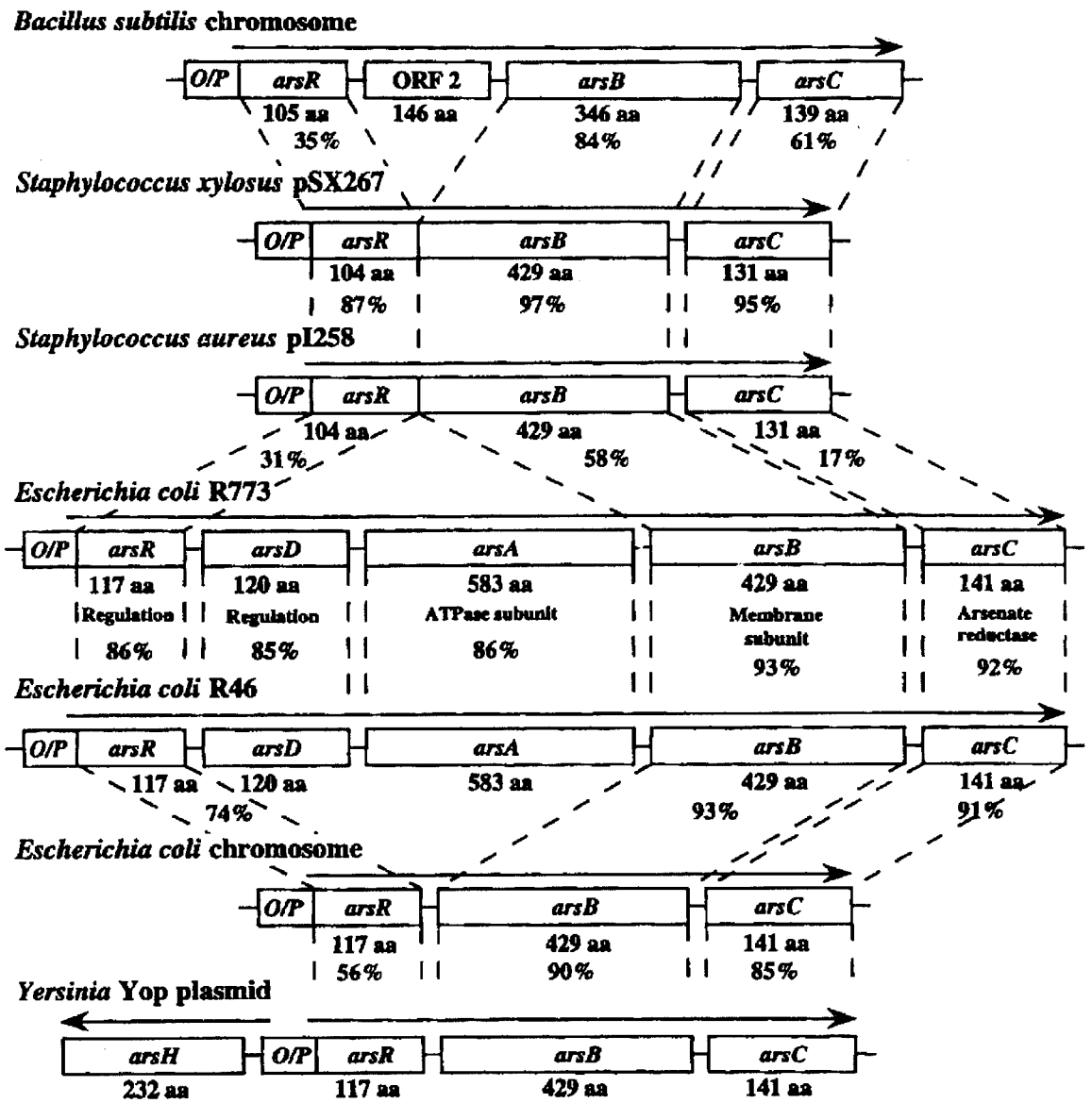

Figure 2.4: The seven gene systems for arsenic resistance in bacteria (Silver 1998).

The resistance systems have at least three genes consisting of the arsR, arsB, and arsC (Figure 2.5). The two *E. coli* systems have two extra genes, the arsD and arsA. ArsR and arsD both encode for regulatory proteins for the ars operons (Xu et al. 1998). The protein that results from the arsR genes is a dimeric trans-acting repressor protein with arsenite, antimonite, and bismuth serving as inducers (arsenate can also serve as an

inducer in vivo) (Cervantes, et al. 1994). The resulting protein from arsD is believed to be an inducer-independent trans-acting regulatory protein (Silver and Phung 1996) with a lower affinity for the same binding site as the arsR protein (Xu et al. 1998). The arsA protein is a membrane-associated oxyanion (arsenite and antimonite) stimulated ATPase and is attached to the inner-membrane arsB protein (Figure 2.5) (Silver and Phung 1996).

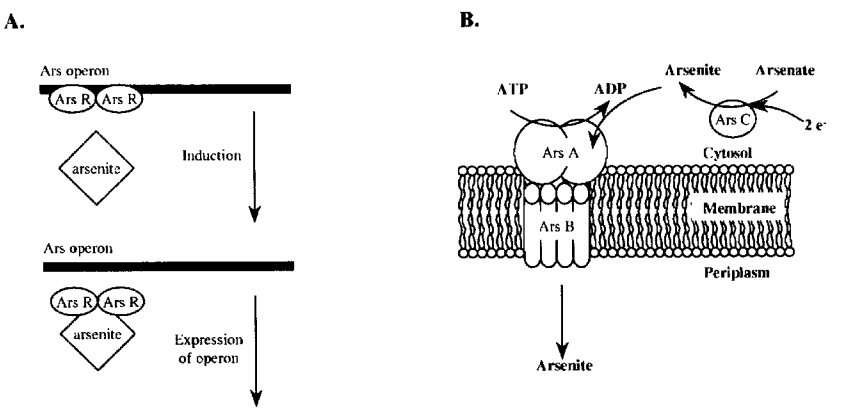

Figure 2.5: Arsenic detoxification A. Role of arsR protein B. Role of arsA, arsB, and arsC in primary arsenite efflux pump (modified from Rosen et al. 1994).

The arsA-arsB complex serves as an ATP-coupled arsenite efflux pump, which is the primary pump requiring chemical energy. In systems where the arsA gene is nonexistent, the arsB protein functions as a secondary arsenite-efflux transporter driven by electrochemical energy (membrane potential) (Silver 1996). However, the arsA-arsB complex confers a higher level of resistance than the arsB protein alone (Xu et al. 1998). Finally, the product of the arsC gene is a small soluble arsenate reductase that reduces arsenate to arsenite, which is then transported by the arsB transport protein (Silver and Phung 1996; Silver 1996). The newest gene, the arsH on the Yersinia plasmid, needs further study but is thought to be involved in the regulation of the operon (Silver 1998).

2.1.6 Rapid Oxidation of Arsenic at Hot Creek

Hot Creek is one of the tributaries of the Owens River and is located in the Long Valley Caldera in the eastern Sierra Nevada (Figure 2.6).

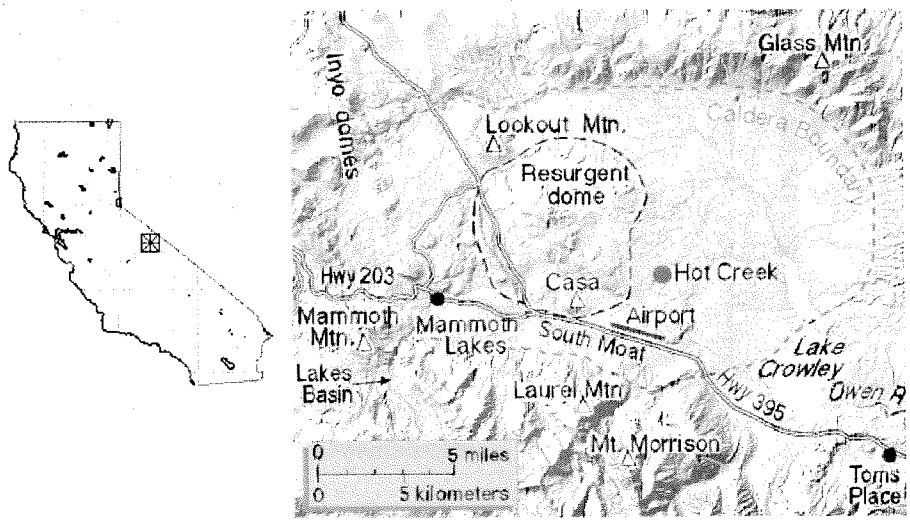

Figure 2.6: Map of Hot Creek in the Long Valley Caldera (U.S. Geological Survey).

The major inputs of arsenic are geothermal, occurring along Hot Creek Gorge, a 370 m portion of Hot Creek (Eccles 1976). The creek is characterized as having an average pH of 8.3 and temperatures that range from 23 to 28° C annually (Wilkie and Hering 1998). Arsenic concentrations are reported to be in excess of 13 μM in the hot spring pools which is diluted into the creek to final concentrations of 2.7 μM (Eccles 1976). The sampling conducted by Wilkie and Hering also reported values ranging from 10 – 18 μM in the hot spring pools where the fraction of the total arsenic in the form of arsenite ranged from 0-73 %. Concentrations of arsenic in the creek were approximately 3 μM (Wilkie and Hering 1998; Wilkie 1997). After the initial mixing of the geothermal waters with the creek waters, arsenite constituted approximately 41% of the total arsenic;

however, 1200 m below the gorge area, the contribution of arsenite dropped to 4% of the total (Wilkie and Hering 1998). A pseudo first-order half-life of 0.3 hr was calculated for the oxidation of arsenite to arsenate using an estimated flow velocity of 0.4 $m \cdot s^{-1}$ for the creek (Figure 2.7).

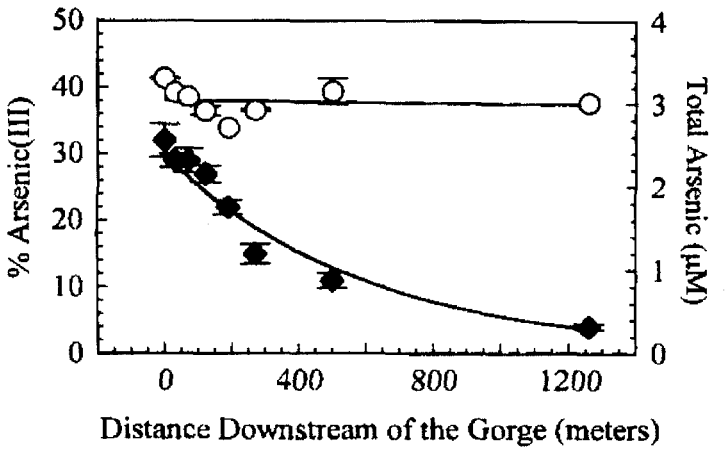

Figure 2.7: Oxidation of arsenite at Hot Creek, (o) total arsenic and (♦) % arsenite (Wilkie and Hering 1998).

Field incubation studies conducted at the site indicated that this oxidation was microbial in nature (Figure 2.8).

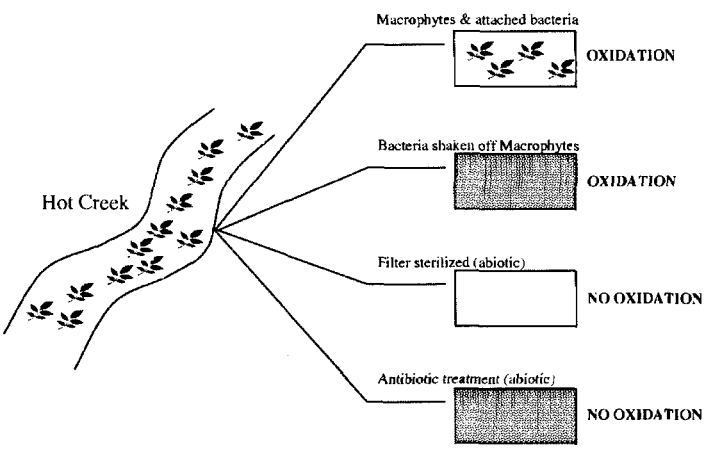

Figure 2.8: In situ experiments at Hot Creek with aquatic macrophytes and bacteria.

Experiments revealed that oxidation was associated with the aquatic macrophyte *Potamogeton pectinatus*, which is abundant in the creek directly below the gorge area. Experiments with the plants or the bacteria shaken off the plants resulted in the oxidation of arsenite with rates similar to those observed in situ. Additionally, sterile filtration or antibiotic treatment inhibited the oxidation. Thus, the evidence suggested that microbial oxidation of arsenite was occurring in the creek (Wilkie and Hering 1998). The current project was motivated by these observations at Hot Creek.

2.2 Microbial Diversity

2.2.1 Measuring Microbial Diversity by Molecular Techniques

Over the last 20 years, the techniques of molecular biology have been used to study the diversity, ecology, abundance and evolution of microorganisms (Head et al. 1998). In the study of microbial communities, molecular tools have provided information and analysis where traditional isolation and cultivation techniques of microbiology have been unsuccessful. The application of classical cultivation methods to describe the composition of microbial communities has been seriously limited by the lack of morphological variability among the prokaryotes and the difficulty in mimicking ambient conditions for microbial growth under laboratory conditions (Amann et al. 1995; Muyzer and Ramsing 1996). The selection imposed by culture-dependent methods has prevented the accurate depiction of natural bacterial communities and has resulted in the underestimation of the richness and abundance of microbial diversity (Theron and Cloete

2000). With the advent of molecular tools in environmental microbiology, the limitations due to selectection have mostly been circumvented and more complete descriptions of communities have been obtained.

Fundamental to molecular techniques has been the comparative analysis of ribosomal ribonucleic acids (rRNA) sequences. This comparative study utilizes rRNA as a marker because of its presence in all known organisms as a dominant cellular macromolecule (Amann et al. 1995; Muyzer and Ramsing 1996; Amann 2000). The existence of highly conserved and also variable regions of rRNA sequences make it an ideal candidate to use for the design of polymerase chain reaction (PCR) primers and probes to target general and specific organisms. Finally, rRNA genes are not horizontally transferred among organisms making this marker a unique "fingerprint" for a given organism (Amann et al. 1995; Muyzer and Ramsing 1996; Amann 2000).

The rRNA molecule has three subunits: the 5S, 16S, and 23S in ascending order by size. In the early phases of comparative analysis of rRNA, the 5S molecule was utilized as the marker although its small size (120 nucleotides) limited its effectiveness in studying complex communities (Theron and Cloete 2000). In recent years, the 16S molecule with its 1500 nucleotides of sequence information has emerged as the yardstick for identifying bacteria and determining phylogenetic relationships among different organisms (Muyzer and Ramsing 1996). Although the 23S rRNA molecule has the greatest amount of information (3000 nucleotides) of the three molecules, current sequence databases for the 16S rDNA genes are much larger than those of the 23S, which allows for better comparisons among organisms. This remains true despite the fact that in some cases the 16S rRNA is considered too well conserved to discriminate between

organisms that are highly related (Amann and Ludwig 2000). At present the 16S approach remains the "gold standard" for explaining bacterial phylogeny (Ludwig and Schleifer 1999).

Many different molecular techniques can be used in the analysis of environmental samples. Figure 2.9 presents a simplified flow chart of the procedure and different molecular techniques used in this work.

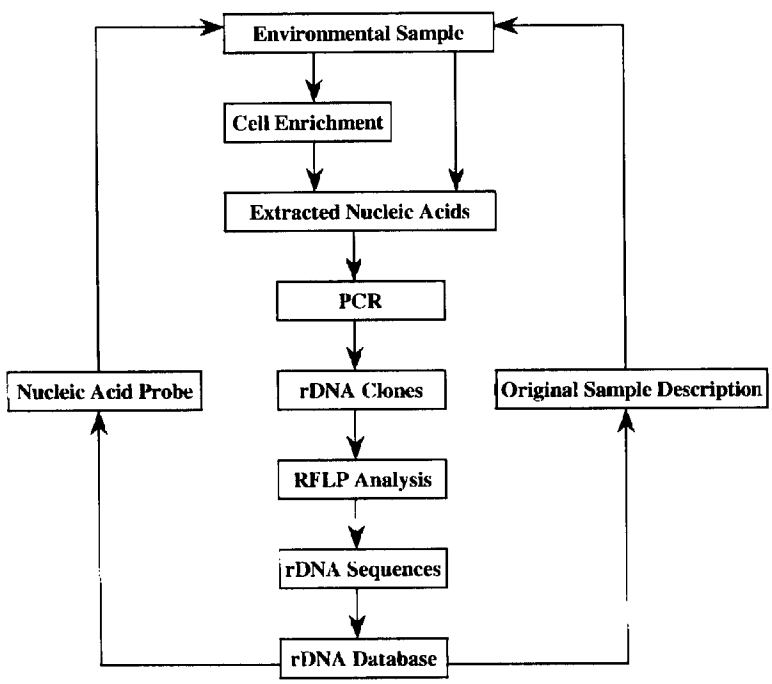

Figure 2.9: Flow chart for molecular techniques used in environmental microbiology.

An environmental sample, such as plant matter, water, or soil is collected. Using chemical and physical mechanisms to lyse cells, the nucleic acids present in that sample are extracted. Universal primers designed based on the highly conserved regions of the rRNA sequence are used to amplify the 16S rDNA genes of the microorganisms in that original sample by PCR and the genes are cloned into *E. coli* cells. The clones are

analyzed for uniqueness using restriction fragment length polymorphism (RFLP) analysis. The clones yielding unique patterns are then sequenced and a phylogenetic tree describing the original sample is constructed.

Furthermore, sequence information can be used to design probes that bind to specific 16S rRNA molecules. In a technique called fluorescent in situ hybridization (FISH), samples are hybridized with fluorescently labeled oligonucleotide probes with complementary targets on portions of the 16S rRNA. This technique, when successful, produces fluorescent images of the sample under observation with information about the three-dimensional distribution of individual bacterial cells within the community. The use of this technique in conjunction with the sequencing of 16S rDNA genes from the natural community allows for the identification, enumeration and visualization of the actual cells represented by the retrieved sequences (Amann 1995).

Many other molecular techniques are available to environmental microbiologist for the analysis of microbial communities without cultivation. However, the methods outlined in Figure 2.8 are limited to the techniques predominantly used in this project.

2.2.2 Limitations of Molecular Methods in Environmental Microbiology

Molecular techniques in environmental microbiology are very powerful tools but are not without their limitations and biases. For the extraction of nucleic acids alone several potential problems arise. In a mixed complex community (soils, plant matter, animal tissue with Gram-negative and positive bacteria), it can be challenging to extract a clean, representative sample of community nucleic acids. Gram-positive bacteria as well as

small bacterial cells (0.3 to 1.2 μm) are classically known to be more resistant to lysis and thus their nucleic acids are harder to access (Theron and Cloete 2000). After acquiring a sample of community nucleic acids, the PCR amplification step can pose further challenges. "Dirty" original samples can introduce impurities such as humic acids that strongly inhibit *Taq* polymerases or other DNA modifying enzymes used in PCR and thus prevent successful amplification reactions (Wintzingerode et al. 1997). Additives such as bovine serum albumin (BSA) can reduce the inhibitory effects of contaminants resulting from extractions of feces and fresh or marine water samples and can increase the tolerance to fulvic acids, tannic acids or $FeCl_3$ (Wintzingerode et al. 1997). Even if amplification is successful, the amplification efficiencies may not be the same for all molecules and there is the concern that preferential amplification of the 16S rDNA of some bacteria over others might occur. As one example, higher G+C content (percent of total DNA bases as Guanine and Cytosine) templates dissociate less efficiently than lower G+C content templates during the denaturation step of PCR, resulting in preferential amplification of lower G+C content templates (Wintzingerode et al. 1997). Contamination in the PCR reaction tube may lead in successful amplification but biased results. For example, it is possible to amplify "naked" DNA present in the sample that is not derived from intact bacterial cells present in the community being studied (Amann et al. 1995). In addition, the products that are formed depend strongly on the specificity of the primers and the PCR conditions (Wintzingerode et al. 1997).

Further limitations may arise if the presence of fragmented nucleic acid templates gives rise to PCR amplification artifacts such as the formation of chimeric products, which incorporate parts of two different sequences. Fragmented DNA can result when

bead-beating procedures are used to access community DNA (Wintzingerode et al. 1997). Chimeric sequences can also result because highly conserved regions of the 16S rDNA genes allow strands of DNA from different organisms to anneal after denaturation in PCR (Amann et al. 1995). In cloning, where the procedures are almost entirely standardized and often utilize cloning kits, researchers have reported differences in clone libraries depending on the cloning vectors used. Ultimately, given the great number of biases, the frequencies of clones should not be used as a measure of cell frequency in the natural environment (Amann and Ludwig 2000).

In FISH, significant limitations also exist. For the technique to work well, probes must penetrate a bacterial cell and bind to target sites. Thus, the first challenges involve permeability, particularly with Gram-positive bacteria or archeae (Amann 1995; Amann et al. 1995; Muyzer and Ramsing 1996). To overcome this limitation, chemical treatment with aldehydes is used to stabilize cell morphology and treatment with denaturing agents, such as alcohols is used to increase cell permeability (Amann 1995; Amann et al. 1995). A second limitation is that the intensity of the fluorescence signal may be too low to detect if cells do not have sufficient targets for hybridization (i.e., they have low numbers of ribosomes because they are not actively metabolizing or are dormant) (Amann 1995; Amann et al. 1995). There is a direct correlation between the number of ribosomes present within a given cell and the general metabolic activity of that cell (Amann 1995). This can particularly be true for environmental samples where cells might be subject to starvation conditions. Hybridization can also be prevented if the rRNA molecules are not accessible due to very stable secondary structures of the molecule itself in its interactions with ribosomal proteins (Theron and Cloete 2000).

With environmental samples, strong background autofluorescence from phototrophic bacteria (such as cyanobacteria), plant matter or minerals can also interfere with the detection of signals from probes. If there are no permeability, intensity or background autofluorescence concerns, there is still a possibility that non specific binding can highlight bacteria that are not being targeted specifically. Finally, in dealing with environmental samples, there is also the possibility that sample heterogeneity could result in the analysis of unrepresentative samples (Amann 1995). Even if all these limitations are overcome, there is still the issue of designing "specific" probes using the current data set on 16S rDNA genes. It is evident that the microbial diversity has not been fully described since new species are being identified in almost every environment. This implies that many unknown organisms may be present in environments under study and that probes could target some of these organisms because their sequence information was not available during design of the probe (Amann and Ludwig 2000). However, despite all these limitations, the power of molecular tools in describing communities and diversity previously unknown to the scientific community is inarguable.

Chapter Three

ISOLATION AND CHARACTERIZATION OF AGROBACTERIUM ALBERTIMAGNI STRAIN AOL15

3.1 Introduction

Geothermal waters often contain elevated concentrations of arsenic and can be an important source of arsenic to both surface and groundwater (Welch et al. 1988). In the eastern Sierra Nevada, California, the concentrations of arsenic in Hot Creek, a tributary of the Owens River, averages 2.7 μM as a result of inputs of geothermal water containing arsenic in concentrations in excess of 13 μM (DWR 1967; Eccles 1976). Arsenic in the geothermal water at Hot Creek occurs primarily in the +III oxidation state (arsenite) but, after mixing with meteoric surface water, undergoes rapid *in situ* oxidation to As(V) or arsenate (Wilkie and Hering 1998), which is thermodynamically favored in oxic surface waters (Ferguson and Gavis 1972; Cullen and Reimer 1989). Field incubation studies demonstrated that the oxidation was associated with an aquatic macrophyte, *Potamogeton pectinatus*. Rapid arsenite oxidation was observed in the presence of the plant or of particulate material detached from the plant surfaces by shaking. Inhibition by antibiotics and filtration suggested that arsenite oxidation was mediated by bacteria colonizing the surface of the aquatic macrophytes (Wilkie and Hering 1998).

To date, several microorganisms are known to catalyze transformations of arsenic including oxidation, reduction, and methylation (Cullen and Reimer 1989; Dowdle et al. 1996; Newman et al. 1998; Stolz and Oremland 1999). Arsenite-oxidizing bacteria have been isolated from many different environments (i.e., cattle-dipping fluids, soil, sewage, mines and mine waters, and aquatic environments) and have been studied under laboratory conditions. Table 2.1 (in Chapter 2) summarizes the different studies on arsenite-oxidizing isolates or consortia. Although the ambient concentrations of arsenic were not reported for many of these studies, the concentrations used in the laboratory studies were highly elevated in some cases (e.g., 100 mM for isolates from cattle-dipping fluids) (Green 1918; Turner 1949; Turner 1954; Turner and Legge 1954; Legge 1954; Legge and Turner 1954). In the studies where whole-cell or enzyme kinetics were examined, Michaelis-Menten K_s or K_m values range from 2-1540 μM (Phillips and Taylor 1976; Osborne and Erhlich 1976). In the current study, the ambient concentrations of arsenic are near 2.7 μM and the experimental concentrations of arsenic are low (2-450 μM for kinetic studies) relative to other reports of arsenite oxidation.

Although numerous studies have reported on arsenite oxidation, its physiological role is not always well understood or described. In two studies, arsenite-oxidizing strains isolated from mine waters, *Pseudomonas arsenitoxidans* (Ilyaletdinov and Abdrashitova 1981) and strain NT-26 (Santini et al. 2000), were shown to be capable of chemolithoautotrophic growth, deriving energy from the oxidation of arsenite. In other cases, arsenite oxidation is generally presumed to be a detoxification mechanism without experimental observations of any toxic effects. This explanation is commonly offered because differential levels of toxicity are associated with arsenite and arsenate. The

toxicity of arsenite results from its affinity for sulfhydryl groups; various enzymes can be inactivated when arsenite binds to the cysteine residues of these proteins (Ferguson and Gavis 1972; Summers and Silver 1978). Arsenate, an analogue for inorganic phosphate, exerts a lower level of toxicity by substituting for phosphate in membrane transport systems (Summers and Silver 1978).

Here we examine the kinetics and physiological role of arsenite oxidation by the strain *Agrobacterium albertimagni*, strain AOL15. The kinetic studies demonstrate that, at the ambient concentrations of arsenic at Hot Creek, AOL15 oxidizes arsenite at about half of its maximum rate. In trying to assess the physiological role of AOL15 and possible explanations for its arsenite oxidizing capability, observations from laboratory and field incubation studies are compared but with the caveat that this organism is not a dominant member of the microbial community attached to the Hot Creek plant surfaces.

3.2 Experimental Methods

3.2.1 Isolation Procedure

In August 1997, fresh samples of *Potamogenton pectinatus* were collected in sterile polypropylene bottles, transported to the laboratory on ice, and stored at 4° C for one day. Clippings of the plant samples were then placed into a sterile, 15 ml polypropylene centrifuge tube with 5 ml of deionized water. The centrifuge tube was vigorously mixed with a vortex mixer and 1 ml of the resulting suspension was inoculated into a liquid citrate medium (which was selected to provide a chemically well-defined, simple growth

medium). The medium was amended with 30 μM arsenite and within one week, the resulting turbid medium showed a complete oxidation of the arsenite to arsenate. At this point, the culture was transferred to fresh arsenite-amended citrate medium and, after several transfers, an enrichment culture was established. To increase selectivity for arsenite-resistant microorganisms, arsenic concentrations in the enrichment cultures were gradually increased from 30 μM to 500 μM during the isolation process. A serial dilution of the liquid culture was plated and all resulting colonies were transferred to liquid media to screen for arsenite oxidation using the $KMnO_4$ method (described below).

3.2.2 Media

The medium used for the establishment of the enrichment culture and eventual isolation of arsenite oxidizing microorganisms was a minimal medium with citrate as the carbon source, herein referred to as citrate medium (composition [g/L]: KH_2PO_4 (0.75), K_2HPO_4 (0.61), NH_4Cl (0.67), $MgSO_4 \cdot 7H_2O$ (0.2), $CaCl_2$ (0.023), $FeCl_3$ (0.0024), $MnCl_2 \cdot 4H_2O$ (0.003), $Na_2MoO_4 \cdot 2H_2O$ (0.001), sodium citrate (3.64) with 30 μM arsenite for isolation and a final concentration of 500 μM arsenite for the pure culture). After isolation, the citrate medium was modified to improve growth by the addition of 1g/L tryptone to the defined medium. A mannitol-based medium (modified from Kerr) (Kerr 1992) was also used for growth studies, herein referred to as mannitol medium (composition [g/L]: K_2HPO_4 (0.5), $MgSO_4 \cdot 7H_2O$ (0.4), NaCl (0.2), yeast extract (0.3), L-glutamate (2.0), mannitol (10.0) with variable final concentrations of arsenite ranging from 0 to 5mM). For variable pH growth studies, the phosphate-buffered medium consisted of 10% Luria-

Bertani (Difco) with pH ranging from 4 to 13 (desired pH obtained by addition of citric acid, hydrochloric acid, tris, glycine, or sodium hydroxide).

3.2.3 DNA extraction, 16S rDNA sequencing and DNA-DNA hybridizations

For the extraction of genomic DNA, a 100 ml cell suspension was centrifuged at 10,000 g for 15 minutes and resuspended in 4 ml dilute Tris-EDTA buffer (0.01 M Tris, 0.005 M EDTA). The sample was treated sequentially with (a) lysozyme (1 mg/ml for 30 minutes at 37° C) followed by addition of l ml of concentrated Tris-EDTA buffer (0.21 M Tris, 0.08 M EDTA) (b) SDS, sodium dodecyl sulfate (1% solution for 60 minutes at 60° C) (c) proteinase K and RNAase (0.5 mg/ml and 0.01 mg/ml respectively for 45 minutes at 37° C). The DNA was separated from the bulk solution using a series of phenol and chloroform extractions. The DNA was then precipitated using a combined ethanol and 0.3 M sodium acetate solution, vacuum dried, redissolved in Tris-EDTA buffer (20 mM Tris and 5 mM EDTA), and stored at –20° C (method modified from Ausubel et al. 1992 and Gerhardt et al. 1994). Purified genomic DNA from liquid-grown cultures were quantified and ~10 ng of DNA was used as the template for PCR amplification. Universal primers [S-D-Bact-0011-a-S-17 (5' to 3': GTTTGATCCTGGCTCAG) and S-D-Bact-1492-b-A-16 (5' to 3': TACCTTGTTACGACTT)] (Wheeler et al. 1996; Kane et al. 1993) were used to amplify the 1.4-kb PCR fragment per protocols established by Ruimy et al. 1994. Directly following purification on Qiagen columns (Qiagen, Valencia, Calif.), amplicons thus generated were sequenced. The identity of a given PCR product was verified by sequencing at the DNA Sequencing Core Facility at the Beckman

Institute at Caltech using the dideoxy chain termination method with Sequenase DNA sequencing kit (United States Biochemical Corporation, Cleveland, Ohio) and with an ABI 373A automatic sequencer as recommended by the manufacturer (Perkin-Elmer Corp., Foster City, California). The phylogenetic relationships of organisms examined in this study were determined by comparison of individual 16S rDNA sequences to existing sequences in the public database (NCBI). The resulting 1412 base pair sequence was analyzed using MacVector™, GENETYX-MAC 8.0, AssemblyLIGN™, Genetic Data Environment (GDE) v. 2.0, Phylip version 3.6 (J. Felsenstein and the University of Washington, Seattle [public domain]). DNA-DNA hybridizations were carried out with biotinylated DNA by flurometric hybridizations in microdilution wells as previously described (Ezaki et al. 1989; Satomi et al. 1998; Satomi et al. 1997).

3.2.4 Growth and toxicity studies

In determining growth rates and doubling times, mannitol medium was used exclusively. Cell numbers were determined microscopically using the fluorochrome DAPI to stain cells. Stained cells were retained on 0.2 μm pore filters before viewing and counting (Kepner and Pratt 1994). In determining the ability of AOL15 to grow in variable pH or NaCl media, positive results were reported for solutions with minimum optical density of 0.25 at 600 nm. Plate counts were used to determine cell numbers in experiments monitoring growth and oxidation concurrently. For the variable salt content growth studies (%NaCl), the medium consisted of neutral pH (pH 7) solution of 1% tryptone with salt content (%NaCl) ranging from 1 to 10%. To determine if AOL15 was capable

of chemolithoautotrophic growth by arsenite oxidation, a medium was prepared with bicarbonate as the carbon source and arsenite at 1 or 5 mM as the energy source (Santini et al. 2000), herein called bicarbonate medium.

The ability of AOL15 to grow anaerobically in mannitol medium with nitrate (5 mM), ferric iron (20 mM), sulfate (5 mM), sulfite (5 mM), thiosulfate (5 mM), arsenate (5 mM), fumarate (20 mM), malate (10 mM), and DMSO (10 mM) as terminal electron acceptors was tested at 30°C.

For the carbon-source utilization characterization of AOL15, API 20 NE strip tests (BioMerieux S. A., Marcy l'Etoile, France) and Biolog GN microplates (Biolog Inc., Hayward, CA) were used. Results for AOL15 were compared with those for *Agrobacterium tumefaciens* (ATCC #23308) and *Blastobacter aggregatus* (ATCC #43293), two species that are phylogenetically related to AOL15.

In order to determine the toxic effects of arsenite and arsenate, LB plates with variable concentrations of either arsenite or arsenate ranging from 10 μM to 50 mM were prepared. Cultures of AOL15, *A. tumefaciens*, and *B. aggregatus* were plated and incubated at 30°C and colony formation was monitored.

3.2.5 Analyses

In kinetics experiments, arsenite oxidation was monitored by measuring As(III) concentrations over time. Arsenic (III) and As(V) in filtered samples were separated using anion exchange columns filled with AG 1-X8 resin, dry mesh size 100-200 in the acetate form (Bio-Rad, Hercules, CA) as described by Wilkie and Hering 1998. Total

arsenic concentrations were measured in the initial filtered samples and arsenite concentrations were measured in samples processed through the anion exchange columns. Arsenic concentrations were determined by inductively coupled plasma mass spectrometry (ICP-MS) on a Perkin- Elmer ELAN 4000.

A qualitative $KMnO_4$ screening technique was used to monitor the consumption of arsenite and production of arsenate in culture growth media. Thirty µl of 0.01 M $KMnO_4$ were added to 1 ml of the culture medium containing 500 µM total arsenic. A pink color for the resulting mixture indicated that arsenate (which does not react with permanganate) was present and thus was a positive result for arsenite oxidation. A clear or orange colored solution indicated that arsenite (which reacts with permanganate) was present and thus was a negative result for oxidation.

Additionally, AOL15, *A. tumefaciens* and *B. aggregatus* were sent for fatty acid methyl ester (FAME) analysis (Microbial ID, Inc., Newark, DE). Fatty acids were separated by high-resolution gas chromatography and the resulting fatty acid profiles were analyzed as previously described (Ringelberg et al. 1994).

3.2.6 Kinetics of arsenite oxidation

To determine the kinetic constants for whole cell suspensions (K_s and V_{max}), cultures of AOL15 were used. In a standardized procedure, frozen stocks of AOL15 were used to inoculate into mannitol medium without arsenite at a dilution of 1:50 and allowed to grow for 24 hours. After 24 hours, the fully grown culture was transferred into mannitol medium with 500 µM arsenite at a dilution of 1:1000. After 24 hours of growth in the

presence of arsenite, the cultures reached late exponential/early stationary phase and were harvested by centrifugation at 12,000 g for 20 minutes at 4°C with two wash steps using 10 mM HEPES buffer at pH 7. The washed cells were resuspended in HEPES buffer and allowed to equilibrate to 30°C; kinetic experiments were initiated by the addition of arsenite. Samples were collected, sterilized by filtration (0.2 μm filter) and analyzed for arsenite and total arsenic as described above. Kinetic parameters were determined from a plot of initial rate vs. initial substrate concentrations using Scientist (Micromath Scientific Software). The variability associated with cell counts resulted in a 32% error in the V_{max} value and a calculated error of 65% in K_s. For data sets with low initial substrate concentrations, initial rates were calculated from K_s and V_{max} values fit to the individual data sets. To compare V_{max} values with literature values, protein concentration determinations were made using the Bio-Rad DC protein assay (Hercules, CA).

3.2.7 Transmission Electron Microscopy

Standard methods for transmission electron microscopy (TEM) were used for AOL15 samples. Cells grown in mannitol medium were pelleted and fixed in a 2.5% glutaraldehyde solution and stained with saturated uranyl acetate for TEM based on the procedures outlined by Robinson et al. 1987. Samples were observed on a Philips EM 201 transmission electron microscope at 80 kV.

3.2.8 Nucleotide accession numbers

The nucleotide sequence for strain AOL15 reported here has been deposited with GenBank nucleotide sequence databases under accession number AF316615.

3.3 Results and Discussion

3.3.1 Isolation and identification of AOL15

The isolation procedure described above yielded two strains capable of arsenite oxidation. *Agrobacterium albertimagni* strain AOL15 (Figure 3.1) was selected for further study after 16S rDNA analysis revealed that these strains were 100% identical.

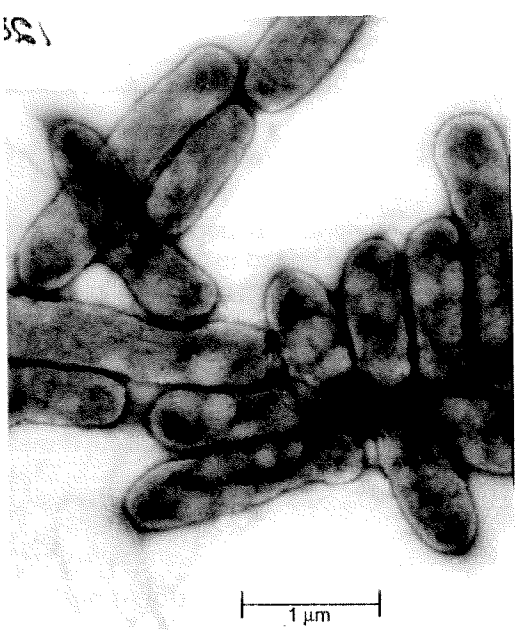

Figure 3.1: Negatively stained transmission electron micrograph of AOL15 grown in mannitol medium without arsenite (stained with uranyl acetate).

A polar flagellum was observed by microscopy and AOL15 was found to be motile in mannitol medium but immotile in citrate medium (a similar observation was also made for Green's arsenite oxidizer) (Green 1918). Images of AOL5 in citrate medium and mannitol medium are presented in Appendix A.

Phylogenetic analysis by 16S rDNA (mask: comparing 1329 of the 1412 aligned base pairs) showed that AOL15 was 97.0 % identical to *B. aggregatus* and 97.7% identical to *A. tumefaciens* (Figure 3.2).

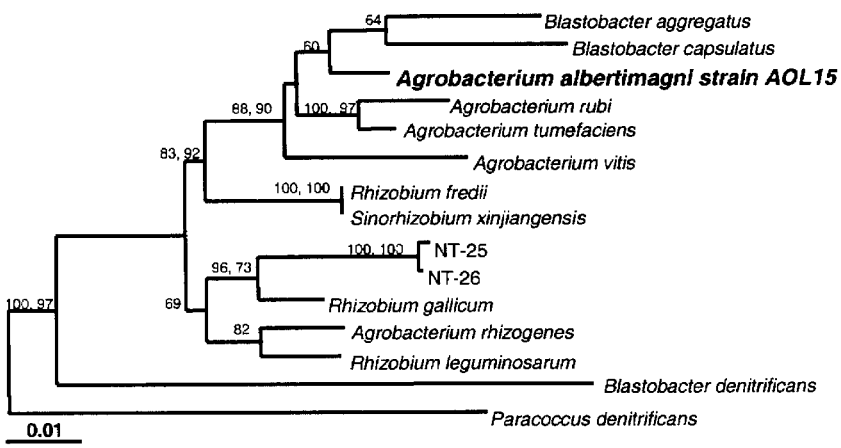

Figure 3.2: Phylogenetic Tree of AOL15. Numbers at branch points are bootstrap values for a distance (first value) and parsimony (second value) based analysis. Single bootstrap values are for distance-based analysis only. Accession numbers: *Blastobacter aggregatus* (X73041), *Blastobacter capsulatus* (X73042), *Agrobacterium albertimagni strain AOL15* (AF316615), *Agrobacterium rubi* (D12787), *Agrobacterium tumefaciens* (D12784), *Agrobacterium vitis* (D01258 and D14502), *Rhizobium fredii* (D12792), *Sinorhizobium xinjiangensis* (D12796), *NT-25* (AF159452), *NT-26* (AF159453), *Rhizobium gallicum* (U86343), *Agrobacterium rhizobenes* (X67224), *Rhizobium leguminosarum* (U29386), *Blastobacter denitrificans* (S46917), *Paracoccus denitrificans* (X69159).

Of the previously-described arsenite oxidizers, the chemolithoautotrophic strains NT-25 and NT-26 are the closest to AOL15 (94.2% similarity) and are included in the

phylogenetic tree. DNA-DNA hybridizations confirmed that AOL15 and *B. aggregatus* were more closely related (30% similarity) than AOL15 and *A. tumefaciens* (10-15% similarity) but that AOL15 was a new species (less than 70% identical) (Wayne et al. 1987). However, since the genus *Blastobacter* may be reclassified in the near future (as an *Agrobacterium*) (Hugenholtz et al. 1994), we suggest that strain AOL15 be grouped with the genus *Agrobacterium*. The similarity matrix for the phylogenetic analysis and the DNA-DNA hybridization experiments appear in Appendix B.

The phenotypic profiles showed that AOL15 was metabolically similar to both *Agrobacterium tumefaciens* and *Blastobacter aggregatus*. All three strains (AOL15, *A. tumefaciens*, and *B. aggregatus*) were positive for esculin hydrolysis, β-galactosidase activity, and oxidase activity and were negative for indole formation, glucose fermentation, arginine dihydrolase activity, and gelatinase activity. All three strains utilized the same 41 carbon sources of the 95 tested. In the FAME analysis, the relatedness of the three species (*A. tumefaciens*, *B. aggregatus*, AOL15) was determined by applying a Euclidean distance method to analyze the fatty acid profiles (Microbial ID, Inc., Newark, DE). This analysis revealed that, of these three strains, AOL15 and *B. aggregatus* were more closely related than AOL15 and *A. tumefaciens* or *B. aggregatus* and *A. tumefaciens*.

3.3.2 Growth and toxicity studies

AOL15 was grown at three different temperatures (25°, 30°, and 37° C) with varied concentrations of arsenite. An attempt was also made to grow the culture without arsenic

at 4° and 42° C. The optimal growth temperature was 30° C (which is comparable to field temperatures ranging from 23° to 28° C) with a doubling time of 1.3 hours in mannitol medium when grown without arsenic (Table 3.1).

Table 3.1:Doubling time for AOL15

Temp. (°C)	[As(III)],(μM)	Doubling Time, (hr)
25	0	2.0
25	5	1.9
25	500	2.0
30	0	1.3
30	50	1.3
30	500	1.6
37	0	1.5

Only slight differences in the growth rates were observed with variations in arsenite concentration up to 500 μM. However, cultures grown at 1 mM and 2.5 mM arsenite mannitol medium exhibited significant lag periods before entering exponential growth phase. This lag suggests that higher concentrations of arsenite are toxic to AOL15. Consistent with this hypothesis, it was observed that AOL15 could grow on solid media in the presence of 50 mM arsenate (the highest level tested) but growth was not observed in the presence of 5 mM arsenite. Although the strains *A. tumefaciens* and *B. aggregatus* (which are closely related to AOL15) were tolerant to elevated concentrations of arsenite, neither strain was capable of oxidizing arsenite (as determined by the permanganate assay). *A. tumefaciens* could grow in the presence of 500 μM arsenite but not at 5mM. *B. aggregatus* could grow at 400 μM arsenite but not at 500 μM. In the literature, the highest levels of tolerance reported by Green (100 mM

arsenite) and Turner (60 mM arsenite) are significantly higher than the levels observed here (Green 1918; Turner 1949).

Arsenite did not support chemolithoautotrophic growth of AOL15 in bicarbonate medium. Growth was observed, however, when the bicarbonate medium was amended with 500 μM mannitol. In addition, growth experiments with gradual increases of arsenite did not show increases in cell numbers compared with parallel batches grown without arsenite. Thus, arsenite oxidation does not appear to be linked to chemolithoautotrophic growth, rather, given the toxic affects of arsenite, it appears to be a detoxification mechanism for AOL15.

AOL15 was not able to grow using any of the tested terminal electron acceptors other than molecular oxygen nor did it exhibit fermentative growth. This is consistent with the reports on the *Agrobacterium* genus although some strains have been reported that are capable of anaerobic respiration in the presence of nitrate (Kersters and De Ley 1984). Optimal growth of AOL15 was observed at neutral pH (pH 7 and 8), comparable to field conditions (pH 8.3), and at low salt conditions (less than 2 % NaCl although no concentrations below 1% were tested).

3.3.3 Arsenite oxidation

The growth of AOL15 and the redox speciation of arsenic were monitored simultaneously. As shown in Figure 3.3, AOL15 grew exponentially for 15 hours and then reached stationary phase. The decrease in the measured arsenite concentration shows that oxidation occurred during the late exponential phase, once the culture had reached a high cell density. Oxidation of 585 μM arsenite (i.e., 290 μmole) was

complete within 24 hours. Arsenite oxidation in short term assays (<5 hrs) was not observed in suspensions of washed cells from cultures grown in the absence of arsenite (data not shown) but cells that had previously been grown in the presence of arsenite were able to oxidize arsenite immediately. This capacity to oxidize arsenite was not lost even after 10 consecutive transfer and growth cycles in arsenite-free medium. This implies that arsenite oxidation is an inducible activity that is likely to be encoded on the chromosome.

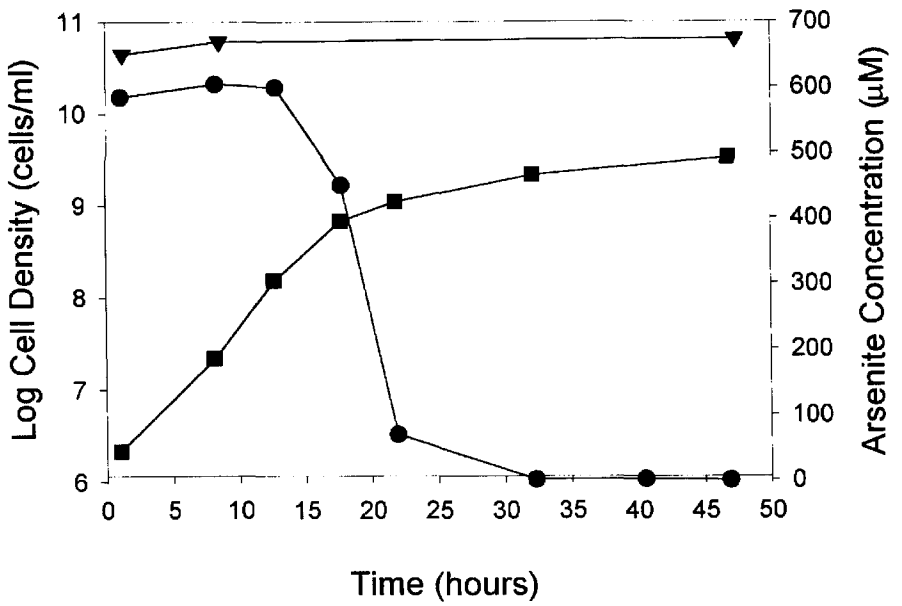

Figure 3.3: Growth of AOL15 in the presence of approximately 500 μM (585μM) arsenite in mannitol medium at 30° C (Representative data set). Symbols: (■) cell growth measured by plate counts, (▼) arsenite in control experiments of mannitol solution without bacterial cells, (●) arsenite in mannitol solution with growing cells. Lines are included only as a guide.

The kinetic parameters for arsenite oxidation by AOL15 were determined using washed and resuspended whole cells harvested at late exponential/early stationary phase. The detailed data and analysis for these experiments is presented in Appendix D. The

values of the kinetic parameters for arsenite oxidation are K_s = 3.4 ± 2.2 μM and V_{max} = 1.81 ± 0.58 x 10^{-12} μmole·cell^{-1}·min^{-1} (0.043 ± 0.017 μmole·mg protein^{-1}·min^{-1}) (Figure 3.4). Further kinetic studies with cells harvested in the exponential growth phase and in stationary phase showed comparable rates of arsenite oxidation (data presented in Appendix E). Thus the apparent localization of arsenite oxidation to the late exponential/early stationary phase (Figure 3.3) is attributable to the fact that the number of cells present in the early part of the growth experiment was not sufficient to oxidize arsenite at a detectable rate.

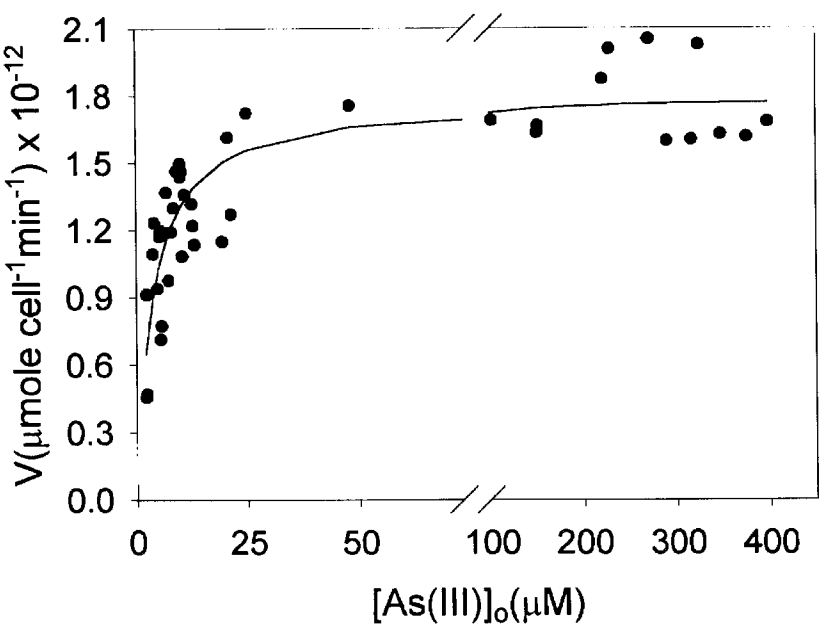

Figure 3.4: Oxidation rate as a function of initial arsenite concentration $[As(III)]_o$. Data points (●) fit with theoretical line with K_s = 3.4 ± 1.1 μM and V_{max} = 1.81 ± 0.58 x 10^{-12} μmole·cell^{-1} min^{-1}.

The K_s value for AOL15 is substantially lower than previously-reported values (ranging from 70 – 1540 μM) for arsenite oxidation by whole cell suspensions (cf. Table 2.1). The arsenic concentration in Hot Creek averages 2.7 μM thus the K_s value observed here is close to the conditions experienced by AOL15 in its natural setting. The protein-

normalized V_{max} reported here (0.043 ± 0.58 μmole·mg^{-1}·min^{-1}) compares very well with the V_{max} reported for whole cell studies of *Alcaligenes faecalis* (0.05 μmole·mg^{-1}·min^{-1}) (Phillips and Taylor 1976) and for the cell-free extracts of *A. faecalis* (0.023 μmole·mg^{-1} min^{-1}) (Anderson et al. 1992). The arsenite oxidase from *Alcaligenes faecalis* is the only enzyme for arsenite oxidation that has been purified and characterized. It has been described as an oxomolybdenum enzyme and its activity has been localized to the periplasmic space of the bacterial cell (Anderson et al. 1992, McNellis and Anderson 1998). It has also been suggested that arsenite oxidation is a resistance mechanism that occurs by a periplasmic electron transfer chain with arsenite oxidase as the first protein in the transfer sequence (Anderson et al. 1992, McNellis and Anderson 1998).

3.3.4 Implications of Arsenite Oxidation at Hot Creek

For AOL15, arsenite is clearly more toxic than arsenate and the enzymatic transformation of arsenite to the less toxic form may be a mechanism for resistance and detoxification. This is in contrast with the arsenic resistance (in Gram-negative and Gram-positive bacteria) associated with the *reduction* of arsenate to arsenite. In these cases arsenite is exported from the cell into a low-arsenite external medium along a favorable chemical gradient (Silver 1996; Rosen 1996). In Hot Creek, however, the elevated concentrations of arsenite in the external cell environment could result in passive diffusion of arsenite (as the uncharged species H_3AsO_3) into the cell. In this case, arsenite oxidation could minimize arsenic uptake into the cell.

The potential contribution of a microorganism like AOL15 to the rapid *in situ* oxidation observed at Hot Creek can be illustrated by comparing the kinetics of oxidation

in the field and in laboratory studies with AOL15. In field incubation studies, pseudo first-order oxidation of arsenite was observed both at the ambient arsenite concentration and in samples spiked with 2 μM arsenite with an average pseudo first-order rate constant of 0.050 min^{-1}. For Michaelis-Menten kinetics, pseudo first-order kinetics are expected for the initial substrate concentration $[S]_o < K_s$, then

$$V = \frac{V_{max}[S]}{K_s} \qquad (1)$$

and the pseudo first-order rate constant corresponds to V_{max}/K_s. In the field study, this assumption is not entirely valid since $[As(III)]_o$ is less than the K_s for AOL15 at the ambient concentration of ca. 0.5 μM (Wilkie 1997) but is comparable to K_s in the spiked sample. For illustrative purposes, however, Eqn. 1 can be used to estimate the cell density required to achieve the pseudo first-order rate constant observed in the field incubations. With the values of V_{max} and K_s for AOL15, that estimated cell density is 10^8 cells/mL. This value cannot be interpreted as an observation of ambient conditions since it is an estimate of the number of cells shaken off the plant surface and not an estimate of the number of planktonic cells present in the creek or in association with the biofilm on the surface of the plants. However, it is a reasonable *estimate* of the number of cells required to account for the observed oxidation and can be even more informative if the density of the biofilm is determined in the future. This calculation must be viewed with some caution since the kinetic parameters determined in the laboratory for AOL15 may not apply under ambient conditions and since microorganisms other than AOL15 may contribute wholly or in part to the arsenite oxidation observed in the field. It is highly likely that other oxidizers are present on the surfaces of the macrophytes that were not

selected for in these isolations because the arsenic concentrations in the enrichment media (30 and 500 μM) were 10 to 170 times the ambient concentrations.

3.3.5 Description of *Agrobacterium albertimagni* strain AOL15 sp. nov

Agrobacterium albertimagni is named after the Dominican scholar Albertus Magnus who was the first person to describe arsenic.

AOL15 (Figure 3.1) is a gram-negative rod, 1.5μm long by 0.5 μm wide. When the microorganism is grown in mannitol medium, one polar flagellum is observed by transmission electron microscopy and the species is motile although it is immotile in citrate medium.

Strict aerobe. Positive for esculin hydrolysis, β-galactosidase activity, and oxidase activity but negative for indole formation, glucose fermentation, arginine dihydrolase activity, and gelatinase activity. From the assimilation tests, able to utilize D-glucose, L-arabinose, D-mannose, D-mannitol, N-acetyl-D-glucosamine, maltose, L-malic acid, dextrin, D-arabitol, D-fructose, L-fucose, D-galactose, gentiobiose, α-D-glucose, m-inositol, α-D-lactose, lactulose, D-melibiose, β-methyl-D-glucoside, D-psiscose, D-raffinose, L-rhamnose, D-sorbitol, sucrose, trehalose, turanose, methyl pyruvate, mono-methyl succinate, D,L-lactic acid, L-aspartic acid, L-glutamic acid, L-ornithine, L-proline, L-pyroglutamic acid, urocanic acid, inosine, uridine, glycerol, glucose-1-phosphate, and glucose-6-phosphate.

Optimal growth occurs at 30° C on mannitol, at neutral pH (7 or 8) and at low % NaCl (1 – 4). The strain can oxidize arsenite but does not appear to grow chemolithoautotrophically.

Phylogenetically the species is 97.0% identical to *Blastobacter aggregatus* and 97.7% identical to *Agrobacterium tumefaciens.* Based on DNA-DNA hybridizations, AOL15 is 30 – 31% identical to *Blastobacter aggregatus* and 10 – 15% identical to *Agrobacterium tumefaciens,* which confirms that it is a new species.

Source: Isolated from the surface of the aquatic macrophyte *Potamogeton pectinatus* in Hot Creek, California.

Type strain: AOL15. Deposited in the American Type Culture Collection (ATCC BAA-24).

Chapter Four

A DESCRIPTION OF THE MICROBIAL BIOFILM COMMUNITY ON THE SURFACE OF AQUATIC PLANTS BY MOLECULAR TECHNIQUES

4.1 Introduction

The ability of AOL15 to oxidize arsenite was demonstrated in Chapter 3. However, the relative importance of AOL15 as an arsenite oxidizer within the biofilm community was not established. Molecular techniques can be used to characterize the genetic diversity within microbial communities without needing to cultivate the microbiota (Amann et al. 1995; Muyzer and Ramsing 1996). Thus, a "molecular" approach was employed to complement the cultivation-based study. Molecular tools were used to inventory numerically dominant members of the biofilm present on the leaf surfaces of the submerged macrophyte *Potamogeton pectinatus* and to determine whether AOL15 could be detected within the inventory. It should be noted that this inventory does not reflect the functional role of the community microbiota.

PCR-based methods were used to amplify the 16S rDNA genes of the biofilm community and to construct a clone library. Additionally, a primer was designed to amplify with specificity the DNA of AOL15 (or similar organisms) from the complex mixture of DNA extracted from samples of *Potamogeton pectinatus*. Finally, an attempt

was made to visualize the several different ribotypes (subtypes of bacteria based on DNA fragment patterns) present in this community by fluorescence in situ hybridization (FISH).

4.2 Experimental Methods

4.2.1 Reagents

DNA extraction reagents are presented in Table 4.1. PCR and gel electrophoresis reagents are presented in Table 4.2, and the reagents for microscopy are presented in Table 4.3. All solutions were prepared in high purity, 18 MΩcm water (Millipore) unless otherwise specified. These solutions are referred to by their names in the text.

Table 4.1: Reagents for DNA extraction.

Reagent Name	**Composition**
Phosphate Buffered Saline (PBS)	NaCl (8 g/L) KCl (0.2 g/L) $Na_2HPO_4 \cdot 7H_20$ (2.68 g/L) KH_2PO_4 (0.24 g/L), pH adjusted to 7.4
Extraction Buffer A	NaCl (200 mM) Tris (200 mM) Sodium citrate (2 mM) CaCl2 (10 mM) EDTA (50 mM), pH adjusted to 8.0
20% SDS Solution	SDS (20 g/L)
Phenol:Chloroform:Isopropanol Solution	Phenol:chloroform:isopropanol 1:1:0.02 by volume
DNA Precipitation Solution	3 M sodium acetate:isopropanol 0.1:1 by volume
Tris EDTA Buffer (TE Buffer)	Tris (10 mM) EDTA (1 mM), pH adjusted to 8.0
TE-RNAase A Solution	Tris (50 mM) EDTA (10 mM) RNAase A (Sigma) (100 mg/ml)
NaOH-SDS Solution	NaOH (200 mM) SDS (1%)
Neutralizing Solution	Sodium Acetate (3 M), pH adjusted to 5.5

Table 4.2: Reagents for PCR and gel electrophoresis.

Reagent Name	Composition
PCR Reaction Buffer (GeneAmp® Buffer from Perkin Elmer, #N808-0006)	Tris (100 mM) KCl (500 mM)
PCR Reaction Solution	PCR Reaction Buffer (1:10 dilution in water) BSA (Bovine Serum Albumin) (0.9 μg/ml) Nucleotides (0.9 mM) $MgCl_2$ (1.5 mM) Forward Primer (2 μg/ml) Reverse Primer (2 μg/ml) Taq Polymerase (Perkin Elmer) 1.25 units /25 μl
PCR Reaction Solution with Betaine	PCR Reaction Solution Betaine (1M)
Tris Acetate EDTA Buffer (TAE Buffer)	Tris-acetate 40 mM EDTA 1 mM, pH adjusted to 8.3
1% Agarose Gel	Agarose (10 g/L) Ethidium Bromide (0.05 μg/ml) Prepared in TAE Buffer
2.5% Low Melting Point Agarose Gel	Agarose (25 g/L) Ethidium Bromide (0.05 μg/ml) Prepared in TAE Buffer (Table 4.1)

Table 4.3: Reagents for microscopy.

Reagent Name	Composition
Gelatin Slide Coating Solution	Gelatin (0.1%) Chromium potassium sulfate (0.01%)
Hybridization Buffer	Tris (100 mM) NaCl (0.9 M) SDS (0.1%) Formamide (10%), pH adjusted to 8.0
Wash Buffer	Tris (100 mM) NaCl (0.9 M) SDS (0.1%) EDTA (5 mM) Formamide (10%), pH adjusted to 8.0
DAPI Solution	DAPI (0.1 μg/ml)

4.2.2 Sample Collection

On June 30, 2000, fresh clippings of *Potamogeton pectinatus* were collected from Hot Creek in sterile Eppendorf tubes. The collected plants were treated in one of four ways: (1) stored in ambient creek water (sample name: HC), (2) rinsed with 70% ethanol and

stored in 70% ethanol (sample name: EtOH), (3) rinsed with (and stored in) PBS solution (sample name: PBS), or (4) rinsed with DI water and stored in 3.7% paraformaldehyde by combining three parts 4 % paraformaldehyde with one part sample (sample name: 4% Para). All samples were transported on ice to the laboratory for further processing.

4.2.3 DNA Extraction

DNA was extracted from the HC, EtOH, and PBS samples using techniques described in Dawson (2000). Plant clippings from these samples were placed into individual tubes with 600 µl of extraction buffer A and 100 µl of 0.5 mm glass beads and vortexed at a low speed for three minutes. Then, 500 µl of the resulting solution was transferred to a clean tube for the extraction of DNA by bead-beating. Acid washed fine zirconium beads (0.1 mm diameter) were added to the solution with 200 µl of 20% SDS and 700 µl phenol:chloroform:isopropanol solution. The samples were then placed on a bead beater (Mini Bead Beater, Biospec Products) for two minutes on low setting. After beating, the samples were centrifuged for three minutes at 12,000 × g. The sample was extracted again with the phenol:chloroform:isopropanol solution resulting in a 500 µl final product. The DNA in this product was precipitated by adding 500 µl of DNA precipitation solution and placing the sample on ice for 20 minutes. After precipitation the DNA was pelleted by centrifugation at 4000 × g, at 4° C for 30 minutes. The resulting DNA pellet (brown in color) from the three different samples (HC, EtOH, and PBS) was washed once with 70% ethanol, allowed to air dry and then resuspended in TE buffer. The final extracted DNA product was stored at –20° C for future use.

4.2.4 PCR, Cloning, RFLP and Sequencing

The extracted community DNA from the three plant samples (HC, EtOH, and PBS) was used as a template for PCR. The primers used in these amplifications are listed in Table 4.4.

Table 4.4: List of primers used for amplification from extracted community DNA samples.

Primer Name	Specificity	Sequence 5' to 3'
8F	Bacteria	AGAGTTTGATCCTGGCTCAG
1492R	Bacteria	GGTTACCTTGTTACGACTT
4F	Archaea	TCCGGTTGATCCTGCCRG
515F	Universal	GTGCCAGCMGCCGCGGTAA
1195F	Eukarya	GGGCATCACAGACCTG
ALF	α-Proteobacteria	CTGGCTCAGARCGAACG
AOL15	*A. albertimagni* strain AOL15	GTGGTTAGCTGCCTCCCTTG

The PCR amplifications from community DNA were conducted in a 25 µl reaction containing template and PCR reaction solution with betaine. The primer annealing temperature was varied ($62^{\circ} \pm 10^{\circ}$ C) to optimize reaction conditions using the MasteCycler Gradient PCR machine (Eppendorf). Where explicitly stated, betaine was omitted from the PCR reaction solution.

The reaction product was separated by electrophoresis on a 1% agarose gel and visualized by staining with ethidium bromide and UV illumination of the gel. The products were then cloned into *E. coli* cells using the TOPO TA Cloning kit from Invitrogen (Carlsbad, California) following recommended procedures by the manufacturer. Plasmids were purified from the *E. coli* cells by growing the cultures for

18 hours, spinning them down at 4,000 × g and lysing the cells for 15 minutes at –80° C. These minipreps were carried out in 96 well (deep well, two ml volume) culture plates by an alkaline lysis procedure (Ng et al. 1996). One hundred microliters of TE-RNAse A solution was added to the pellets and the plates were vortexed at medium speed for three minutes. After vortexing, 100 µl of NaOH-SDS solution was added to the mixture and vortexed on a low setting for a few seconds to mix the sample. The suspension was placed on ice for five minutes after which 100 µl of neutralizing solution was added. The suspension was vortexed on low for five minutes and placed on ice for another 20 minutes. Finally, the cell lysates were centrifuged for 15 minutes at 4000 × g to pellet the cell debris. Two hundred microliters of the supernatant (containing the plasmid DNA with the 16S rDNA insert) was transferred to a sterile 96 well culture plate and 200 µl of cold isopropanol was added to precipitate the plasmid DNA. The solution was centrifuged at 4° C at 4000 × g for 10 minutes. The supernatant was removed by inverting the culture plate and the plasmid DNA was allowed to air dry in the wells before resuspension in 40 µl of TE buffer. The plasmid product was used as a template to re-amplify the 16S rDNA insert by primers T3 (5' to 3': TAATACGACTCACTATA), and T7 (5' to 3': ATTAACCCTCACTAAAGGGA) and the reaction products were analyzed by restriction fragment length polymorphism (RFLP).

For the restriction digest, the enzymes Hin PII and Msp I (New England Biolabs) were used at final concentrations of 30 units of enzyme/ml. The digestion reactions were incubated at 37° C overnight, and visualized by ethidium bromide staining and UV illumination of digestion products separated by electrophoresis on a 2.5% low melting point agarose gel. Unique clones were then sequenced using primers T3, T7 and 515F at

the DNA Sequencing Facility at the University of Colorado at Boulder. Sequences were edited using Sequencher (Genecodes Corp.) and analyzed and aligned using the ARB software package (Strunk et al. 1998). Sequences were identified initially using the Basic Local Alignment Search Tool (BLAST; Altschul et al. 1990). Chimeric sequences were identified using the CHIMERA_CHECK program of the Ribosomal Database Project (RDP; Maidak et al. 2000). Distance, parsimony and maximum likelihood phylogenetic based inferences were determined using ARB. Bootstrap analysis (resampling of 100 replicates of the individual sequence dataset being analyzed by maximum parsimony) was performed to determine the relative robustness of the resulting phylogenetic tree topology. The consensus phylogenetic trees were further modified using Treeview (Version 1.6.5; Page 1996).

4.2.5 16S rDNA Probes and FISH

Samples were collected and stored in 4% paraformadehyde for microscopy based on reported techniques (Amann et al. 1990; Amann 1995; Amann et al. 1995, Dawson 2000). The fixed cells were stored at 4° C overnight after which the parformaldehyde was replaced with 95% ethanol. The samples were then stored at –20° C until further use (samples stored in this way can be preserved for several months) (Dawson 2000). The probes used for these studies are presented in Table 4.5. One probe, Probe AOL15, based on the 16S rDNA sequence for *Agrobacterium albertimagni* strain AOL15 was designed using the Probe Design feature of the ARB software package (Strunk et al. 1998) and synthesized by Synthegen (Synthegen LLC, Texas).

Eight well microscope slides were coated with warmed solution (70° C) of gelatin slide coating solution. The slides were allowed to air dry before the samples were applied to the wells. These gelatin coated slides were stored for later use at 4° C. Three microliters of fixed sample stored in ethanol was added to each well of the microscope slides and allowed to air dry. The samples were dehydrated by sequentially soaking in 50%, 80% and 95% ethanol. Each dehydration step was carried out for three minutes. After the final dehydration step, the sample slides were allowed to air dry before hybridization. One hundred sixty microliters of hybridization solution consisting of 153.6 µl of hybridization buffer and 6.4 µl of probe (stock concentration of 50 ng/µl) was prepared for each slide. Twenty microliters of hybridization solution was added to each well in the dark and the slides were each covered with a cover slip while avoiding the formation of bubbles. The slides were then placed in a hybridization chamber consisting of a sealed, darkened container humidified with hybridization buffer. The slides in the chamber were incubated overnight at 37° C.

Table 4.5: Probe list for FISH.

Probe Name	Specificity	Sequence of Probe (5' to 3')	Reference
ALF1b-Cy3	α-proteobacteria, several members of δ-proteobacteria, most spirochetes	CGTTCGYTCTGAGCCAG	1
BET42a-Cy3	β-proteobacteria	GCCTTCCCACTTCGTTT	1
GAM42a-Cy3	γ-proteobacteria	GCCTTCCCACATCGTTT	1
CF319a-Cy3	Cytophaga-flavobacterium cluster of Cytophagales	TGGTCCGTGTCTCAGTAC	2
BONE23a-Cy3	β1-proteobacteria	GAATTCCATCCCCCTCT	3
B1055-Cy3	Bacteria	CACGAGCTGACGACRGCCRT	4
AOL15-FITC	*Agrobacterium albertimagni* strain AOL15	GTGGTTAGCTGCCTCCCTTG	-

(1)Manz et al. 1992; (2)Manz et al. 1996; (3)Amann et al. 1996; (4)Amann et al. 1990.

After incubation, the slides were placed in the wash buffer equilibrated at 37° C and agitated for 10 minutes in the dark. After this first wash step, the slides were washed again in wash buffer for another 10 minutes in the dark. As a final rinse, the slides were briefly rinsed in DI water before air-drying in the dark. Once dry, the slides were counterstained with DAPI by adding 20 µl of 0.1 µg/ml DAPI to each well and incubated for five minutes. The DAPI was also rinsed off with DI water and the sample was allowed to dry completely before being mounted in a fluorescence antibleaching reagent (ProLong Anti-Fade, Molecular Probes) according to the manufacturer's instructions. The sample was sealed with a cover slip followed by a final drying step in the dark before visualization by fluorescence microscopy.

4.3 Results and Discussion

4.3.1 Extraction of Community DNA and PCR Amplification of 16S rDNA

Bead-beating yielded "total community DNA" samples that were adequate for amplification via PCR. Figure 4.1 shows the extracted DNA, separated by electrophoresis on a 1% agarose gel. Amplification of the 16S rDNA genes from these samples was successful for all the different primers used with samples EtOH and PBS. The HC samples were the brownest in color (possibly due to the presence of humic substances which interfere with the PCR reaction) and, perhaps not surprisingly, did not successfully amplify (Wintzingerode et al. 1997). A representative PCR reaction product gel is shown in Figure 4.2. Since amplification with the EtOH and PBS samples was

successful, no attempt was made to optimize amplification conditions for the HC samples. For the remaining analysis, the EtOH and PBS extracted samples were used exclusively.

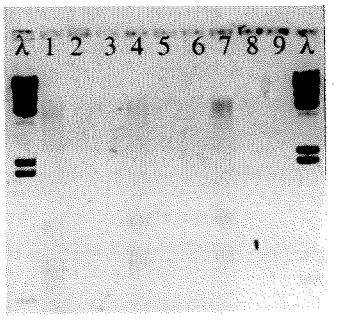

Figure 4.1: Genomic DNA extracted by bead-beating. Outer lanes are λ DNA digested with HinPII to provide a standard ladder. Lane 1 is the DNA from HC sample, lane 4 is the DNA from the EtOH sample, and lane 7 is the DNA from the PBS sample. The other lanes are diluted DNA samples that were not successfully visualized.

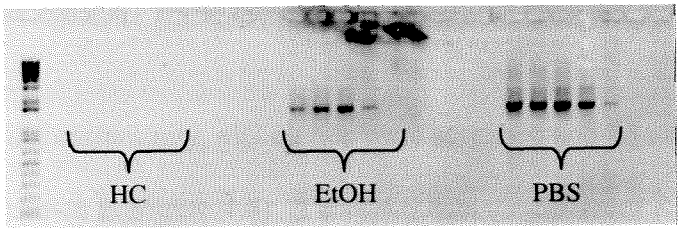

Figure 4.2: PCR product using universal bacterial primers. Similar results were obtained with Archaea, Eukarya, Alpha and AOL15 primers. The PCR cycle here was set for a gradient and thus the successful amplification in the first four reaction tubes corresponds to temperatures of 53.5°, 55.3°, 57.7°, and 60.5° C respectively for both EtOH and PBS. The HC samples did not amplify.

4.3.2 RFLP Analysis

PCR will amplify from and yield a heterogeneous mixture of 16S rDNA genes. This mixture can then be resolved or separated by cloning. The individual clones can then be screened via restriction enzyme digestions in order to identify and investigate the

diversity of "amplicons" (PCR generated amplified end products). A schematic of the overall RFLP analysis is presented in Figure 4.3.

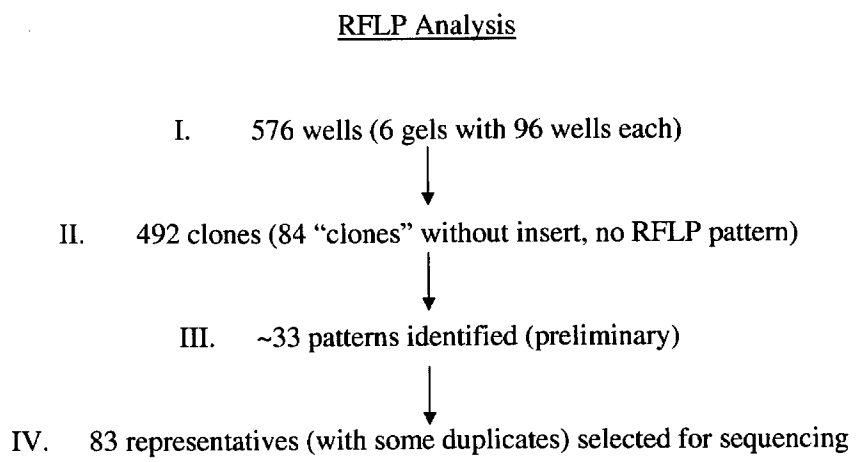

Figure 4.3: RFLP analysis flow chart. Eighty four "clones" (Line II) did not have an insert (i.e., the cloning step was unsuccessful). These lanes on the gels do not have any patterns to analyze.

For the analysis of the community, 492 clones were screened and 83 clones were selected for sequencing (as shown in Figure 4.4). Table 4.6 lists the different RFLP gel images generated during this analysis. Appendix F contains all of these RFLP gel images except for one representative gel presented here in Figure 4.4 for discussion purposes. Although Eukarya, Archaea, α-Proteobacteria, and AOL15 specific primers were also used in this analysis, the generated clone libraries were not analyzed in depth or sequenced.

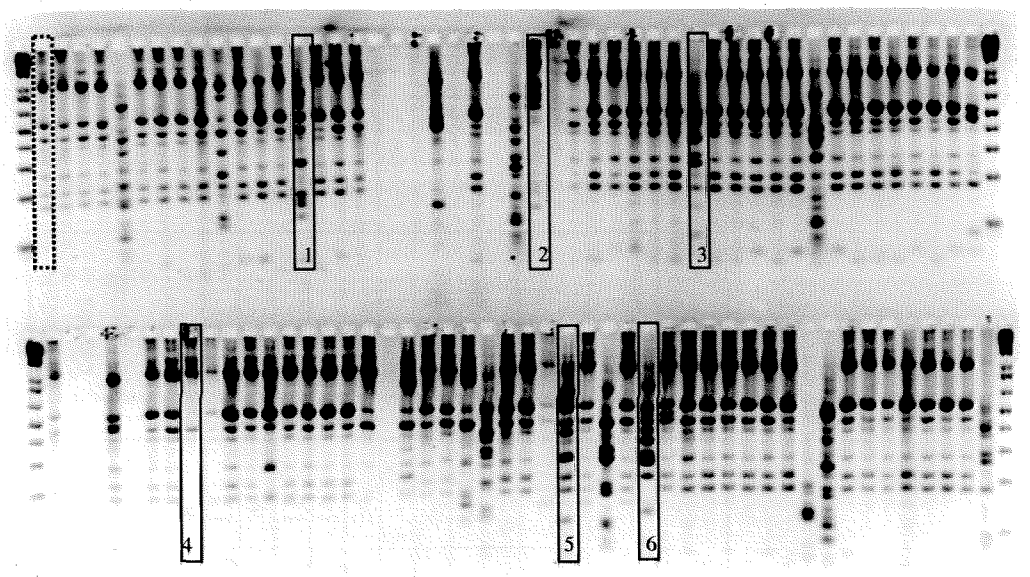

Figure 4.4: (from 070900). EtOH sample PCR product using bacterial primers 8F and 1492R digested with HinPII and MspI. The clones represented by the RFLP patterns that were selected for sequencing are outlined by a black box. Hatched line box for dominant pattern (*O. sinensis*).

The RFLP analysis, as shown in the representative gel of Figure 4.4, revealed a single dominant pattern (shown outlined by a hatched box in Figure 4.4). Several clones with this pattern were sequenced (see section 4.3.3). The analysis revealed that this dominant clone was most similar to a Eukaryotic, phototrophic diatom, the stramenopile *Odontella sinensis*. Stramenopiles are protists (Eukarya) composed of both photosynthetic and nonphotosynthetic members (Dawson 2000). On average, 75% of the clones carried the *O. sinensis* 16S rDNA insert.

Table 4.6: List of RFLP gel images with descriptions (percent of the patterns on a given gel that represent the stramenopile *O.sinensis*; the total number of clones that were sequenced from a given gel and the number of successfully sequenced clones).

Gel Name	Primer	Figure	# of clones	# as *O. sinensis pattern or sequence*	% as *O. sinensis*	# of nonsense inserts	# of total clones sequenced	# of completely sequenced clones
070900-EtOH	8F, 1492R	4.3	85	72	85	8	6	3
070900-PBS	8F, 1492R	F.1	86	63	74	17	22	9
071600-EtOH	8F, 1492R	F.2	70	60	86	4	7	6
071600-PBS	8F, 1492R	F.3	83	61	73	11	15	7
071700-PBS	8F, 1492R	F.4	83	64	77	14	10	2
071700-PBS w/o Betaine	8F, 1492R	F.5	85	48	56	24	23	5
072700-EtOH/PBS	ALF, 1492R	F.6	92	-	-	-	-	-
072700-EtOH/PBS	8F, AOL15R	F.7	57	-	-	-	-	-
071500-EthOH	515F, 1195R	F.8	95	-	-	-	-	-
071500-PBS	515F, 1195R	F.9	82	-	-	-	-	-
071500-EthOH	4F, 1492R	F.10	70	-	-	-	-	-
071500-PBS	4F, 1492R	F.11	86	-	-	-	-	-

This dominance of an *O. sinensis*-like organism suggests one of two conclusions. *O. sinensis*-like organisms may actually be the most abundant organisms in this community and thus be accurately represented in the RFLP analysis. Alternatively, the experimental conditions may bias the extraction, amplification and cloning of the 16S rDNA genes of this rather than other templates. The possibility of such bias has been reviewed in the literature; such biases could be identified if the effects of modifying conditions for DNA extraction, amplification and cloning conditions were thoroughly evaluated (Wintzingerode et al. 1997). Some differences were observed in the proportion of *O. sinensis* clones resulting in the EtOH (82-86% *O. sinensis*) and PBS (56-76% *O. sinensis*) gels. However, since the reproducibility of these results was not rigorously assessed and since the highest values (82% *O. sinensis* by EtOH and 76% by PBS) are not very different, it is not possible to evaluate bias based on these results. Further attempts to evaluate bias were not made since the goal of this study was to obtain a rough estimate of the genetic diversity in this community and to determine whether AOL15-like organisms were represented in the inventory.

4.3.3 Sequences of Clones from Unique RFLP Groups

Further analyses of community diversity were made based on the sequences obtained for representatives of the 83 unique RFLP groups. Figure 4.5 is a schematic of the overall sequence analysis of these RFLP groups.

Sequence Analysis

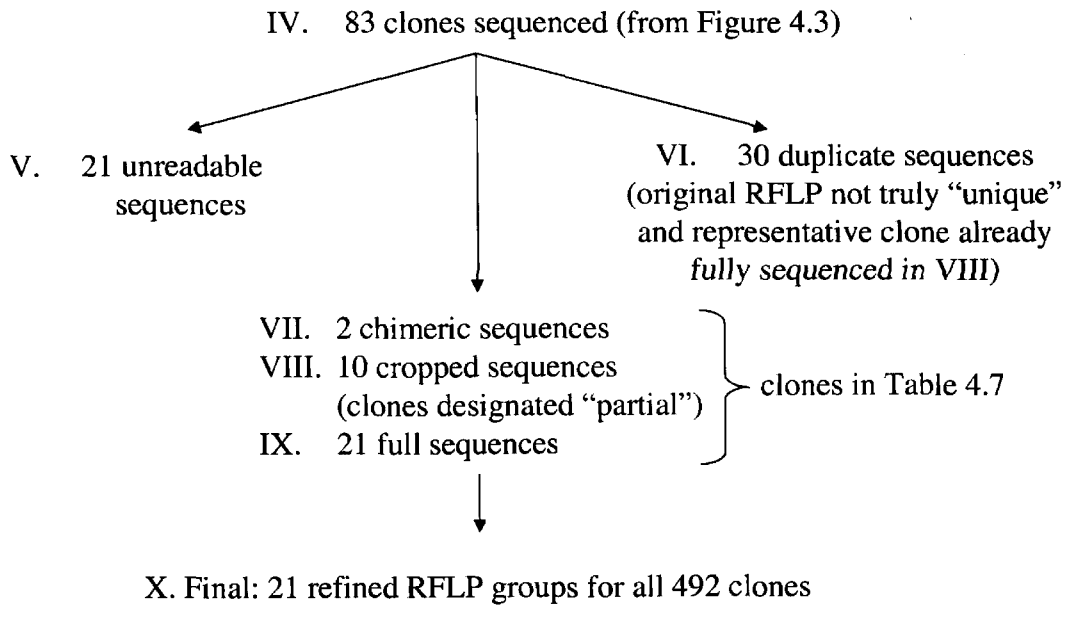

Figure 4.5: Flow chart for sequence analysis of 83 selected clones. The numbers in VII, VIII and IX add up to 84 because Clone #25 was separated into two parts Clone #25a and Clone #25b.

The clones selected for sequencing are indicated by the numbered boxes in the gel images (e.g., clones #1-6 in Fig. 4.4). An example of the phylogenetic tree generated for these clones is shown in Figure 4.6, which illustrates the similarity between clones #8 and 42 (partial) and the stramenopile *O. sinensis* (as discussed in section 4.3.2).

In total, 83 clones were sequenced from these gels but only 32 of these samples yielded clean sequences. Since two partial sequences resulted from Clone #25, 32 clean sequences were obtained for only 31 clones.The samples that were successfully sequenced are listed in Table 4.7. Phylogenetic trees for all the clones in Table 4.7 are presented in Appendix G.

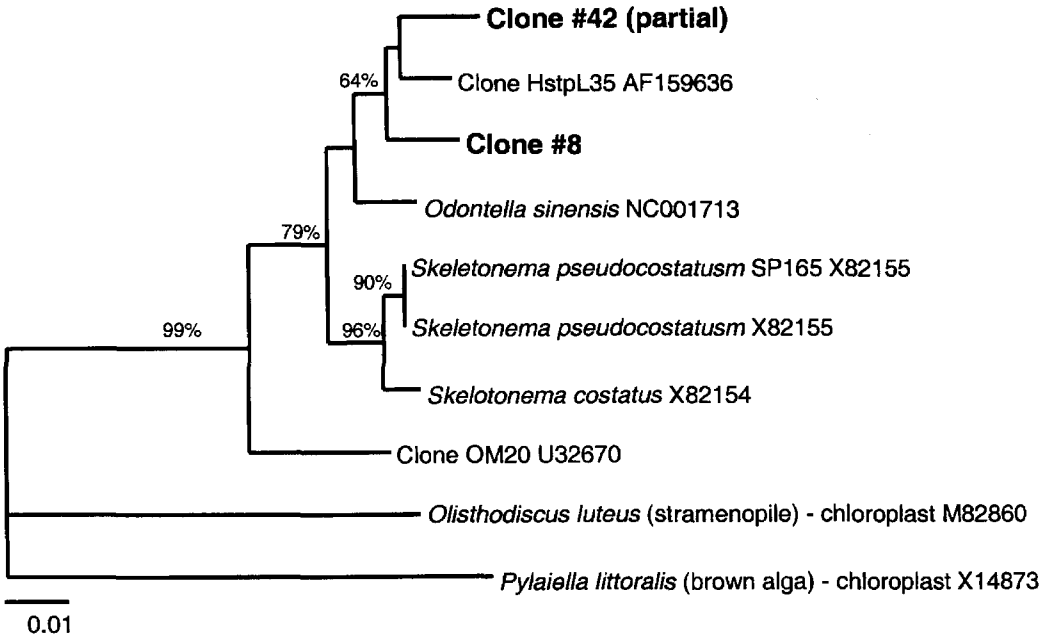

Figure 4.6: Phylogenetic tree for Clones #8 and 42 (partial) by maximum likelihood algorithm in ARB program. The topology of this tree was also supported by a parsimony and distance based tree. Numbers at branch points are bootstrap values that support the tree topology by parsimony. Only bootstrap values greater than 64% are reported in the tree. The accession numbers for the species are shown in the figure.

One complication that arose in the analysis was the probable presence of chimeric sequences, revealed by the CHIMERA_CHECK program (Maidak et al. 2000). In chimeric sequences, contiguous portions of the cloned amplicon are derived from distant organisms and thus not truly reflective of a "real" genetic group. Chimeric sequences were cropped and truncated in order to retain as much sequence information as possible. These clones are designated as "partial," since several bases of the foreign sequence were removed resulting in shorter final sequences. From the chimera analysis, two clones, Clone #12 and Clone #80 were eliminated from the remainder of the analysis because they were chimeric and clean (i.e., distinct) sequences could not be obtained by cropping.

Table 4.7: Complete list of successfully sequenced clones.

Clone	Sequence Length	Closest Identity	% Similar	Group
Clone #1	1389	*Nicotiana tabacum (chloroplast)*	98.8	Chloroplast
Clone #2	1414	*Cytophaga hutchinsonii*	81.2	CFB*
Clone #3	1434	*Polaromonas vaculota*	96.8	β–Proteobacteria
Clone #7 (partial)	1020	*Aeromonas sobria*	99.5	γ–Proteobacteria
Clone #8	1432	*Odontella sinensis (chloroplast)*	97.3	Stramenopile
Clone #10	1350	*Hydrogenophaga flava*	89.3	β–Proteobacteria
Clone #11	1353	*Roseateles depolymerans*	95.7	β–Proteobacteria
Clone #12	Chimera	-	-	-
Clone #20	1472	*Bdellovibrio bacteriovorus*	92	δ–Proteobacteria
Clone #23	1367	*Idonella dechloratans*	97	β–Proteobacteria
Clone #25a (partial)	400	*Sphingomonas rosa*	97.4	α–Proteobacteria
Clone #25b (partial)	705	*Rhodobacter blasticus*	98.4	α–Proteobacteria
Clone #27 (partial)	1050	*Anaeroflexus maritimus*	87	CFB
Clone #29	1414	*Idonella dechloratans*	97.4	β–Proteobacteria
Clone #30	1380	*Rhodobacter apigmentum*	97.6	α–Proteobacteria
Clone #31	1467	*Clostridium punecium*	99.2	Clostridium
Clone #32	1496	*Aqualspirillum delicantum*	93.7	β–Proteobacteria
Clone #33	1386	*Uncultured soil bacterium*	85.5	-
Clone #35	1462	*Gemmata obscuriglobus*	86.5	Planctomycetaceae
Clone #37 (partial)	1000	*Aeromonas sobria*	99.5	γ–Proteobacteria
Clone #38	1460	*Idonella dechloratans*	97.2	β–Proteobacteria
Clone #39	1389	*Aqualspirillum delicantum*	90	β–Proteobacteria
Clone #42 (partial)	900	*Odontella sinensis (chloroplast)*	97.2	Eukarya
Clone #44 (partial)	291	*Hydrogenophaga flava*	99.3	β–Proteobacteria
Clone #48 (partial)	950	*Variovorax paradoxus*	96.1	β–Proteobacteria
Clone #49 (partial)	1165	*Haliscomenobacter hydrossis*	99.6	CFB
Clone #58	1486	*Aeromonas salmonicida*	99.7	γ–Proteobacteria
Clone #60	1309	*Aeromonas veronii*	98.8	γ–Proteobacteria
Clone #61	1292	*Planktothrix rubescens*	90.7	Cyanobacteria
Clone #64 (partial)	1260	*Aquaspirillum sinuosum*	86.2	β–Proteobacteria
Clone #66	1266	*Pseudomonas fluorescens*	92.7	γ–Proteobacteria
Clone #80	Chimera	-	-	-
Clone #83	1448	*Cytophaga aurantiaca*	84.5	CFB

*Cytophaga/Flexibacter/Bacteriodes group.

4.3.4 Overall Community Inventory (Sequence and RFLP Analysis Summary)

Table 4.8 summarizes the combined RFLP and sequence results. In this table, 21 final RFLP groups are defined based on the refinement of the 33 preliminary patterns using the sequence data.

By combining the RFLP and sequence results, the diversity represented in this inventory can be assessed. On this basis, *O. sinensis* is identified as the dominant organism representing 368 (or 75%) of the 492 clones. The genus *Aeromonas* (γ-proteobacteria) accounted for the next highest number of clones (15 of the 492). It was, however, very difficult to compare RFLP patterns among the gels. Thus, the final RFLP groups designated in Table 4.8 may include clones with differing RFLP patterns. These differences in RFLP patterns were ignored when two or more clones were identified as belonging to the same phylogenetic group based on the sequence results. A more concise survey of the overall community by both RFLP and sequence analysis can be obtained by further consolidation of the clones listed in Tables 4.7 and 4.8 (i.e., combining all β-proteobacteria, γ-proteobacteria, etc.) as illustrated in Figure 4.7.

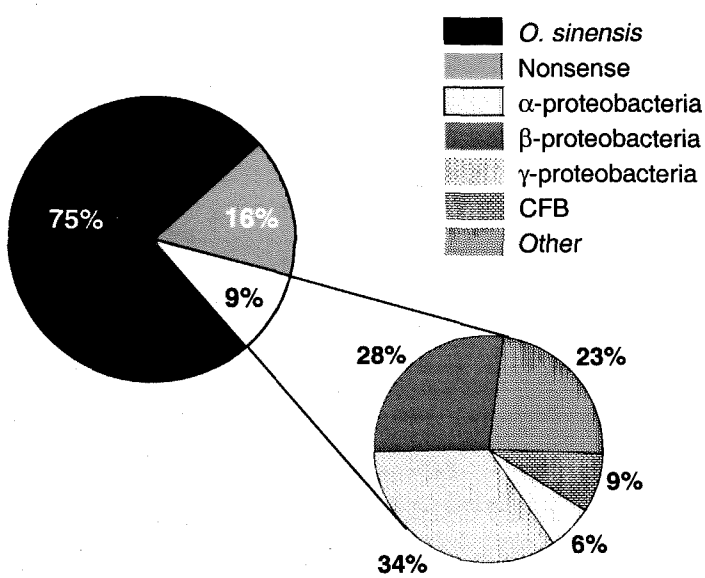

Figure 4.7: Pie chart showing the representation of different bacterial groups in this survey. The other category contains 1 cyanobacterium clone, 1 δ-proteobacterium clone, 1 clostridium, 1 chloroplast and 2 unknown/novel clones.

Table 4.8: Summary of community inventory based on RFLP and sequence analysis.

Final RFLP group	**# of clones**	**Representative clones sequenced**		
		Clone #	Gel	Group
A	354	8 42(partial)	070900-PBS 071600-PBS	Eukarya
B	15	7(partial) 37(partial) 58 60	070900-PBS 071600-PBS 071700-PBS 071700-PBS	Aeromonas (γ–proteobacteria)
C	4	2 27(partial) 49(partial) 83	070900-EtOH 070900-PBS 071600-PBS 011700-PBS w/o Betaine	CFB[a] cytophaga/flexibacter/bacteriodes
D	3	32 39 64(partial)	071600-EtOH 071600-PBS 071700-PBS w/o Betaine	Aquaspirillum (β–proteobacteria)
E	3	23 29 38	070900-PBS 071600-EtOH 071600-PBS	Idonella (β–proteobacteria)
F	3	3	070900-EtOH	Polaromonas (β–proteobacteria)
G	2	10 44(partial)	070900-PBS 071600-PBS	Hydrogenophaga (β–proteobacteria)
H	2	25b(partial) 30	070900-PBS 071600-EtOH	Rhodobacter (α–proteobacteria)
I	1	25a(partial)	070900-PBS	Sphingomonas (α–proteobacteria)
J	1	11	070900-PBS	Roseateles (β–proteobacteria)
K	1	48(partial)	071600-PBS	Variovorax (β–proteobacteria)
L	1	66	071700-PBS w/o Betaine	Pseudomonas (γ–proteobacteria)
M	1	20	070900-PBS	Bdellovibrio (δ–proteobacteria)
N	1	31	071600-EtOH	Clostridium
O	1	1	070900-EtOH	Chloroplast
P	1	61	071700-PBS w/o Betaine	Cyanobacterium
Q	1	33	071600-EtOH	Novel (unknown)
R	1	35	071600-EtOH	Novel (unknown)
S	3	-		Unsequenced[b]
T	2	-		Unsequenced[b]
U	78	12 80	070900-PBS 071700-PBS w/o Betaine	Nonsense inserts[c]

[a]These clones were all members of the CFB group (a very diverse group) and the RFLP patterns appeared "unique" for each of these clones; however, they are classified together here in this analysis.

[b]These clones had unique sequences each but where never fully sequenced.

[c] These nonsense inserts included chimeric sequences, smeared RFLP patterns or clones that could not be successfully identified due to unclean sequence reads.

Sixteen percent of the clones had nonsense inserts (chimeric or unreadable sequences, or unresolved, smeared RFLP patterns). Nine percent of the clones represented the α, β and γ-proteobacteria, the cytophaga/flexibacter/bacteriodes (CFB) group and other species (δ-proteobacteria, cyanobacteria, clostridium, chloroplast and unknown/novel bacteria). After the stramenopile, the groups with the highest representation were the β- and γ- proteobacteria, which each accounted for almost 3% of the clones in this survey.

4.3.5 Attempts at Molecular Identification of AOL15 in the Biofilm Community

In the entire community analysis, the sequence for AOL15-like organisms was not retrieved. Thus further attempts were made to determine whether AOL15-like organisms could be identified by molecular techniques. The 16S rDNA genes from pure cultures of AOL15 were cloned to determine its RFLP pattern. The 16S rDNA genes from the extracted community DNA (both EtOH and PBS samples) were amplified using the ALF (α-proteobacteria) and AOL15 primers to try to isolate the AOL15 genes from among the community DNA. These products were cloned and analyzed by RFLP (shown in Appendix F).

From analysis using the ALF primer, the pattern for *O. sinensis*-like organisms was not evident, which was expected since this organism is not an α-proteobacterium and should not be amplified by these primers. One of the patterns did match the previously determined pattern from AOL15 (determined from DNA extracted and amplified from the pure culture). However, analysis of one clone with this RFLP pattern produced a

sequence for *Sphingomonas adhaesive*, which is not an exact match for AOL15 though both are α-proteobacteria.

This result indicates that the RFLP patterns do not resolve all subgenera differences, and that the design of the AOL15 primer was not sufficiently stringent. Nevertheless, the primer probably amplified the 16S from a small subset of α-proteobacteria, and even so, the sequences of AOL15-like organisms were not retrieved. Since the signature of AOL15 was not detected using either general bacterial primers or more specific primers, it is unlikely that AOL15 is a dominant member of this community.

4.3.6 Hybridizations

The attempt to visualize communities of phylogenetically diverse organisms on the surface of macrophytes in Hot Creek was not very successful. All the probes listed in Table 4.2 were used in this analysis. At first, the probes were tried with pure cultures of isolates growing under laboratory conditions. Figure 4.8 shows a typical result, in this case of AOL15 stained with DAPI and hybridized with ALF-1b-Cy3 probe.

The similar appearance of the two panels in Figure 4.8 (one DAPI stained and one hybridized with ALF-1b-Cy3 probe) demonstrates that the probe successfully hybridized with its target. Additionally, negative controls confirmed that no hybridization took place when ALF-1b-Cy3 probes were used with γ-proteobacteria targets and vice versa (data not shown). However, the AOL15 probes were not specific to AOL15 since the probe did hybridize with non-AOL15 α-proteobacteria targets.

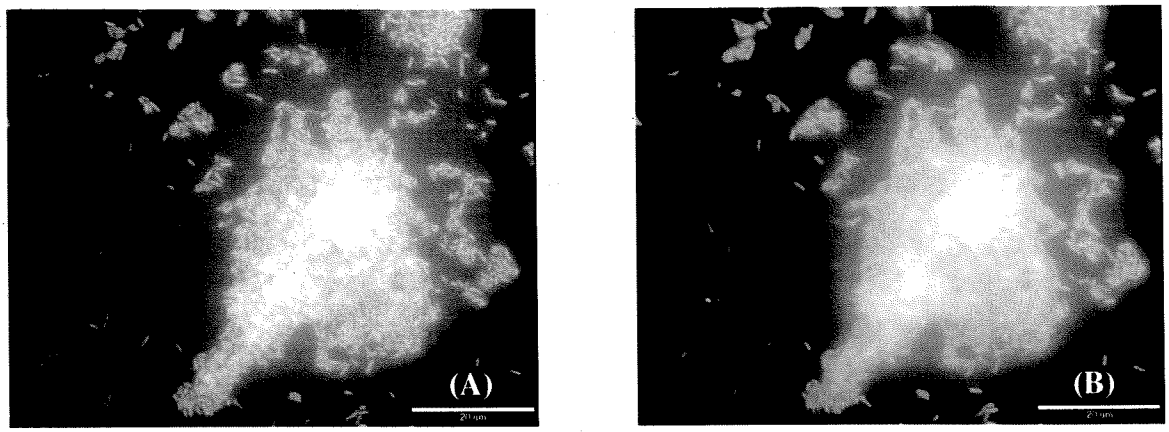

Figure 4.8: Image (A) AOL15 stained with DAPI and image (B) AOL15 hybridized with ALF-1b-Cy3 probe. Bar represents 20 μm.

Although the results with the pure cultures were successful, the visualization of probe-hybridized cells from the natural environment was much more challenging. Much of the difficulty was the result of intense autofluorescence associated with the samples, which obscured any signal from the probe. Long, filamentous cyanobacteria greatly interfered with imaging of the hybridized samples due to this autofluorescence. This problem is illustrated by the series of images of a sample from Hot Creek shown in Figure 4.9.

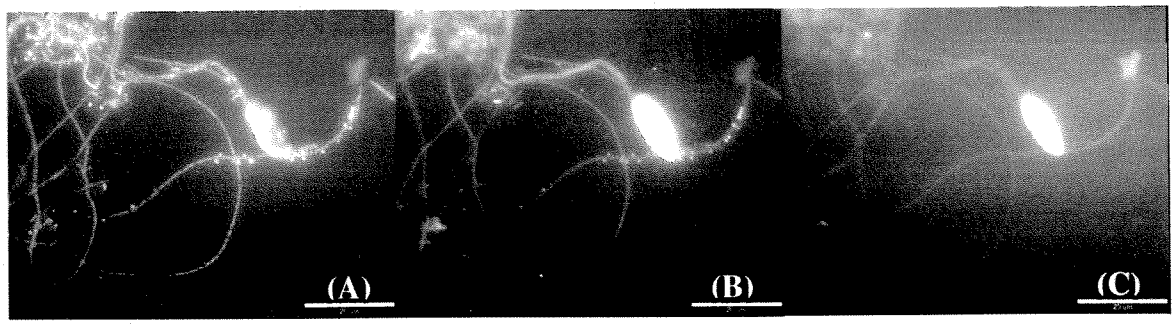

Figure 4.9: Image of 4% Para sample (A) stained with DAPI; (B) hybridized with BONE23a-Cy3 probe; (C) autofluorescence. Bar represents 20 μm.

The β-proteobacteria attached to the filaments are visible both with the DAPI stain (panel A) and hybridized with BONE23a-Cy3, β-proteobacteria probe (panel B). The last panel (panel C), although of poorer quality, reveals the background autofluorescence that was encountered.

Figure 4.10 reveals a more typical result where many of the cells do not fluoresce after probe hybridization. This was observed with all the probes that were used (with the exception of the BONE23a-Cy3 probe in Figure 4.9). Thus phylogenetic groups other than the β-proteobacteria could not be visualized and a comprehensive microscopic analysis of the community was not possible.

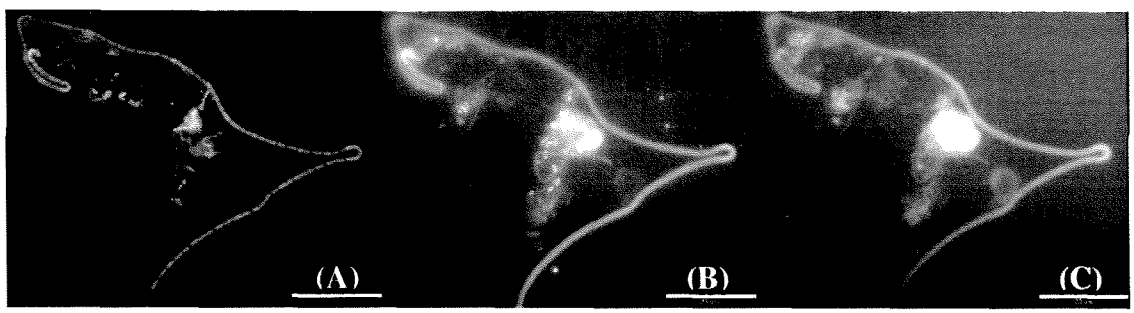

Figure 4.10: Image of 4% Para sample (A) stained with DAPI; (B) hybridized with BET42a-Cy3 probe; (C) autofluorescence. Bar represents 20 μm.

4.3.7 Implications for Hot Creek

The sequences of AOL15-like organisms were not among those retrieved in this generated clone library. Thus there is no molecular evidence to suggest that AOL15-like organisms are dominant members of the natural community attached to *Potamogeton pectinatus*. The molecular analysis did reveal the apparent dominant abundance of *O. sinensis*-like organisms. However, the functional role of Eukaryotic phototrophs (and

their influence on the in situ rates of arsenite oxidation) was not among the questions investigated.

Two independent molecular techniques suggest that β-proteobacteria are numerically significant bacteria in the community. This group accounted for 2.6% of the sequence inventory based on both RFLP patterns and sequence analysis and was visualized by FISH using β-proteobacteria probes. Taken together, these results suggest that other arsenite oxidizers, rather than AOL15, might play more significant roles in the *in situ* oxidation of arsenite reported by Wilkie and Hering (1998).

Finally, the inventory also retrieved several "novel" sequences. Two of these sequences (Clone #33 and #35) are deeply divergent, perhaps at the level of novel phyla. These sequences deserve further study and suggest that Hot Creek, because of its thermal and redox gradients, would be a valuable site for the study of novel organisms.

Chapter Five

ISOLATION AND CHARACTERIZATION OF THREE NOVEL ARSENITE OXIDIZING BACTERIA FROM HOT CREEK

5.1 Introduction and Motivation

Enrichment and isolation conditions can strongly influence the resulting cultures that are established in the laboratory. Enrichment techniques in general do not permit all bacteria an equal opportunity for growth. Many variables including the concentration and form of media components, incubation conditions and individual growth rates of the bacteria affect the time course of an enrichment culture. The isolation of AOL15 was achieved after the establishment of an enrichment culture. However, the characterization of the bacterial biofilm by molecular techniques and the resulting absence of AOL15's signature in the sequences of the clone library suggested that there might be other, more numerous arsenite oxidizers present at Hot Creek. Thus the isolation conditions described in Chapter 3 were restructured to try to maximize for the selection of oxidizers that might be predominant in the ambient environment.

The media for the new isolations were designed so that they mimicked ambient conditions more closely than that used to isolate AOL15. Particular care was taken to include a wide suite of trace components (i.e., metals and vitamins) to allow for the

growth of diverse bacteria. The comparison of results obtained with several media suggest that a heterotrophic medium prepared with yeast extract (the YE medium) was "well designed," that is, the composition of this medium allowed the isolation of dominant microorganisms in the microbial community. Using this "well-designed" medium, three new arsenite oxidizers were isolated.

5.2 Experimental Methods

5.2.1 Sample Collection and Inoculum Preparation

In October of 2000, fresh samples of *Potamogeton pectinatus* were collected in sterile polypropylene bottles, transported to the laboratory on ice, and processed immediately. The plant samples were placed into a sterile, 250 ml polypropylene bottle and filled with sterilized Hot Creek water. The bottle was vigorously mixed with a vortex mixer for five minutes and the resulting suspension was used as the undiluted inoculum (sample name: undiluted HC) for subsequent experiments. This undiluted HC sample was used to prepare a tenfold dilution series of the original sample into sterilized creek water (sample names: 1:10 HC to $1:10^9$ HC). One hundred µl of each of these samples (undiluted HC to $1:10^9$ HC) was used to inoculate both liquid and solid media (described below) for the isolation of arsenite oxidizers.

5.2.2 Media

The isolation approach for the arsenite oxidizers reported here placed more emphasis on isolation from solid media rather than the establishment of an enrichment culture. Six different media were used for these isolations from agarose plates. For each type of medium, a liquid enrichment was also established, mainly for the purpose of monitoring the arsenite oxidizing activity in the dilution series. The six media that were selected were (1) citrate medium, as described in Chapter 3, (2) mannitol medium, as described in Chapter 3, (3) an autotrophic medium (here called AUTO), (4) a heterotrophic medium with acetate as the carbon source (here called ACETATE), (5) a heterotrophic medium with yeast extract (here called YE), and (6) a medium designed to mimic ambient conditions as closely as possible (here called HOT). The arsenite concentration was 100 μM for all the media. The pH for the citrate and mannitol media was adjusted to 7 to mimic conditions used for the enrichment and isolation of AOL15, all other media were adjusted to pH 8. The composition of these media is summarized in Table 5.1.

The solid media was prepared with 1% agarose. The preparations of these media were based on recipes of Dr. Jared Leadbetter designed for the Woods Hole Microbial Diversity course. Although at the onset of this study all these different media were used, gradually over the course of the isolation procedure the YE medium emerged as the most successful for the isolation of arsenite oxidizers. This analysis is primarily the report of the bacteria isolated from the YE medium plates. The more detailed reasons for this narrowing of the analysis are described in the Results and Discussion section.

Table 5.1: Media Composition. All media and components mentioned below were sterilized by filtration.

Medium or Medium Component	**Composition**
Vitamin Supplement A (12-Vitamin)	10 mM phosphate buffer adjusted to pH 7.2 and containing: riboflavin (10 mg/100 ml), thiamine•HCl (100 mg/100 ml), L-ascorbic acid (100 mg/100 ml), D-Ca-pantothenate (100 mg/100 ml), folic acid (100 mg/100 ml), niacinamide (100 mg/100 ml), nicotinic acid (100 mg/100 ml), 4-aminobenzoic acid/PABA (100 mg/100 ml), pyridoxine•HCl (100 mg/100 ml), lipoic acid (100 mg/100 ml), NAD (100 mg/100 ml), thiamine pyrophosphate (100 mg/100 ml)
Vitamin Supplement B (Vitamin B_{12})	cyanocobalamin (100 mg/ml)
Trace Metal Supplement	EDTA (5200 mg/L) $FeSO_4•7H_2O$ (2100 mg/L) H_3BO_3 (30 mg/L) $MnCl_2•4H_2O$ (100 mg/L) $CoCl_2•6H_2O$ (190 mg/L) $NiCl_2•6H_2O$ (24 mg/L) $CuCl_2•2H_2O$ (2 mg/L) $ZnSO_4•7H_2O$ (144 mg/L) $Na_2MoO_4•2H_2O$ (36 mg/L) $NaVO_3$ (25 mg/L) $Na_2SeO_3•5H_2O$ (6 mg/L) $Na_2WO_4•2H_2O$ (8 mg/L) pH adjusted to 6.0
AUTO	NaCl (1.0 g/L) $MgSO_4•6H_2O$ (0.4 g/L) $CaCl_2•2H_2O$ (0.1 g/L) KH_2PO_4 (0.2 g/L) KCl (0.5 g/L) HEPES (1.19 g/L) Vitamin Supplement A (1ml/L) Vitamin Supplement B (1ml/L) Trace Metal Supplement (1ml/L) 2 mM bicarbonate
ACETATE	Same as AUTO without 2 mM bicarbonate sodium acetate (82 g/L)
YE	Same as AUTO without 2 mM bicarbonate yeast extract (1g/L)
Plant Extract Supplement	*Potamogeton pectinatus* (90 g wet weight) heated in 800 ml of DI water and filtered
HOT	Creek water (900 ml/L) Plant Extract Supplement (100 ml/L)

5.2.3 Analyses

For growth studies with the new isolates where arsenite oxidation was measured, the anion exchange method outlined in Chapter 3 was used for the separation of arsenite and arsenate. Arsenic concentrations were determined by inductively coupled plasma mass spectrometry (ICP-MS) on a Perkin- Elmer ELAN 4000.

The qualitative $KMnO_4$ screening technique developed and described for the isolation of AOL15 in Chapter 3 was used extensively in the isolations described here. Six µl of 0.002 M $KMnO_4$ were added to 200 µl of the culture medium containing 100 µM total arsenic. A pale pink color for the resulting mixture indicated that arsenate (which does not react with permanganate) was present and thus was a positive result for arsenite oxidation. A clear colored solution indicated that arsenite (which reacts with permanganate) was present and thus was a negative result for oxidation.

Sulfide concentrations were determined using the methylene blue method (Franson 1981).

5.2.4 Isolations

Arsenite oxidizers were isolated from solid media. For each of the described media, 100 µl of the dilution series solutions (undiluted HC sample to $1:10^9$ HC sample) were inoculated onto both agarose plates and into tubes with 5 ml of liquid media. For each of the dilution plates, colonies that formed were transferred into 1.5 ml of liquid culture. To allow for larger throughput, 96 well deep tissue culture plates were used to grow the

isolates in liquid culture. After growth was established, 200 µl of the cultures in the 96 well plates were sampled and checked for oxidation by the permanganate assay. The bacteria in the wells that were positive for arsenite oxidation were then streaked onto plates (composed of the same medium as the liquid from which they were transferred). The isolates were transferred from solid medium to solid medium several times to achieve a pure culture. Isolates purified in this way were repeatedly checked for arsenite oxidation by transferring back into liquid medium and using the permanganate assay. Stock cultures of all the isolates were prepared in 20% glycerol and frozen at –80° C.

5.2.5 DNA extraction, Cloning, RFLP and Sequencing

Once the new arsenite oxidizers were isolated, molecular techniques were used in conjunction with colony morphology and distinguishable physiological characteristics to identify unique oxidizers. Genomic DNA of the isolates was obtained using the DNeasy™ Tissue Kit (Qiagen, Valencia, CA) following the manufacturer's recommended procedure. The 16S rDNA genes of the isolates were amplified by PCR using universal bacterial primers [S-D-Bact-0008-a-S-20 (5' to 3': AGAGTTTGATCCTGGCTCAG) and S-D-Bact-1492-b-A-16 (5' to 3': TACCTTGTTACGACTT)] (Wheeler et al. 1996; Kane et al. 1993) using protocols established by Ruimy et al. (Ruimy et al. 1994) and described in Chapter 3.

The resulting 1.5 kb PCR product was visualized on a 1% agarose gel and cloned into *E. coli* cells using the TOPO TA Cloning kit from Invitrogen (Carlsbad, California) by the methods detailed in Chapter 4. Plasmids were purified from the *E. coli* cells using

the Plasmid Mini Kit (Qiagen, Valencia, CA) following the manufacturer's recommended procedure. The plasmid was used as template for PCR by primers T3 (5' to 3': TAATACGACTCACTATA), and T7 (5' to 3': ATTAACCCTCACTAAAGGGA) and the reaction products were analyzed by RFLP as described in Chapter 4. The resulting PCR product was then sequenced using primers T3, T7, the bacterial primers 356F (5' to 3':ACTCCTACGGGAGGCAGCA), 805F (5' to 3': ATTAGATACCCTGGTAGTC), 907R (5' to 3':CCGTCAATTCCTTTRAGTTT) and 1200R (5' to 3':GTAGCRCGTGTGTMGCCC) at the DNA Sequencing Core Facility at the Beckman Institute at Caltech using the dideoxy chain termination method with Sequenase DNA sequencing kit (United States Biochemical Corporation, Cleveland, Ohio) and with an ABI 373A automatic sequencer as recommended by the manufacturer (Perkin-Elmer Corp., Foster City, California). Sequences were edited and analyzed by the methods described in Chapter 4.

5.2.6 Characterization of New Isolates

The physiological characteristics of the new isolates were determined by testing their ability to grow on various carbon sources and to respire electron acceptors other than molecular oxygen. The carbon sources that were used were acetate (0.012 M), mannitol (0.006 M), succinate (0.004 M), citrate (0.003 M), sucrose (0.003 M), D(-)fructose (0.006 M), glycerol (0.011 M), D(-)glucose (0.006 M), D(+)mannose (0.006 M), formate (0.015 M), D(+)galactose (0.006 M), pyruvate (0.01 M), lactate (0.01 M) and propionate (0.005 M). The ability of the new isolates to grow anaerobically was tested in YE medium (at

30° C) with nitrate (5 mM), ferric iron (20 mM), sulfate (5 mM), sulfite (5 mM), thiosulfate (5 mM), arsenate (5 mM), fumarate (20 mM) or DMSO (10 mM) as terminal electron acceptors. Positive results for growth were based on absorbance readings near 0.2 at 630 nm.

For each of the new isolates, the growth and oxidation were determined concurrently. For these experiments the arsenite concentrations were measured by ICP-MS as described in the Analysis section and plate counts were used to determine cell numbers in monitoring growth on YE medium with 100 μM arsenite.

5.2.7 Transmission Electron Microscopy

Standard methods for transmission electron microscopy (TEM) were used for the three new isolates (YED1-18, YED6-4 and YED6-21) grown in YE medium. The cultures were pelleted and fixed in a 2.5% glutaraldehyde solution and stained with saturated uranyl acetate for TEM based on the procedures outlined by Robinson et al. (Robinson et al. 1987). Samples were observed on a Philips EM 201 transmission electron microscope at 80 kV.

5.3 Results and Discussion

5.3.1 Colony Formation and Arsenite Oxidation Activity in Dilution Series

Using the dilution series (undiluted HC to $1:10^9$ HC samples), the various plates and liquid media were inoculated. The liquid cultures that were established contained 10 μM

arsenite initially (in contrast to all other experiments with liquid and solid media where arsenite concentrations were 100 μM). The arsenite oxidation in these liquid cultures was assayed after 10 days incubation at 30° C. Table 5.2 summarizes the results from these liquid enrichments as a qualitative determination of the extent of arsenite oxidation.

Table 5.2: Arsenite oxidation in liquid enrichment cultures of various media in duplicate*.

Dilution	Mannitol I	Mannitol II	AUTO I	AUTO II	ACETATE I	ACETATE II	YE I	YE II	HOT I	HOT II
None	+	+	+	+	+	+	+	+	+	+
1:10	+	+	+	+	+	+	+	+	+	+
$1:10^2$	+	+	+	+	+	+	+	+	+	+
$1:10^3$	+	+	+	+	+	+	+	+	+	+
$1:10^4$	+	+	+	+	+	+	+	+	+	+
$1:10^5$	+	+	+	+	-	-	+	+	+	+
$1:10^6$	-	-	+	-	-	-	-	-	+	+
$1:10^7$	-	-	-	-	-	-	-	-	-	-
$1:10^8$	-	-	-	-	-	-	-	-	-	-
$1:10^9$	-	-	-	-	-	-	-	-	-	-

* Citrate medium not reported since chemical oxidation of arsenite was observed in every dilution and in the negative controls.

The arsenite concentration in these "enrichments" was one order of magnitude lower in concentration than in the solid media. Ten days were allowed for the oxidation reaction to go to completion before determining arsenic redox speciation. It was hypothesized that even small numbers of arsenite oxidizers in the original inocula could deplete the amount of arsenite present in these batches within 10 days. Thus, by this reasoning, Table 5.2 reflects the natural abundance of oxidizers in materials shaken off aquatic macrophytes of Hot Creek. Thus it appears that arsenite oxidizers were present in the $1:10^5$ to $1:10^6$ dilution inocula. This observation is in accord with the results from the solid media.

Colony formation on the agarose plates of the various media was monitored over several days. Table 5.3 summarizes the results of the colony formation on the solid media.

Table 5.3: Colony formation on various media using HC samples (undiluted to $1:10^9$ dilution) as inoculum.

Media	Undiluted	1:10	$1:10^2$	$1:10^3$	$1:10^4$	$1:10^5$	$1:10^6$	$1:10^7$	$1:10^8$	$1:10^9$
CITRATE	120	9	-	-	-	-	-	-	-	-
MANNITOL	many	many	many	269	50	7	-	-	-	-
AUTO	many	many	many	many	30	7	-	-	-	-
ACETATE	many	many	many	many	54	6	-	-	-	-
YE	many	many	many	many	120	87	60	-	-	-
HOT	many	many	many	many	125	14	2	-	-	-

The results in Table 5.3 show that some of the designed media allowed for growth of greater numbers of colonies (i.e., were less selective). The citrate medium, since it yielded the lowest colony counts was not used further for isolations. The HOT medium, although very promising in its design, was difficult to work with because of analytical limitations. The HOT medium was greenish in color, making it very difficult to distinguish the difference between positive and negative results using the permanganate arsenite oxidation assay. For this reason, isolation from this medium was not further pursued.

The AUTO and ACETATE media yielded very small colonies that were difficult to transfer and which often did not grow upon transfer. These media were initially designed with the intention of isolating autotrophic arsenite oxidizers; however, the concentrations of arsenite were very low (100 μM on the plates) compared to the concentrations of 5-10 mM used by Santini (2000) or 13.3-26.7 mM used by Illyaletdinov and Abdrashitova (1982) to isolate autotrophic arsenite oxidizers. This

might explain the very small size of the resulting colonies. The lack of success in transferring these colonies could mean that the colonies that initially formed grew on trace amounts of nutrients that were carried over in the inoculation step. These media were not further pursued because of these limitations. To improve the conditions necessary for the isolation of such organisms, higher initial arsenite concentrations (in the mM range) might prove more successful in future studies at Hot Creek.

After these eliminations, only the Mannitol and YE media remained for further analysis. From the agarose plates of these two media, many colonies were selected, transferred into 96 well deep culture plates of liquid media and analyzed for growth and arsenite oxidation. Table 5.4 summaries the numbers of colonies that were transferred from each dilution plate and the resulting number of arsenite oxidizers among the selected colonies.

Table 5.4: Number of colonies selected for further study and resulting arsenite oxidation assays.

Dilution Plate	Total Number of Colonies	Number of Colonies Transferred into Liquid	Number of Arsenite Oxidizers	Percentage of Transferred Colonies Positive for Arsenite Oxidation
YE-undiluted	many	0	-	-
YE-1:10	many	96	73	76
YE-1:10^2	many	48	26	54
YE-1:10^3	many	192	142	74
YE-1:10^4	120	86	54	63
YE-1:10^5	87	65	53	82
YE-1:10^6	60	60	42	70
Man-undiluted	many	0	-	-
Man-1:10	many	0	-	-
Man-1:10^2	many	0	-	-
Man-1:10^3	many	48	3	6
Man-1:10^4	50	6	0	0
Man-1:10^5	7	4	1 or 0 (?)*	0-25(?)
Man-1:10^6	0	0	-	-

* Arsenite oxidation unclear (sample may be weakly positive).

From the analysis summarized in Table 5.4, the mannitol medium did not appear to be a very good choice for the isolation of arsenite oxidizers, leaving the YE medium isolates for further study.

Overall 390 arsenite oxidizers were isolated from the YE dilution plates. Several isolates from the 1:10 dilution plate were selected for further study because of distinctly different colony color and morphology. Of the remaining isolates, the colonies from dilutions $1:10^2$ through $1:10^5$ were catalogued and frozen with 20% glycerol at –80° C. Only the 42 isolates from the $1:10^6$ dilution plate were studied in depth. The motivation for this was that these isolates appeared to be dominant members of the community (persisting after a $1:10^6$ dilution from the original sample). It was hypothesized that the isolates that could be further purified and identified from this final dilution on the YE plate would potentially be significant oxidizers in the field.

5.3.2 Isolation Summary and Identification of Unique Isolates

The 42 isolates from the $1:10^6$ dilution plate and the selected isolates from the 1:10 dilution plate were transferred several times to assure the purity of the cultures. Some of the samples appeared to be mixed cultures and a few of the isolates did not grow or maintain the arsenite oxidation activity after subsequent transfers. At the end of the analysis, 36 isolates from the $1:10^6$ dilution plate remained. The DNA from these 36 isolates and the selected isolates from the 1:10 dilution was extracted, the 16S rDNA genes were amplified, cloned and analyzed by RFLP. Figure 5.1 shows a representative gel image from this RFLP analysis.

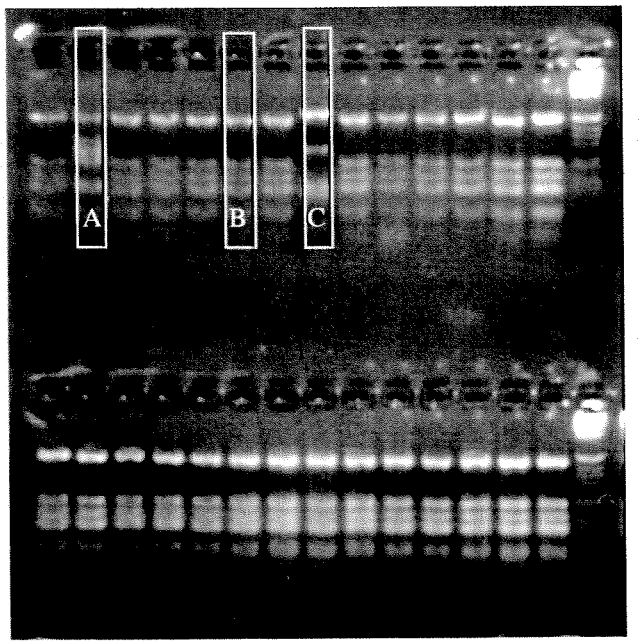

Figure 5.1: RFLP analysis of isolated arsenite oxidizers. Patterns A, B, and C outlined in the figure were the three unique patterns that were obtained.

The RFLP analysis resulted in three main patterns (A, B, and C) shown in Figure 5.1. All three of these patterns were found for isolates from the 1:10 dilution plate. The 36 isolates from the $1:10^6$ plates exhibited only pattern B and thus would be considered identical based on RFLP analysis. In Chapter 4, however, identical RFLP patterns were reported for different species in the case of the *Sphingomonas* clone that was sequenced using AOL15 primers and had a pattern identical to AOL15. To determine whether the isolates were actually unique, the 16S rDNA genes of several of the isolates with RFLP pattern B were sequenced in addition to the isolates represented by pattern A and C. The sequencing reaction for the pattern C isolate failed completely and so this isolate was not pursued further. From the 1:10 dilution plate, the one isolate with pattern A (named isolate YED1-16) was successfully identified as a *Pseudomonas* strain.

The 16S rDNA genes were sequenced for several of the isolates with pattern B. These isolates were all identified as members of the genus *Hydrogenophaga*. Since it would have been difficult to characterize all 36 isolates, two representative strains, YED6-4 and YED6-21, were selected for further study. These two isolates were chosen because there appeared to be two distinct groups of oxidizers within the 36 isolates. One group (from which YED6-21 was selected) had a tendency to aggregate and form flocs of cells in growing culture while the other group (from which YED6-4 was selected) did not. Of the 1:10 dilution purified oxidizers, one isolate, YED1-18 (identified as *Hydrogenophaga* by its partial sequence) was also selected for further study because of its close phylogenetic relation to YED6-4 and YED6-21. YED1-18 formed deep yellow colored colonies and was thus easily distinguished from YED6-4 and YED6-21, which formed cream-colored colonies.

At the conclusion of this analysis, four new isolates, three easily distinguishable *Hydrogenophaga* strains and one *Pseudomonas* were isolated. During the course of the characterization of these isolates, the *Pseudomonas* isolate culture became contaminated. Since this isolate was from the 1:10 dilution plate and its signature was not found in the $1:10^6$ dilution plate, it was concluded that YED1-16 was not a dominant member of the community. For these reasons, the further study and characterization of the isolate was not pursued even though it was phylogenetically distinct from the other oxidizers (this isolate was a *Pseudomonas* strain of the gamma-proteobacteria whereas the other isolates were *Hydrogenophaga* of the β-proteobacteria). .

On the basis of the isolations using the YE medium, it appears that *Hydrogenophaga* strains are significant oxidizers in the community. The actual

dominance of these organisms under ambient conditions depends on how well the YE medium and isolation conditions were designed and how closely they mimicked ambient growth conditions. It can be argued that, of all the media described here, the HOT medium (which was discarded from the analysis due to the problems it posed for the permanganate assay for arsenite oxidation) was the medium that mimicked ambient conditions best. Thus the natural diversity of the environment should be best captured by the HOT medium and the numbers of colonies that formed on HOT medium can be taken as an upper limit on the number of cultivatable bacteria using a well-designed medium. However the summary present in Table 5.3 showed that similar numbers of colonies were obtained with both the HOT and YE media. Although it is possible that these two media selected for different members of the community, the correspondence between the number of colonies on the YE and HOT plates suggests that the YE medium was well designed for this environment and the isolates obtained from the $1{:}10^6$ dilution plates with YE medium are significant arsenite oxidizers under ambient conditions.

5.3.3 Description and Characterization of New Isolates

The isolation procedure described above yielded three new Gram-negative arsenite oxidizing strains, YED6-4, YED6-21, and YED1-18 shown in Figure 5.2.

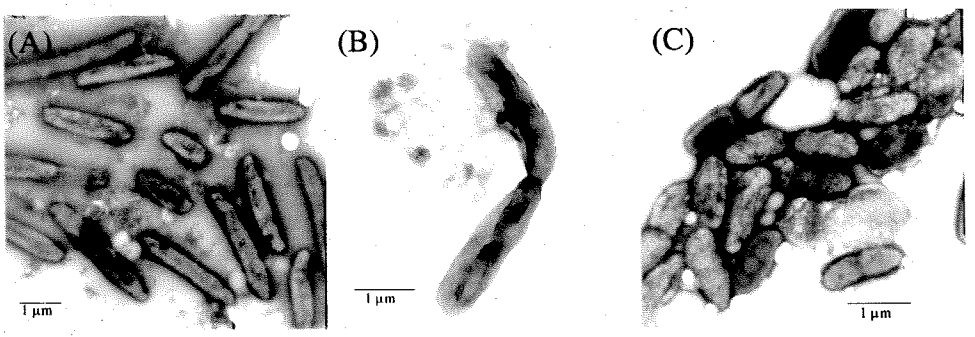

Figure 5.2: Negatively stained transmission electron micrograph of (A) YED6-4, (B) YED6-21 and (C) YED1-18 grown in YE medium without arsenite (stained with uranyl acetate).

Phylogenetic analysis by 16S rDNA (mask: comparing 1408 of the aligned base pairs) showed that YED6-4 (1421 bases), YED6-21(1432 bases), and YED1-18 (1437 bases) were all over 98% similar (based on a maximum likelihood algorithm in the ARB software package) to *Hydrogenophaga pseudoflava* of the β-proteobacteria. Figure 5.3 is a phylogenetic tree for these three new arsenite oxidizers. The similarity matrix for these isolates is presented in Appendix H.

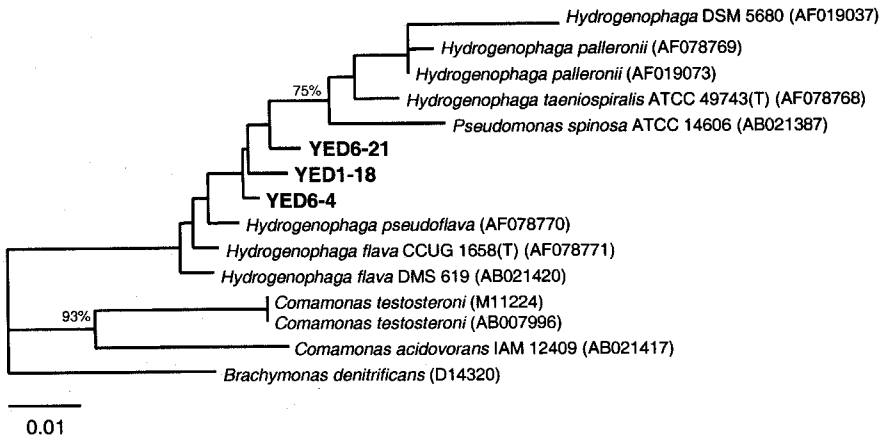

Figure 5.3: Phylogenetic tree for YED6-4, YED6-21, and YED1-18 by maximum likelihood algorithm in ARB program. The topology of this tree was also supported by a parsimony and distance based tree. Numbers at branch points are bootstrap values that support the tree topology by parsimony. Only bootstrap values greater than 70% are reported in the tree. The accession numbers for the species are shown in the figure.

The phenotypic profiles demonstrated that there were some discernible differences among these strains despite the very high phylogenetic similarities among them. Table 5.5 summarizes the ability of these new isolates to grow on various carbon sources and to respire electron acceptors other than molecular oxygen or grow fermentatively.

Table 5.5: Carbon utilization and respiration profiles of new isolates.

Compound	YED6-4	YED6-21	YED1-18
Bicarbonate	-	-	Not determined
Acetate	+	+	+
Mannitol	-	+	+
Succinate	+	+	+
Citrate	+	+	+
Sucrose	-	+	+
D(-)Fructose	+	+	+
Glycerol	+	-	
D(-)Glucose	+	+	+
D(+)Mannose	+	+	+
Formate	-	-	-
Maltose	-	+	+
D(+)Galactose	-	-	+/-
Pyruvate	+	+	+
Lactate	+	+	+
Propionate	-	+/-	-
Nitrate	+	-	-
Sulfate	-	-	-
Sulfite	-	-	-
Thiosulfate	-	-	-
Arsenate	-	-	-
Fumarate	+	-	-
DMSO	-	-	-
Fe Oxide	-	-	-
YE (fermentative)	+	+	+

The results from the respiration experiments were very difficult to interpret. It appeared that all three strains were able to grow fermentatively on YE and thus it was necessary to discriminate between turbidity due to respiratory or fermentative growth. These experiments were repeated several times and only clear positive results are presented in Table 5.5. Many of the results were negative because the turbidity in the vials could not be distinguished from the turbidity (at 630 nm) due to fermentative growth. Additionally, in highly turbid vials initially spiked with DMSO, thiosulfate or sulfate, no chemical transformations of the sulfur-containing electron acceptors to sulfide were detected by the methylene blue assay. This confirms the negative results for respiration of these electron acceptors.

The *Hydrogenophaga* genus is described as a member of the mesophilic (growing optimally at temperatures between 18° and 40° C) hydrogen-oxidizing (knallgas) bacteria, which fix CO_2 for growth using gaseous hydrogen as the electron donor and oxygen as the terminal electron acceptor (Aragno and Schlegel 1999). This ability was not confirmed for the three isolates described here. It was hypothesized that given the ability of the genus to grow autotrophically on hydrogen gas, these new isolates might be good candidates for chemolithoautotrophic growth by arsenite oxidation. However it was shown that arsenite oxidation could not support the growth of YED6-4 and YED6-21 on bicarbonate (YED1-18 was not tested).

The knallgas bacteria have also been described as facultative autotrophs since they are able to grow on organic substrates as has been demonstrated for the new isolates in Table 5.5). Interestingly, knallgas bacteria have been found associated with H_2

producing cyanobacteria (Aragno and Schlegel 1999). Microscopic analysis of the plant samples from Hot Creek reveals cyanobacterial cells present on this surface.

The growth of YED6-4, YED6-21, and YED1-18 and the redox speciation of arsenic were monitored simultaneously and the results are shown in Figure 5.4. The data for these experiments are tabulated in Appendix I.

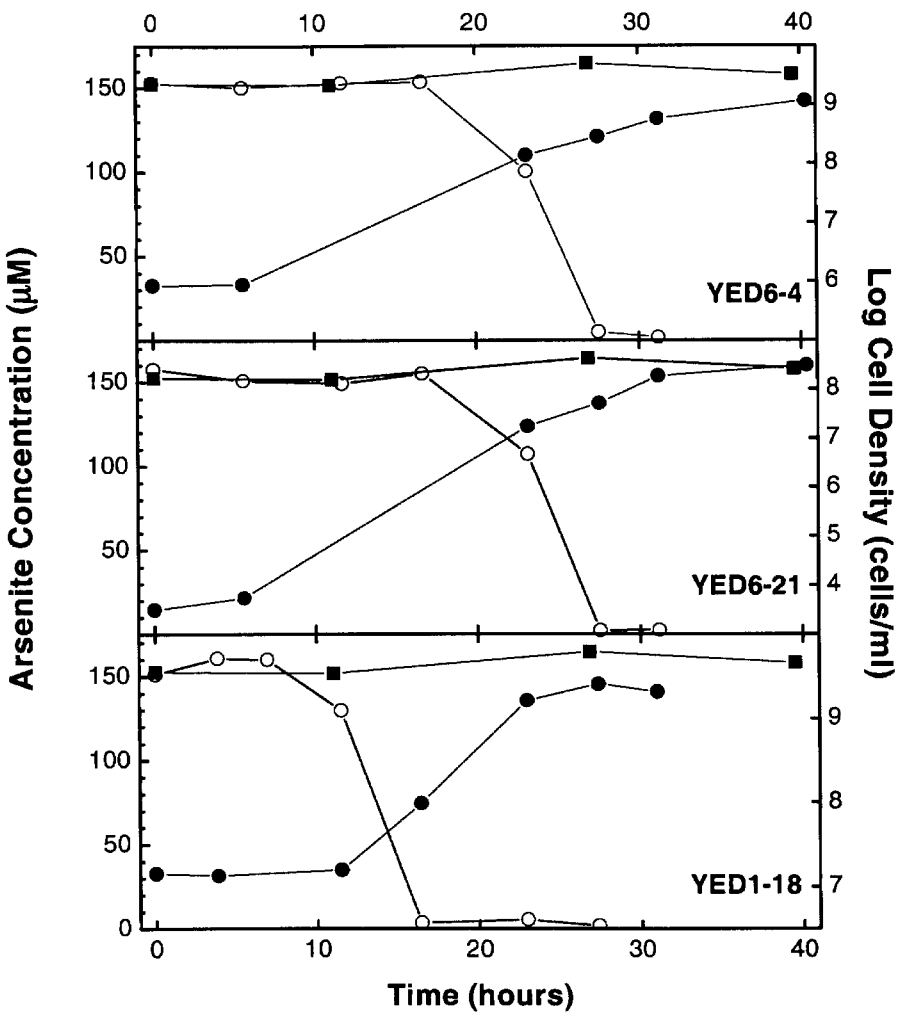

Figure 5.4: Growth of YED6-4, YED6-21, and YED1-18 in the presence of approximately 150 μM arsenite in YE medium at 30° C (Representative data set). Symbols: (●) cell growth measured by plate counts, (■) arsenite in control experiments of mannitol solution without bacterial cells, (○) arsenite in mannitol solution with growing cells. Plot of one representative experiment where lines are included only as a guide. The variable initial cell concentrations are due to difference in cell densities in the inocula.

To compare these data with the growth and oxidation data of AOL15, a plot of the normalized arsenite concentration can be plotted against cell density to correct for variations in both initial arsenite concentrations and doubling times of the isolates. Thus, the growth and oxidation profiles of AOL15 (initial arsenite concentration 585 μM) and the new isolates (initial arsenite concentration 150 μM) can be compared qualitatively. This comparison is shown in Figure 5.5 and indicates that fewer cells of the *Hydrogenophaga* isolates than of AOL15 are required to yield a detectable change in arsenite concentrations in the culture medium. For YED6-21 and YED1-18, the oxidation of arsenite is complete by the time the cells have reached a density of 10^8 cells/ml. For AOL15, a density of over 10^9 cells/ml density is reached in the growing culture before arsenite oxidation is complete. Qualitatively, this would suggest that the *Hydrogenophaga* isolates are "faster" oxidizers (i.e., fewer *Hydrogenophaga* cells are required to account for an equivalent amount of arsenite oxidation by AOL15).

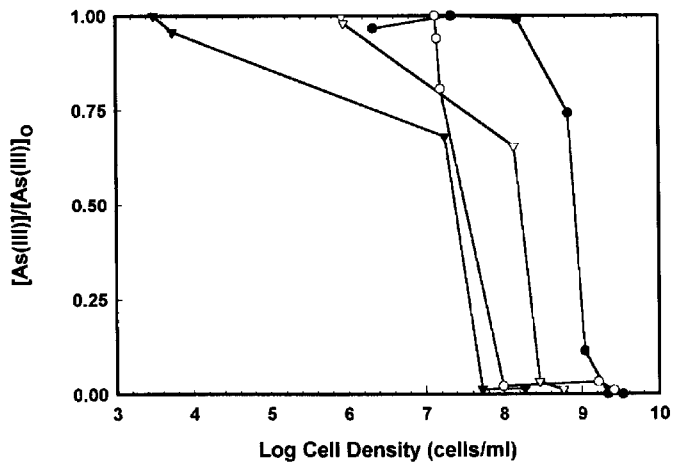

Figure 5.5: Plot of normalized arsenite concentration with cell density for all isolated arsenite oxidizers. Symbols: (●) AOL15, (○) YED1-18, (▽) YED6-4, (▼) YED6-21. Lines are included only as a guide.

5.3.4 Implications for Hot Creek

The findings of this analysis have significant implications for Hot Creek. One very interesting observation is the prevalence of arsenite oxidizers in the field. Based on the information for the isolation from the YE medium, 42 of the 60 colonies (70%) selected from the $1:10^6$ dilution plate were positive for arsenite oxidation. This suggests that arsenite oxidizers are abundant in this biofilm and could constitute up to 70% of the cultivatable population. This observation is further confirmed by the results in liquid culture (Table 5.2) that showed oxidation of arsenite in enrichment cultures established from material shaken off aquatic plants of Hot Creek even after a 10^5 or 10^6 fold dilution. These findings confirm the importance of the aquatic macrophytes in Hot Creek as a locus for bacterial oxidation (Wilkie and Hering 1998).

Three new arsenite oxidizers (YED1-18, YED6-4, and YED6-21) of the genus *Hydrogenophaga* were isolated during this analysis. All of the arsenite oxidizers isolated from the final $1:10^6$ dilution plate of the YE medium had identical RFLP patters and were identified as *Hydrogenophaga* by partial sequencing, suggesting that the *Hydrogenophaga* are the predominant arsenite oxidizers at Hot Creek. Although the kinetics of arsenite oxidation by the *Hydrogenophaga* isolates were not determined in this project, it can be seen qualitatively that fewer cells of *Hydrogenophaga* than of AOL15 are required to produce similar levels of arsenite oxidation as by AOL15.

Finally, the results here are also supported by the findings in Chapter 4. One of the clones reported in Chapter 4 (Clone #44 partial) was identical in its sequence to YED6-21 (Figure 5.6).

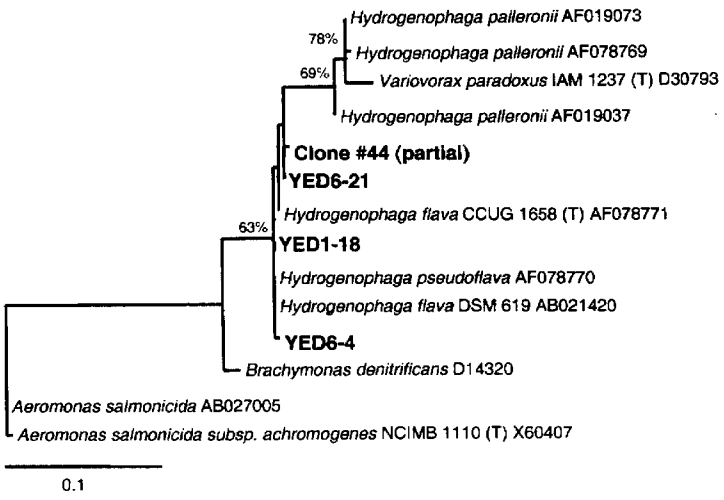

Figure 5.6: Phylogenetic tree for YED6-4, YED6-21, YED1-18, and Clone #44 (partial) by maximum likelihood algorithm in ARB program. The topology of this tree was also supported by a parsimony and distance based tree. Numbers at branch points are bootstrap values that support the tree topology by parsimony. Only bootstrap values greater than 70% are reported in the tree. The accession numbers for the species are provided in the tree.

This phylogenetic analysis (mask: comparing 286 of the aligned base pairs since Clone #44 (partial) was only 291 bases long) showed that Clone #44 (partial) was 99.6% similar to YED6-21. The similarity matrix for this tree is located in Appendix F of Chapter 4.

Furthermore, the FISH analysis of Chapter 4 demonstrated that β-proteobacteria can be detected in this environment. Since the *Hydrogenophaga* genus is a member of the β-proteobacteria, these isolates could be among the bacterial cells that were visualized using the β probes. It is notable that the signature of the *Hydrogenophaga* isolates was found in this environment (using the molecular analysis described in Chapter 4) several months before these isolates were purified from the field. The independent report of the *Hydrogenophaga* sequence within the clone library and identification of the new isolates as *Hydrogenophaga* strengthen the argument that *Hydrogenophaga* are dominant arsenite oxidizing members of the microbial community attached to the aquatic macrophytes of Hot Creek.

Chapter Six

DETERMINATIONS OF CELL DENSITIES AND RATES OF ARSENITE OXIDATION IN SUSPENSIONS DERIVED FROM NATURAL BIOFILMS

6.1 Introduction

In studying the oxidation of arsenite by bacteria isolated from Hot Creek, some of the most interesting questions to be addressed deal with oxidation of arsenite under ambient conditions. The observation that motivated this project is presented in Figure 6.1 (Wilkie 1997) where the rates for *in situ* oxidation with plants or solutions containing the material shaken off plants were determined.

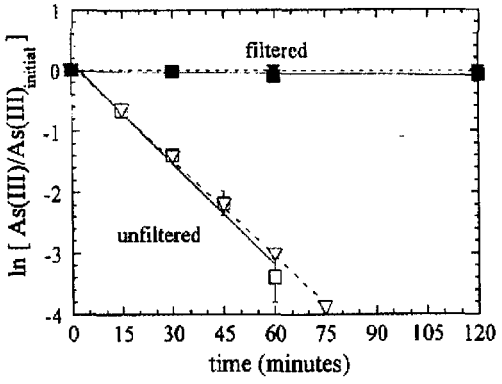

Figure 6.1: Pseudo first-order plots of As(III) oxidation for sterile filtered (solid) and unfiltered (open) systems. Sterile filtered samples were filtered through a 0.22 μm filter. Experiments conducted under ambient conditions (□,■) and 2 μm As(III) spike (▽,▼) (Wilkie 1997).

In Chapters 3 and 5, the arsenite oxidizing ability of isolated bacteria under laboratory conditions was described. In this chapter, an attempt was made to measure the density of the bacterial biofilm at Hot Creek and to determine oxidation rates, expanding on the work done by Wilkie and Hering (1998).

6.2 Experimental Methods

6.2.1 Sample Collection and Inoculum Preparation

On two separate occasions in March 2001, fresh samples of *Potamogeton pectinatus* were collected in sterile polypropylene bottles from Hot Creek. The objective was to determine the densities of cells associated with these plants and to relate these values to the observed rates of arsenite oxidation. On March 24, 2001, three 2-L bottles were each filled with plant matter from Hot Creek (to occupy approximately 20% of volume). Sixteen hundred milliliters of creek water was then added to each of these bottles. Samples were then transported back to the laboratory on ice and processed immediately for a series of kinetics experiments. Each bottle (labeled A, B and C) was processed according to the procedure outlined in Figure 6.2. First, the samples were vigorously mixed with a vortex mixer for five minutes resulting in a suspension of bacterial cells and plant debris. This suspension was then used to generate three independent dilution series A, B and C in triplicate (i.e., A-I to A-III). Each of these triplicates incorporated a tenfold dilution series of samples ranging from undiluted (i.e., undiluted A-I) to a $1{:}10^9$

dilution in sterilized Hot Creek water (i.e., $1:10^9$ A-I). Seventy-five microliters of each of these samples in the dilution series was used to inoculate YE medium amended with 100 μM arsenite (as described in Chapter 5) except for the C-III set, which was inoculated with 90 μl. These inoculations were done in triplicate (e.g., A-I-1 to A-I-3), resulting in a total of 270 tubes excluding blanks. The triplicate samples of the liquid series were generated in order to produce a statistically significant data set for the determination of most probable numbers (MPNs) of bacteria associated with macrophytes at Hot Creek.

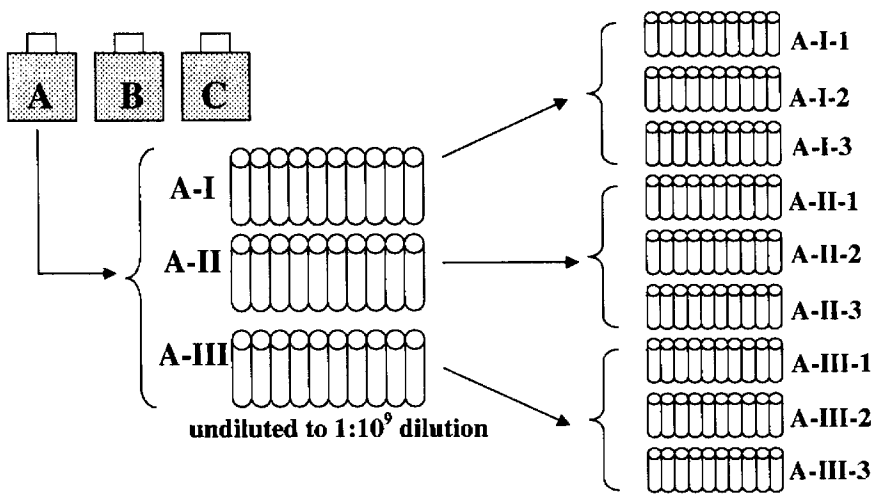

Figure 6.2: Outline of the processing of samples from Hot Creek. The schematic is shown for sample A as an example; however, this procedure was carried out for each of the three samples (A, B and C).

One milliliter of each of the undiluted samples (A, B and C) was fixed with glutaraldeyhyde (final concentration 2.5%) for the determination of total cell numbers by direct counting.

Plate counts were also determined by producing another dilution series in HEPES buffer (10 mM HEPES, pH 7) with the undiluted samples and transferring 10 μl of each

dilution sample onto a 0.2 cm^2 area of a YE medium plate (1% agarose amended with 100 μM arsenite). The dilutions were mixed well before being applied to the plates to result in spatially separated colonies. Typically samples applied to a plate are spread on the entire plate. In this method, the spots were not spread onto the entire plate but rather allowed to dry in place allowing an entire dilution series (in triplicate) to be applied to one plate. Colonies were counted after incubation at 30° C for five days (Figure 6.3).

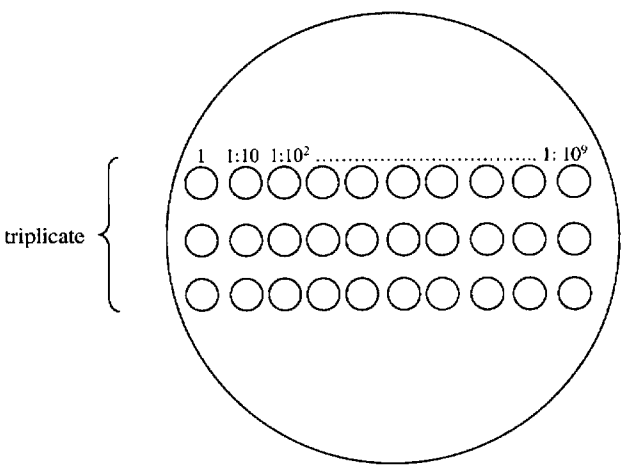

Figure 6.3: Plate count method for cell density determinations.

Finally, the dry weight of the plants in each of the samples was determined by removing all of the plant matter (for each individual sample: A, B, and C) after the initial vortexing step and drying the plant matter in pre-weighed glass beakers at 60° C until no further changes in weight could be detected.

After preparing the dilution series for MPN counts, the three suspensions were combined (sample ABC) to create a single, composite sample for batch kinetic experiments. Larger aggregate matter in this composite sample was allowed to settle out in order to obtain a more homogeneous suspension. The overlying suspension was then

decanted into a large flask to give a final suspension volume of approximately 4800 ml. Portions of this more homogeneous composite suspension (sample ABC*) were removed for direct and plate counts according to the procedure described above. This composite suspension was mixed thoroughly and then aliquots were transferred to flasks for batch kinetics studied of arsenite oxidation.

A second set of experiments was conducted on March 31, 2001, to determine rates of arsenite oxidation in the field. MPNs were not determined in this case. Three 1-L bottles were each filled with plant matter from Hot Creek (to occupy approximately 20% of volume). Eight hundred milliliters of creek water was then added to each of these bottles and the bottles were hand-shaken vigorously on site for five minutes. The resulting suspensions were combined into a single composite sample (sample D) and portions of this sample were used for direct counts (which were fixed with 2.5% glutaraldyhyde and returned to the laboratory on ice) and plate counts (which were diluted and inoculated on site using the method depicted in Figure 6.3). The large aggregates in suspension were allowed to settle out as described for the laboratory experiments. The overlying suspension (sample D*) was used for batch kinetics experiments. A sample of D* was also withdrawn for direct and plate counts.

6.2.2 Batch Experiments

Aliquots of the samples ABC* and D* (described above) were dispensed into flasks for experiments to determine arsenite oxidation rates. All experiments were conducted in duplicate and were initiated (at t=0) by spiking with either 2 or 50 μM arsenite. The 2

μM levels were chosen to approximate ambient arsenic concentrations (2.7 μM) while the 50 μM levels were used to examine reaction kinetics at arsenite concentrations that were elevated compared to ambient levels. Concentrations higher than 50 μM were not used to avoid toxicity effects on the bacteria in suspension. Sample aliquots were removed from the flasks over the course of the experiment and filtered through 0.22 μm filters (cellulose nitrate membrane, VWR) before processing through anion exchange columns. Table 6.1 summarizes the different experiments and conditions for these studies.

Table 6.1: Summary of information on batch experiments.

Location	Sample	Plant Sample	$[As(III)]_o$, μM	Total Sample Volume, ml
Lab	2(ABC*)-I	Composite ABC after settling	2	200
	2(ABC*)-II	Composite ABC after settling	2	200
	50(ABC*)-I	Composite ABC after settling	50	125
	50(ABC*)-II	Composite ABC after settling	50	125
	50(ABC*)-48hr-I[a]	Composite ABC after settling	50	125
	50(ABC*)-48hr-II[a]	Composite ABC after settling	50	125
Field	2(D*)-I	D after settling	2	500
	2(D*)-II	D after settling	2	500
	50(D*)-I	D after settling	50	250
	50(D*)-II	D after settling	50	250

[a]Suspensions were stored at room temperature for 48 hours before conducting experiment.

6.2.3 Analyses

Arsenite concentrations (as total arsenic) in the effluent of anion-exchange columns used to separate arsenic species (see Chapter 3) and total arsenic concentrations in the column

influents were measured by inductively coupled plasma mass spectrometry (ICP-MS) on a Perkin- Elmer ELAN 4000.

The qualitative $KMnO_4$ screening technique developed and described for the isolation of AOL15 (Chapter 3) was used to determine whether or not oxidation had occurred in the different tubes set up for the MPN analysis. Six microliters of 0.002 M $KMnO_4$ were added to 200 µl of the culture medium containing 100 µM total arsenic. A pale pink color for the resulting mixture indicated that arsenate (which does not react with permanganate) was present and thus was a positive result for arsenite oxidation. A clear-colored solution indicated that arsenite (which reacts with permanganate) was present and thus was a negative result for oxidation.

Cell numbers were determined microscopically using the fluorochrome DAPI. Stained cells were retained on 0.2 µm pore size filters before viewing and counting. For each sample, counts were determined both for an untreated sample and after treatment with a dispersant solution (final concentration of 1.2 µM $Na_4P_2O_7 \cdot 10H_2O$) (Kepner and Pratt 1994). Since counts for both treated and untreated samples were similar, only average values are reported here. For the MPN determinations, turbidity readings at 630 nm were used to monitor growth in the YE medium. In all cases, there was a clear distinction between positive results (absorbance near 0.2) and negative results (absorbance below 0.01 and indistinguishable from blanks).

6.3 Results and Discussion

6.3.1 Most Probable Numbers and Cell Counts

In the MPN analysis, positive results for growth and oxidation were separately determined for each of the tubes inoculated using the dilution series produced from the A, B, and C plant samples (tabulated in Appendix J). The MPN values were calculated based on dilution level, the number of positive results for growth or oxidation individually and the volume of the inoculum using MPN tables (Gerhardt et al. 1994). Table 6.2 summarizes the MPN results for the suspensions derived from the surface of *Potamogeton pectinatus* collected in May 2001 including geometric means.

Table 6.2: Summary of MPN determination in suspensions produced after shaking samples of *Potamogeton pectinatus* from Hot Creek.

Sample	MPN (total cells), cells/ml	MPN (oxidizer cells), cells/ml	% of total as oxidizer	MPN (total cells), cells/g (dry wt.)	MPN (oxidizer cells), cells/g (dry wt.)
A-I	3.2×10^6	1.2×10^6	39	5.9×10^8	2.2×10^8
A-II	1.2×10^7	2.0×10^6	16	2.2×10^9	3.7×10^8
A-III	5.7×10^6	3.2×10^5	6	1.0×10^9	5.9×10^7
Geometric Mean (A)	6.0×10^6	9.2×10^5	15	1.1×10^9	1.7×10^8
B-I	2.8×10^6	4.0×10^5	14	4.7×10^8	6.7×10^7
B-II	1.2×10^7	3.2×10^6	26	2.0×10^9	5.3×10^8
B-III	5.7×10^6	3.2×10^6	56	9.5×10^8	5.3×10^8
Geometric Mean (B)	5.8×10^6	1.6×10^6	28	9.6×10^8	2.7×10^8
C-I	1.2×10^7	5.7×10^6	46	3.7×10^9	1.7×10^9
C-II	5.7×10^6	2.0×10^6	35	1.7×10^9	6.1×10^8
C-III	1.0×10^7	1.7×10^6	16	3.0×10^9	5.1×10^8
Geometric Mean (C)	8.8×10^6	2.7×10^6	30	2.7×10^9	8.1×10^8

Based on MPN counts, the bacterial cell density associated with plant samples A, B and C ranged from (0.28-1.2) $\times 10^7$ cells/ml. Of these cells, (0.4-5.7) $\times 10^6$ cells/ml were arsenite oxidizers. However, this comparison is confounded by the difference in the amount of plant matter (in samples A-C) used to prepare the bacterial suspensions. The mass of the plant matter in each sample is reported in Table 6.3 and was used to calculate the values presented in the final two columns of Table 6.2.

Table 6.3: Plant mass and concentration summary.

Plant Sample	Volume of water (ml)	Plant mass (g dry wt.)	Plant concentration (g dry wt./L)
A	1600	8.7	5.4
B	1600	9.61	6.0
C	1600	5.25	3.3
ABC	4800	23.6	4.9
D	2400	12.6	5.3

The MPN values normalized to the amount of plant matter should be more meaningful numbers since the number of cells should be proportional to the amount of plant matter used. The significance of the variability in the MPN values is discussed below. The ranges for the normalized MPN values are (0.47-3.7) $\times 10^9$ total cells/g dry wt. plant and (0.059-1.7) $\times 10^9$ oxidizers cells/g dry wt. plant. The geometric mean values for this range of normalized data are 1.4×10^9 total cells/g dry wt. plant and 3.3×10^8 oxidizer cells/g dry wt. plant. Thus, 24% of the total cells are arsenite oxidizers.

To determine whether or not the estimated MPNs were significantly different, a calculated confidence factor (CF) for a tenfold dilution series with triplicates was used (Woomer 1994). The CF is a tabulated value that varies based on the number of replicates per dilution and the dilution ratio for a given experiment (here, a tenfold

dilution in triplicate). In this case, the CF value is 4.67 (Woomer 1994). Equation 1 is used in assessing the significance of the variations among different estimations of the MPN.

$$CF < \sqrt{\left(\frac{P_U}{P_L}\right)} \quad , \quad (1)$$

where CF = 4.67 (for the 10 fold dilution in triplicate case)

P_U = Upper population estimate

P_L = Lower population estimate

If the calculated value on the right-hand side of Eqn. (1) is greater than the CF value, then the upper and lower MPN estimates are significantly different.

In Table 6.2, the extreme values for the normalized MPNs for total cells are given by samples B-I ($P_L = 4.7 \times 10^8$) and C-I ($P_U = 3.7 \times 10^9$). The square root of the ratio of these values is 2.81, which is less than the CF of 4.67. Thus, the various estimates of the normalized total MPNs are not significantly different. Comparable analyses indicate that the variability in MPN values reported for total or oxidizer cells without normalization is also not significant. Furthermore, no significant differences were observed for the triplicate dilution series for each plant sample, validating the methods used to prepare dilution series here and elsewhere (Chapter 5) in this project. However, the normalized MPNs for the arsenite oxidizers (based on $P_L = 5.9 \times 10^7$ for sample A-III and $P_U = 1.7 \times 10^9$ for sample C-I) do differ significantly.

It was anticipated that normalization for the amount of plant matter would result in a tighter range in the MPN data. Instead, the normalization increased the range in the MPN data slightly (and changed the ordering of some of the MPN values). The effect of

normalization was more pronounced for the arsenite oxidizers than for the total cells. This suggests that the arsenite oxidizers in this biofilm may be less uniformly distributed than the total cells under ambient conditions.

Although the ranges of MPNs reported are the most valid representation of these results, it is useful to have a single value that can be used in simplified calculations. For this purpose, the average plant concentration (4.9 g dry wt./L from Table 6.3) for the composite sample and the geometric mean of the normalized data (1.4×10^9 total cells/g dry wt. plant and 3.3×10^8 oxidizer cells/g dry wt. plant) were used to estimate the concentration of total cells of 7×10^6 total cells/ml and of oxidizer cells of 2×10^6 cells/ml for the composite sample ABC.

Total cell counts were also determined by direct and plate counting. These results are summarized in Table 6.4. The MPN and plate counts agreed within about a factor of two but the MPN values represented only a small fraction of the cells determined by direct counts (between 1 and 5 %). The observation that direct counts are several orders of magnitude higher than counts based on methods requiring cultivation has been well documented (Amann et al. 1995).

Table 6.4: Comparison of MPNs and direct and plate counts.

Sample	Direct count, cells/ml	MPN geometric mean, total cells (cells/ml)	Plate count, cells/ml
A	1.2×10^8	6.0×10^6	2.6×10^6
B	8.2×10^7	2.7×10^6	2.1×10^6
C	7.8×10^8	8.8×10^6	4.6×10^6
ABC	-	$7 \times 10^{6,c}$	-
ABC*[a]	7.3×10^7	-	7.9×10^6
D	1.1×10^8	-	8.1×10^7
D*[b]	1.2×10^8	-	1.9×10^7

[a] Combined sample ABC after removal of settled aggregate plant debris
[b] Sample D after removal of settled aggregate plant debris.
[c] Calculated value, not an actual MPN value.

6.3.2 Rates of Arsenite Oxidation

The composite plant sample suspension (ABC^*) was used in batch experiments to determine rates of arsenite oxidation. For these experiments, the batches were spiked with either 2 or 50 μM arsenite. These values were chosen to correspond to a (lower) level in the range of the K_s for AOL15 and near the ambient concentration and a (higher) level that would be in the range where arsenite oxidation by AOL15 would proceed at its maximum rate (i.e., at the V_{max}). The results for the 2 μM experiments are presented in Figure 6.4 and the data are tabulated in Appendix K.

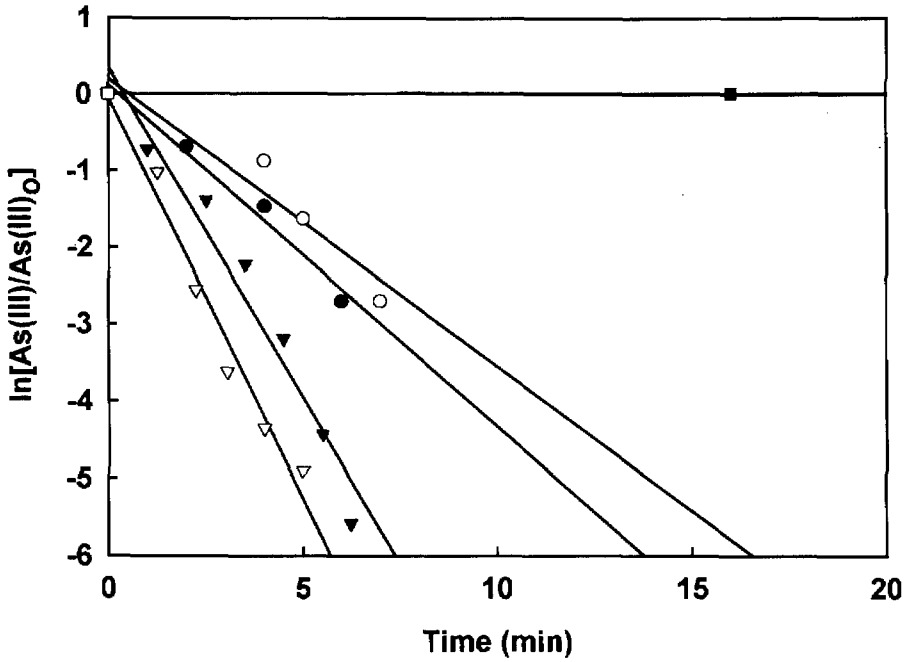

Figure 6.4: Pseudo first-order plots of in situ oxidation of As(III) with material shaken from the surface of the aquatic macrophytes at Hot Creek. (●,○) Plant sample ABC* in duplicate under laboratory conditions; (▼,▽) plant sample D* in duplicate under field conditions; and (■,□) filtered control sample in duplicate.

No arsenite oxidation was observed in the filtered samples, confirming the previous report by Wilkie and Hering (1998). This observation is consistent with the original hypothesis that the oxidation of arsenite at Hot Creek is bacterial in nature; once these bacteria are physically removed from the reaction vessel (by filtering), the oxidation does not proceed. *With the 2 μM arsenite spike, pseudo first-order kinetics* were observed with rate constants of 0.86 – 1.04 min^{-1} in the field incubations and 0.37 – 0.44 min^{-1} in the laboratory incubations (Fig. 6.4). [Data are tabulated in Appendix K.] The same order of the reaction (in arsenite) was observed by Wilkie and Hering (1998) but they reported a significantly lower rate constant of 0.05 min^{-1}. However, in the previous study, the sample of plant and water was collected so as to maintain (to the

extent possible) the ambient concentration of biomass and neither the amount of the plant nor the bacterial cell numbers were quantified. The method of collecting the plant and water sample employed in the present study probably resulted in a significantly higher density of bacteria in the batch experiments.

The results for the 50 μM batch experiments are presented in Figure 6.5 with the data tabulated in Appendix K. In this case, the kinetics are pseudo zero-order and the arsenite concentrations decrease linearly with time. In this study, rate constants of 1.7 $\mu M \cdot min^{-1}$ (field experiments), 0.98 – 1.0 $\mu M \cdot min^{-1}$ (laboratory experiments) and 0.33 – 0.36 $\mu M \cdot min^{-1}$ (laboratory experiments after 48 hours) were determined.

The shift in the (pseudo) reaction order from first order at lower arsenite concentrations to zero order at higher arsenite concentrations is consistent with a microbially mediated process, where the K_s values lies between the lower and higher concentration values. This observation also supports the original hypothesis of microbial oxidation.

The fastest reaction is observed in the 50 μM arsenite experiments in the field incubations and the slowest reaction for experiments conducted in the laboratory with samples stored for over 48 hours. The slowing of the reaction under laboratory conditions can be attributed to the inactivation of arsenite-oxidizing microorganisms during the time between sample collection at Hot Creek and the laboratory experiments. This suggests, not surprisingly, that the activity of the community is highest in its natural environment.

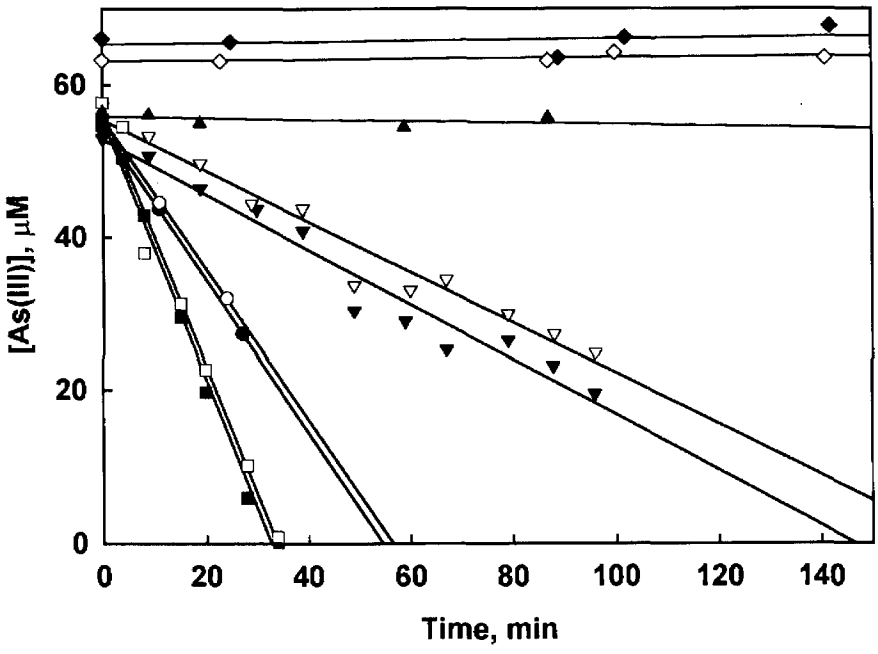

Figure 6.5: Zero-order plot of in situ oxidation of As(*III*) with material shaken from the surface of the aquatic macrophytes at Hot Creek. (●,○) Plant sample ABC in duplicate under laboratory conditions; (▼,▽) plant sample ABC in duplicate under laboratory conditions after 48 hours storage at room temperature; (■,□) plant sample D in duplicate under field conditions; (◆,◇,▲) filtered control sample in triplicate.

6.3.3 Implications of Arsenite Oxidation at Hot Creek

These experiments demonstrate that a significant fraction (on average 24%) of the cultivatable bacteria from the surfaces of macrophytes at Hot Creek are arsenite oxidizers. This suggests it should be possible to isolate arsenite oxidizers from this environment, a hypothesis that has been validated by the isolation and characterization of arsenite oxidizers AOL15, YED1-18, YED6-4, and YED6-21.

Using the value of 1.7 $\mu M \cdot min^{-1}$ for the rate constant obtained in the field for the oxidation experiments with 50 μM arsenite and the normalized density of oxidizers by the MPN counts, a field-V_{max} of 1×10^{-9} $\mu mole \cdot min^{-1} \cdot cell^{-1}$ can be estimated. This value is more than 3 orders of magnitude higher than that determined for AOL15 (1.8×10^{-12}

$\mu mole \cdot min^{-1} \cdot cell^{-1}$). This comparison together with the absence of the genetic signature of AOL15-like organisms in the biofilm community (reported in Chapter 4) suggests that AOL15 is not a dominant organism in this community on either a numerical or activity basis. However, the K_s determined for AOL15 does appear to be representative of the community. The shift from first- to zero- order kinetics (in the 2 μM and 50 μM batch experiments) is consistent with a K_s value in the range determined for AOL15. Furthermore, the isolation of AOL15 (from a very high arsenite enrichment medium) demonstrates that at least some of the microorganisms present in this biofilm can tolerate concentrations of arsenite well above the ambient levels.

Finally, the MPN analysis yielded reproducible counts for total cells attached to the aquatic macrophytes (1.4×10^9 total cells/g dry wt. plant). The MPN analysis also revealed that the distribution of oxidizers could vary significantly depending on the initial plant samples. Furthermore, it was estimated that the arsenite oxidizers constituted a significant fraction (between 6 and 56%) of the community.

Chapter Seven

CONCLUSIONS

7.1 Summary and Conclusions

In this study, the bacterial oxidation of arsenite at Hot Creek was examined. The primary objectives were to characterize the biofilm community on the surface of the submerged macrophytes of Hot Creek in terms of the community make-up, cell densities and arsenite oxidation activity, to isolate (dominant) arsenite oxidizers from the community, and to study the oxidization activity under controlled laboratory conditions. To achieve these objectives, molecular and cultivation techniques were employed.

7.1.1 Characterization of the Attached Microbial Community

On the basis of molecular techniques, an *O. sinensis*-like microorganism was identified as a dominant member of the biofilm community. *O. sinensi* is a photosynthetic stramenopile and its sequence was recovered with high frequency (72% of all clones). Thus, the role of phototrophs may be an important one to understand with respect to the microbial ecology of the biofilm and (possibly) to arsenite oxidation. Molecular techniques also suggested significant representation of β-proteobacteria in this community since several β-proteobacteria sequences were also retrieved. In addition,

microscopic examination by fluorescence *in situ* microscopy (FISH) indicated that β-proteobacteria were present in the biofilm community.

Cell densities were estimated by most probable number (MPN) analysis. The range of MPN values (normalized for the concentration of plant matter used to generate the bacterial suspensions) were $(0.47 - 3.7) \times 10^9$ total cells/g dry wt. plant and $(0.059 - 1.7) \times 10^9$ oxidizers cells/g dry wt. plant. Thus between 6 and 56% of the attached community was capable of arsenite oxidation. Comparison of the MPN values with and without normalization for the concentration of plant matter indicated that despite a uniform distribution of total bacterial cells in this biofilm community, the distribution of oxidizers was subject to greater heterogeneity in the natural environment. Unsurprisingly, the cell density determinations by MPN analysis underestimated the cell numbers obtained by direct counting, which yielded values that were 1 to 2 orders of magnitude greater for total cell numbers.

7.1.2 Isolation and Characterization of Arsenite-Oxidizing Bacteria

Four new arsenite oxidizers were isolated from the surface of the aquatic macrophyte *Potamogeton pectinatus*. The first to be isolated, *Agrobacterium albertimagni* strain AOL15, is an α-proteobacterium, which was fully characterized under laboratory conditions. The kinetics of arsenite oxidation by AOL15 were studied extensively under laboratory conditions and the kinetic parameters K_s (3.4 ± 2.2 μM) and V_{max} (1.81 ± 0.58 x 10^{-12} μmole·cell^{-1}·min^{-1} or 0.043 ± 0.017 μmole·mg protein^{-1}·min^{-1}) were determined. Interestingly, this K_s is near the ambient arsenic levels (2.7 μM) at Hot Creek.

Modification of isolation procedures and media resulted in the isolation of three *Hydrogenophaga* species, YED1-18, YED6-4, and YED6-21. These isolates are members of the β-proteobacteria and were isolated not from enrichment cultures but rather from plates of YE medium. Two of the three *Hydrogenophaga* isolates, YED6-4 and YED6-21 were isolated from a plate inoculated with a $1:10^6$ dilution sample of a suspension of bacteria shaken off the macrophytes of Hot Creek. The persistence of these organisms after a million-fold dilution suggests that they may be significant members of the arsenite oxidizers in the biofilm community.

7.1.3 Relating Field and Laboratory Observations of the Kinetics of Arsenite Oxidation

AOL15 proved not to be a significant member of the attached community on a numerical or activity basis. This conclusion was reached from several independent observations. The 16S rDNA sequence signature of AOL15-like organisms was not found in the survey inventory generated for the attached community (when general and more specific primers were used to amplify the 16S rDNA genes from the biofilm community DNA). In the inventory, the α-proteobacteria made up only 0.6% of the sequences retrieved (lower than the percentages for the β- and γ- proteobacteria at 2.6 and 2.8% respectively). Furthermore, when isolations were attempted on solid media without the establishment of an enrichment culture, AOL15 was not among the cultures that were isolated. These findings suggest that AOL15 is not a numerically significant member of the community.

Further evidence suggested that oxidation by AOL15 does not contribute significantly to the observed arsenite oxidation under ambient conditions. In Chapter 6, rates for arsenite oxidation were determined for batch reactions of bacterial cells shaken off aquatic macrophytes. The rate constants for experiments conducted in the field were 0.86 – 1.04 min^{-1} for the pseudo first-order reaction observed with a 2 μM arsenite spike and 1.7 $\mu M \cdot min^{-1}$ for the pseudo zero-order reaction observed with the 50 μM arsenite spike. Based on the pseudo zero-order rate constant and the MPN estimates for the number of arsenite oxidizers in the biofilm community, a field-V_{max} of 1×10^{-9} $\mu mole \cdot min^{-1} \cdot cell^{-1}$ was estimated. This value is 4 orders of magnitude higher than that determined experimentally for AOL15, which suggests that AOL15 is not a significant contributor to the arsenite oxidization activity observed in the field.

The YED isolates, however, did appear to be significant arsenite oxidizers in this community. Two independent molecular techniques (described in Chapter 4) suggested that β-proteobacteria are numerically relevant bacteria in the community. The β-proteobacteria constituted 2.6 % of the sequence inventory and were the only group of bacteria that could be successfully visualized by FISH using β-proteobacteria probes. Moreover, one of the retrieved sequences in the inventory, Clone #44 (partial), was 99.6% similar to YED6-21. The independent observations of the identification of the YED isolates as members of the *Hydrogenophaga* genus together with the sequence of Clone #44 (partial) suggest that *Hydrogenophaga* species are numerically significant oxidizers at Hot Creek. As further evidence, it was observed that the oxidation of arsenite in growing cultures occurred sooner (i.e., at lower cell densities) for the *Hydrogenophaga* isolates than for AOL15. Although the kinetic constants for these new

oxidizers were not determined, they appear to be "faster" oxidizers than AOL15 and their activity might thus account for the estimated field V_{max}.

It should be noted, however, that the K_s of AOL15 did appear to be representative of the community present at Hot Creek. Also, AOL15 was isolated from very high arsenite containing media, which demonstrates that there are oxidizers present in Hot Creek that are resistant to concentrations of arsenite far greater than the ambient levels. Oxidation of arsenite by AOL15 appeared to be a mechanism for detoxification; none of the isolates tested (AOL15, YED6-4, and YED6-21) were able to growth autotrophically on arsenite.

7.1.4 Wider Implications of This Study and Future Directions

The analysis presented here has answered some of the questions about the bacterial oxidation at Hot Creek. However, several new questions have emerged from this study.

Firstly, in the characterization of the macrophyte community, several interesting observations have been made. One of these involves the presence of the sequence for an *O. sinensis*-like organism in the biofilm, which suggests that the phototrophic community should be more closely examined at this site. Such examination could provide insight not only into the role of an *O. sinensis*-like organism but also into the symbiosis among the different bacteria, cyanobacteria and eukarya (including the host plants) at this site. The relationship between the biofilm bacteria and the host plants is an interesting but (in this study) unposed question. It might also be possible to isolate phototrophic bacteria that are capable of arsenite oxidation from the community.

Secondly, the inventory also revealed two novel sequences that are deserving of further study. This would constitute a separate area of study, different from the arsenite-oxidation based project presented here. The geothermal activity and resulting temperature and redox gradients that occur naturally at Hot Creek make it an exciting study site for the retrieval of novel sequences and the isolation and cultivation of novel bacteria with unusual redox chemistry capabilities. For example, the *Hydrogenophaga* (although identified in this study as arsenite oxidizers) are known to oxidize H_2. The physiological and ecological significance of these two types of oxidation activities in an environment like Hot Creek is not known.

Finally, the physiological role of arsenite oxidation at Hot Creek appears to be associated with detoxification (particularly for AOL15). The possible occurrence of autotrophic arsenite oxidizers at Hot Creek is still an open question that might yield interesting results if studied more carefully and with better-designed media. Prior evidence for autotrophic arsenite oxidation and the observed ability of the biofilm community to oxidize arsenite suggest that this community is an important one to probe for autotrophs.

Appendix A

TRANSMISSION ELECTRON MICROGRAPHS OF AGROBACTERIUM ALBERTIMAGNI STRAIN AOL15

A series of images of AOL15 grown in citrate or mannitol media. Thin sections of AOL15 are also presented.

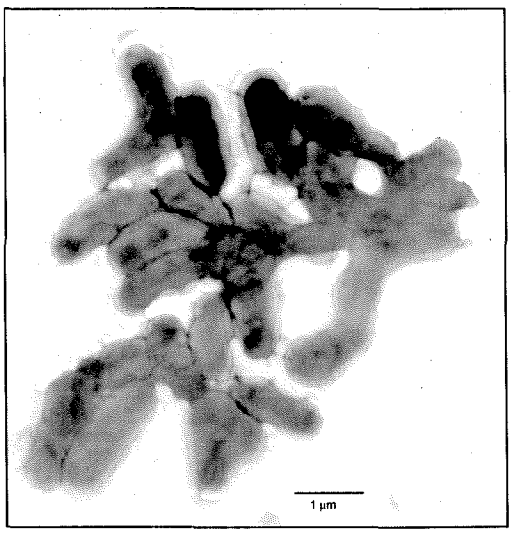

Figure A-1: AOL15 in citrate medium.

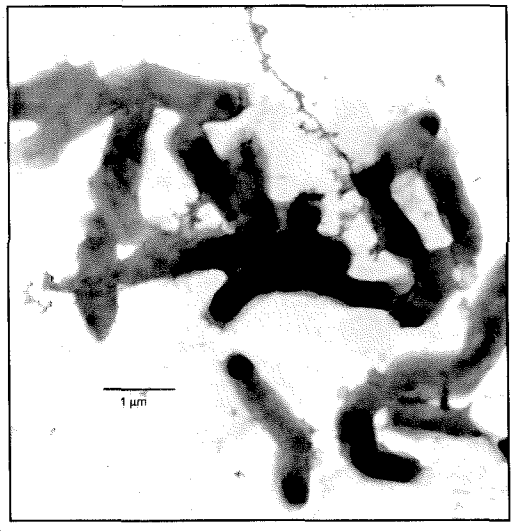

Figure A-2: AOL15 in citrate medium.

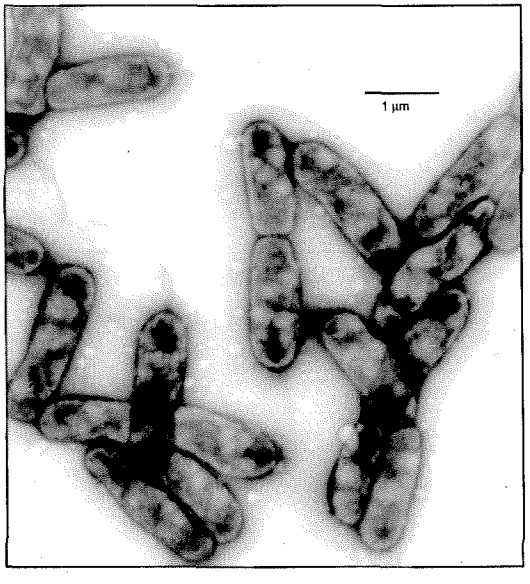

Figure A-3: AOL15 in mannitol medium.

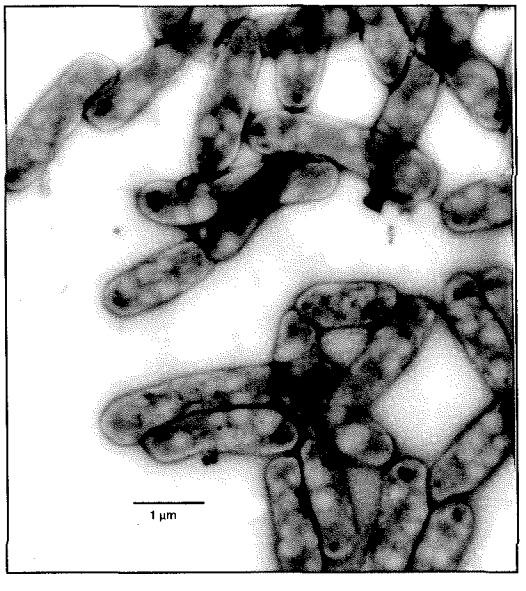

Figure A-4: AOL15 in mannitol medium

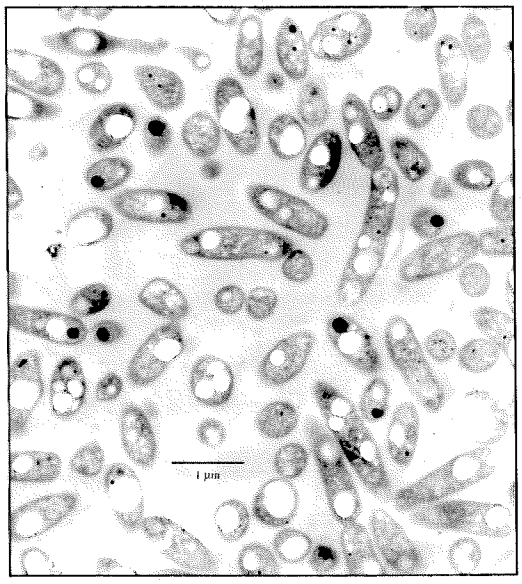

Figure A-5: Thin section of AOL15 in mannitol medium.

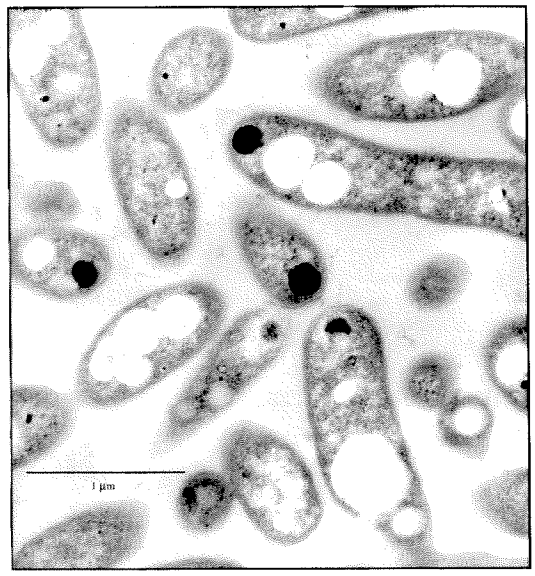

Figure A-6: Thin section of AOL15 in mannitol medium.

Appendix B

MOLECULAR ANALYSIS OF AOL15

The following tables contain data from DNA-DNA hybridization experiments comparing AOL15, *Agrobacterium tumefaciens* and *Blastobacter aggregatus*, and a similarity matrix for AOL15 comparing it with closed related bacteria based on 16S rDNA homology. The DNA-DNA hybridization work was carried out by Dr. Masataka Satomi at the National Research Institute of Fisheries Science, Kanagawa, Japan.

Table B.1: DNA-DNA hybridization results. Numbers are percent similarity between the entire genomic DNA of the strains that are being compared.

Bacteria	Agrobacterium tumefaciens	Blastobacter aggregatus	Agrobacterium albertimagni strain AOL15
Agrobacterium tumefaciens	100	11	15
Blastobacter aggregatus	12	100	31
Agrobacterium albertimagni strain AOL15	10	30	100

Table B.2: Similarity matrix for AOL15 comparing the 16S rDNA genes.

	1	2	3	4	5	6	7	8	9	10	11	12	13	14	15
1. Agrobacterium albertimagni AOL15	100	-	-	-	-	-	-	-	-	-	-	-	-	-	-
2. *Agrobacterium rhizogenes* (X67224)	95.2	100	-	-	-	-	-	-	-	-	-	-	-	-	-
3. *Agrobacterium rubi* (D12787)	96.8	93.7	100	-	-	-	-	-	-	-	-	-	-	-	-
4. *Agrobacterium tumefaciens* (D14505)	94.8	99.3	93.8	100	-	-	-	-	-	-	-	-	-	-	-
5. *Agrobacterium tumefaciens* (M11223)	98.4	94.8	98.3	94.8	100	-	-	-	-	-	-	-	-	-	-
6. *Agrobacterium tumefaciens*-T (D12784)	97.7	94.9	98.3	94.8	99.2	100	-	-	-	-	-	-	-	-	-
7. *Agrobacterium vitis* (D01258, D14502)	95.9	93.9	95.2	94.6	95.9	95.3	100	-	-	-	-	-	-	-	-
8. *Blastobacter aggregatus* (X73041)	97.0	92.6	94.1	92.2	95.6	95.0	94.4	100	-	-	-	-	-	-	-
9. *Blastobacter capsulatus* (X73042)	94.5	92.8	93.1	92.5	93.6	93.5	92.1	95.2	100	-	-	-	-	-	-
10. NT-25 (AF 159452)	94.2	94.6	93.8	94.5	93.6	94.1	93.5	91.6	91.8	100	-	-	-	-	-
11. NT-26 (AF 159453)	94.3	94.7	93.9	94.6	93.8	94.2	93.5	91.7	91.6	99.6	100	-	-	-	-
12. *Rhizobium fredii* (D12792)	95.5	95.8	94.4	96.5	95.2	95.2	94.9	93.4	94.0	94.3	94.4	100	-	-	-
13. *Rhizobium gallicum* (U86343)	94.7	96.4	93.7	96.7	94.5	94.9	94.5	92.1	92.8	96.5	96.7	96.1	100	-	-
14. *Rhizobium leguminosarum* (U29386)	94.7	97.9	93.3	97.5	94.4	94.4	93.4	92.1	92.3	95.6	95.7	95.2	97.3	100	-
15. *Sinorhizobium xinjiangensis* (D12796)	95.6	96.0	94.6	96.0	95.2	95.4	94.4	93.5	94.0	94.3	94.4	99.6	96.0	95.4	100

Appendix C

GROWTH DATA FOR AOL15

This appendix contains data for the growth of AOL15 and its oxidation of arsenite under growth conditions. Also contained in this appendix are the growth data that were used to generate Table 3.1 and to determine the optimal growth temperature for AOL15.

Table C.1: 12-15-98 Experiments. Growth vs. Oxidation Data for AOL15 in Mannitol Medium at pH 7 at 30° C.

Sample Name	Time (hours)	[As(III)] (μM)	Cell Count (cells/ml)
590 μM-A	0.0	589.0	-
	5.1	581.1	-
	10.3	527.7	-
	15.3	540.4	1.20E+07
	20.3	537.6	1.41E+08
	25.2	188.9	2.00E+08
	30.2	5.2	7.00E+08
	35.3	-	7.00E+08
	40.0	-	7.00E+08
590 μM-B	0.0	581.0	-
	5.1	576.9	-
	10.3	545.4	-
	15.3	562.7	1.50E+07
	20.3	577.5	1.41E+08
	25.2	243.0	8.00E+08
	30.2	4.4	7.00E+08
	35.3	-	4.00E+08
	40.0	-	8.00E+08
590 μM-blank	0.0	582.1	-
	5.1	569.9	-
	10.3	569.6	-
	15.3	559.3	-
	20.3	557.4	-
	25.2	575.6	-
	30.2	583.6	-
	35.3	-	-
	40.0	-	-

Table C.2: 04-04-00 Experiments. Growth vs. Oxidation Data for AOL15 in Mannitol Medium at pH 7 at 30° C.

Sample Name	Time (hours)	[As(III)] (μM)	Cell Count (cells/ml)
605 μM	0.5	-	1.46E+06
	9.0	-	2.32E+07
	9.2	606.5	-
	13.6	623.9	-
	16.7	579.8	-
	16.7	-	5.17E+08
	21.1	79.4	-
	24.7	14.6	-
	41.3	14.4	3.04E+09
605 μM-blank	9.2	645.9	-
	13.6	593.7	-
	16.7	588.6	-
	21.1	600.7	-
	24.8	572.8	-
	41.4	582.3	-

Table C.3: 04-15-00 Experiments. Growth vs. Oxidation Data for AOL15 in Mannitol Medium at pH 7 at 30° C.

Sample Name	Time (hours)	[As(III)] (μM)	Cell Count (cells/ml)
1.1 mM	0.9		2.08E+06
	1.0	1180.3	
	8.0		2.70E+06
	8.1	1228.5	
	12.9		1.40E+07
	13.0	1203.8	
	17.9		4.63E+07
	18.0	1222.9	
	22.2		9.63E+07
	22.3	1198.9	
	32.3		5.25E+08
	32.4	1129.7	
	40.4	38.4	
	46.9		2.34E+09
	47.0	-0.7	
1.1 mM-blank	1.2	1267.7	-
	8.5	1289.7	-
	47.3	1308.7	-

Table C.4: Growth vs. Oxidation Data presented in Figure 3.3 for AOL15 in Mannitol Medium at pH 7 at 30° C.

Sample Name	Time (hours)	[As(III)] (μM)	Cell Count (cells/ml)
622 μM	1.0		2150000
	1.1	585.4	
	8.1		21750000
	8.2	605.5	
	12.6		1.53E+08
	12.7	600.2	
	17.6		6.75E+08
	17.7	450.2	
	21.8		1.1E+09
	21.9	69.7	
	32.1		2.15E+09
	32.3	1.0	
	40.5	1.8	
	46.8		3.34E+09
	46.9	0.2	
622 μM-blank	1.3	651.0	-
	8.5	670.3	-
	47.3	674.5	-

Table C.5: 05-25-99 Experiments. Growth Data for AOL15 in Mannitol Medium at pH 7 at 37° C.

[As(III)]	Time (hours)	Cell Count (cells/ml)
0 μM-A	8.8	2.39E+08
	10.6	6.20E+08
	12.2	1.06E+09
0 μM-B	8.9	2.40E+08
	10.6	7.39E+08
	12.2	1.11E+09

Table C.6: 03-12-99 Experiments. Growth Data for AOL15 in Mannitol Medium at pH 7 at 30° C.

[As(III)]	Time (hours)	Cell Count (cells/ml)
0 μM	1.9	6.92E+06
	4.1	4.65E+06
	6.0	2.61E+07
	8.1	6.54E+07
	10.2	2.23E+08
	12.5	5.00E+08
	14.4	8.46E+08
	16.1	1.34E+09
	18.3	1.24E+09
50 μM	2.0	2.19E+06
	4.1	3.79E+06
	6.1	1.99E+07
	8.1	5.16E+07
	10.1	1.55E+08
	13.0	4.43E+08
	14.3	7.45E+08
	16.1	1.01E+09
500 μM	2.0	1.66E+06
	4.0	4.25E+06
	6.0	1.56E+07
	8.2	4.46E+07
	10.2	1.20E+08
	12.6	2.49E+08
	14.3	5.33E+08
	16.0	6.68E+08

Table C.7: 04-14-99 Experiments. Growth Data for AOL15 in Mannitol Medium at pH 7 at 25° C.

[As(III)]	Time (hours)	Cell Count (cells/ml)	[As(III)]	Time (hours)	Cell Count (cells/ml)
0 µM-A	3.0	4.23E+06	**5 µM-B**	3.0	4.33E+06
	6.0	7.45E+06		6.0	7.49E+06
	9.3	1.91E+07		9.3	1.95E+07
	12.1	5.20E+07		12.2	4.88E+07
	15.4	1.58E+08		15.4	1.51E+08
	18.1	4.55E+08		18.2	4.65E+08
0 µM-B	3.0	4.22E+06	**500µM-A**	3.0	3.53E+06
	6.1	8.10E+06		6.0	5.78E+06
	9.3	1.97E+07		9.3	1.40E+07
	12.1	5.10E+07		12.1	4.53E+07
	15.4	1.51E+08		15.5	1.41E+08
	18.1	3.71E+08		18.1	3.10E+08
5 µM-A	3.0	4.58E+06	**500µM-B**	3.0	3.49E+06
	6.0	6.76E+06		6.0	5.17E+06
	9.3	2.01E+07		9.2	1.07E+07
	12.2	5.41E+07		12.1	4.03E+07
	15.4	1.77E+08		15.5	8.73E+07
	18.2	6.03E+08		18.1	2.65E+08

Appendix D

KINETIC DATA

The data presented in this appendix are the entire set of whole cell kinetic experiments for AOL15 harvested in the late exponential/early stationary phase of growth with the exception of experiments T24-3a, 3b, 50a and 50b which are presented in Appendix E. The details for the setup of these experiments are outlined in Chapter 3. Tables D1 and D2 are compiled data for all the experiments and the data sets for individual experiments follow in Tables D3-D48. In these latter tables, the experiment names (for example: E10-5a) represent the experiment number (E10) and the approximate initial concentration of arsenite for the given experiment (5a: 5μM arsenite).

Table D.1: Complete Data Set from all Whole-Cell Kinetic Experiments with AOL15 (all in HEPES Buffer, pH 7, 30° C).

Experiment Name	Cell Numbers (cells/ml)	Initial [As(III)] (μM)	Rate of Oxidation (μmole·cell^{-1}·min^{-1})
E10 2a	2.28E+08	2.07	4.58E-13
E11 2a	7.25E+07	2.25	9.13E-13
E11 2b	7.25E+07	2.25	9.15E-13
E10 2b	2.28E+08	2.27	4.72E-13
E12 4b	1.38E+08	3.68	1.09E-12
E12 4a	1.38E+08	3.98	1.23E-12
E11 5a	7.25E+07	4.67	9.40E-13
E11 5b	7.25E+07	5.14	1.17E-12
E12 6a	1.38E+08	5.3	1.20E-12
E10 5a	2.28E+08	5.36	7.15E-13
E12 6b	1.38E+08	5.45	1.18E-12
E10 5b	2.28E+08	5.58	7.75E-13
E12 7a	1.38E+08	6.27	1.19E-12
E12 7b	1.38E+08	6.71	1.37E-12
E12 8a	1.38E+08	7.17	9.77E-13
E12 8b	1.38E+08	7.79	1.19E-12
E12 9a	1.38E+08	8.28	1.30E-12
E12 9b	1.38E+08	9.02	1.47E-12
E12 10a	1.38E+08	9.81	1.50E-12
E12 11a	1.38E+08	9.82	1.44E-12
E12 11b	1.38E+08	10.07	1.46E-12
E11 10b	7.25E+07	10.23	1.09E-12
E11 10a	7.25E+07	10.81	1.36E-12
E13 12b	1.75E+08	12.45	1.32E-12
E13 12a	1.75E+08	12.65	1.22E-12
E13 13b	1.75E+08	12.99	1.14E-12
E13 13a	1.75E+08	13.05	1.14E-12
E11 20a	7.25E+07	19.26	1.15E-12
E11 20b	7.25E+07	20.56	1.61E-12
E11 25b	7.25E+07	21.26	1.27E-12
E11 25a	7.25E+07	24.76	1.72E-12
E11 50b	7.25E+07	47.83	1.76E-12
E9 100a	3.25E+08	98.7	1.78E-12
E9 100b	3.25E+08	101.31	1.69E-12
E9 150b	3.25E+08	149.77	1.63E-12
E9 150a	3.25E+08	150.52	1.67E-12
E9 200a	3.25E+08	219.7	1.87E-12
E9 200b	3.25E+08	227.48	2.01E-12
E9 250a	3.25E+08	269.64	2.05E-12
E9 250b	3.25E+08	269.71	2.05E-12
E9 300b	3.25E+08	289.19	1.60E-12
E9 350a	3.25E+08	315.99	1.60E-12
E9 300a	3.25E+08	323.63	2.03E-12
E9 350b	3.25E+08	346.82	1.63E-12
E9 400a	3.25E+08	374.86	1.62E-12
E9 400b	3.25E+08	397.59	1.68E-12

Table D.2: Subset of Data from all Whole-Cell Kinetic Experiments with AOL15 (all in HEPES Buffer, pH 7, 30° C) Used to Determine Kinetic Parameters K_s and V_{max}. These data are also presented in Figure 3.4.

Experiment Name	Cell Numbers (cells/ml)	Initial [As(III)] (μM)	Rate of Oxidation (μmole·cell^{-1}·min^{-1})
E11 2a	7.25E+07	2.25	9.13E-13
E11 2b	7.25E+07	2.25	9.15E-13
E12 4b	1.38E+08	3.68	1.09E-12
E11 5b	7.25E+07	5.14	1.17E-12
E12 6a	1.38E+08	5.3	1.20E-12
E10 5a	2.28E+08	5.36	7.15E-13
E12 6b	1.38E+08	5.45	1.18E-12
E10 5b	2.28E+08	5.58	7.75E-13
E12 7a	1.38E+08	6.27	1.19E-12
E12 7b	1.38E+08	6.71	1.37E-12
E12 8a	1.38E+08	7.17	9.77E-13
E12 8b	1.38E+08	7.79	1.19E-12
E12 9b	1.38E+08	9.02	1.47E-12
E12 10a	1.38E+08	9.81	1.50E-12
E12 11b	1.38E+08	10.07	1.46E-12
E13 12a	1.75E+08	12.65	1.22E-12
E13 13a	1.75E+08	13.05	1.14E-12
E9 200a	3.25E+08	219.7	1.87E-12
E9 200b	3.25E+08	227.48	2.01E-12
E9 250a	3.25E+08	269.64	2.05E-12
E9 250b	3.25E+08	269.71	2.05E-12
E9 300b	3.25E+08	289.19	1.60E-12
E9 350a	3.25E+08	315.99	1.60E-12
E9 300a	3.25E+08	323.63	2.03E-12
E9 350b	3.25E+08	346.82	1.63E-12
E9 400a	3.25E+08	374.86	1.62E-12
E9 400b	3.25E+08	397.59	1.68E-12

Table D.3: Individual Data Set (E10-2a).

E10-2a	Time (min)	[As(III)] (μM)
	0.00	2.07
	13.00	1.13
	22.00	0.36
	31.00	0.46
	40.00	0.13
	50.00	0.18
	60.00	0.06
	70.00	0.20
	Cell count (cell/ml)	2.28E+08

Table D.4: Individual Data Set (E11-2a).

E11-2a	Time (min)	[As(III)] (μM)
	0.00	2.25
	15.00	1.38
	24.00	0.97
	36.00	0.61
	46.00	0.36
	56.00	0.14
	66.00	0.08
	76.00	0.05
	Cell count (cell/ml)	7.25E+07

Table D.5: Individual Data Set (E11-2b).

E11-2b	Time (min)	[As(III)] (μM)
	0.00	2.25
	14.00	1.41
	23.00	1.00
	35.00	0.54
	45.00	0.37
	55.00	0.13
	65.00	0.16
	75.00	0.30
	Cell count (cell/ml)	7.25E+07

Table D.6: Individual Data Set (E10-2b).

E10-2b	Time (min)	[As(III)] (μM)
	0.00	2.27
	13.00	1.17
	22.00	0.70
	31.00	0.39
	40.00	0.27
	50.00	0.11
	60.00	0.03
	70.00	0.16
	Cell count (cell/ml)	2.28E+08

Table D.7: Individual Data Set (E12-4b).

E12-4b	Time (min)	[As(III)] (μM)
	0.00	3.68
	18.00	1.46
	33.00	0.38
	46.00	0.11
	59.00	0.27
	71.00	0.13
	83.00	0.04
	94.00	0.03
	Cell count (cell/ml)	1.38E+08

Table D.8: Individual Data Set (E12-4a).

E12-4a	Time (min)	[As(III)] (μM)
	0.00	3.98
	19.00	1.19
	34.00	0.35
	47.00	0.10
	60.00	0.06
	72.00	0.05
	84.00	0.05
	95.00	0.04
	Cell count (cell/ml)	1.38E+08

Table D.9: Individual Data Set (E11-5a).

E11-5a	Time (min)	[As(III)] (μM)
	0.00	4.67
	14.00	4.17
	24.00	3.61
	35.00	2.90
	45.00	2.17
	55.00	1.50
	65.00	1.07
	75.00	1.00
	Cell count (cell/ml)	7.25E+07

Table D.10: Individual Data Set (E11-5b).

E11-5b	Time (min)	[As(III)] (μM)
	0.00	5.14
	14.00	3.91
	24.00	3.31
	34.00	2.42
	45.00	2.19
	55.00	1.38
	65.00	1.02
	75.00	0.69
	Cell count (cell/ml)	7.25E+07

Table D.11: Individual Data Set (E12-6a).

E12-6a	Time (min)	[As(III)] (μM)
	0.00	5.30
	16.00	3.06
	31.00	1.20
	43.00	0.57
	56.00	0.18
	68.00	0.06
	80.00	0.05
	91.00	0.04
	Cell count (cell/ml)	1.38E+08

Table D.12: Individual Data Set (E10-5a).

E10-5a	Time (min)	[As(III)] (μM)
	0.00	5.36
	9.00	4.38
	18.00	2.98
	27.00	2.28
	35.00	1.57
	47.00	0.68
	56.00	0.29
	66.00	0.15
	81.00	0.06
	Cell count (cell/ml)	2.28E+08

Table D.13: Individual Data Set (E12-6b).

E12-6b	Time (min)	[As(III)] (μM)
	0.00	5.45
	15.00	3.74
	30.00	1.33
	42.00	0.66
	55.00	0.19
	67.00	0.06
	79.00	0.45
	90.00	0.02
	Cell count (cell/ml)	1.38E+08

Table D.14: Individual Data Set (E10-5b).

E10-5b	Time (min)	[As(III)] (μM)
	0.00	5.58
	12.00	3.70
	21.00	2.67
	30.00	1.77
	39.00	1.42
	50.00	0.48
	60.00	0.25
	70.00	0.11
	84.00	0.05
	Cell count (cell/ml)	2.28E+08

Table D.15: Individual Data Set (E12-7a).

E12-7a	Time (min)	[As(III)] (μM)
	0.00	6.27
	15.00	3.89
	29.00	2.28
	41.00	1.20
	54.00	0.82
	66.00	0.07
	77.00	0.10
	89.00	0.06
	Cell count (cell/ml)	1.38E+08

Table D.16: Individual Data Set (E12-7b).

E12-7b	Time (min)	[As(III)] (μM)
	0.00	6.71
	14.00	4.29
	28.00	2.41
	40.00	0.91
	43.00	0.40
	65.00	0.14
	76.00	0.09
	88.00	0.05
	Cell count (cell/ml)	1.38E+08

Table D17: Individual Data Set (E12-8a).

E12-8a	Time (min)	[As(III)] (μM)
	0.34	0.34
	0.34	0.34
	0.34	0.34
	0.34	0.34
	0.34	0.34
	0.34	0.34
	0.34	0.34
	0.34	0.34
	Cell count (cell/ml)	1.38E+08

Table D.18: Individual Data Set (E12-8b).

E12-8b	Time (min)	[As(III)] (μM)
	0.00	7.79
	14.00	5.43
	28.00	3.95
	40.00	2.56
	43.00	1.66
	65.00	0.95
	76.00	0.64
	88.00	0.28
	Cell count (cell/ml)	1.38E+08

Table D.19: Individual Data Set (E12-9a).

E12-9a	Time (min)	[As(III)] (μM)
	0.00	8.28
	10.00	8.00
	17.00	5.69
	25.00	5.48
	34.00	2.68
	42.00	1.66
	49.00	1.11
	57.00	0.68
	Cell count (cell/ml)	1.38E+08

Table D.20: Individual Data Set (E12-9b).

E12-9b	Time (min)	[As(III)] (μM)
	0.00	9.02
	10.00	6.87
	17.00	6.12
	25.00	4.50
	34.00	2.70
	41.00	1.70
	49.00	1.26
	56.00	0.69
	Cell count (cell/ml)	1.38E+08

Table D.21: Individual Data Set (E12-10a).

E12-10a	Time (min)	[As(III)] (μM)
	0.00	9.81
	9.00	7.88
	16.00	6.64
	24.00	4.87
	33.00	3.03
	41.00	2.65
	48.00	1.74
	55.00	1.05
	Cell count (cell/ml)	1.38E+08

Table D.22: Individual Data Set (E12-11a).

E12-11a	Time (min)	[As(III)] (μM)
	0.00	9.82
	8.00	8.11
	15.00	7.11
	24.00	5.65
	32.00	4.01
	40.00	3.05
	47.00	0.93
	54.00	2.10
	Cell count (cell/ml)	1.38E+08

Table D.23: Individual Data Set (E12-11b).

E12-11b	Time (min)	[As(III)] (μM)
	0.00	10.07
	7.00	7.97
	15.00	7.38
	24.00	5.12
	31.00	3.95
	39.00	3.07
	47.00	2.50
	53.00	1.54
	Cell count (cell/ml)	1.38E+08

Table D.24: Individual Data Set (E11-10b).

E11-10b	Time (min)	[As(III)] (μM)
	0.00	10.07
	7.00	7.97
	15.00	7.38
	24.00	5.12
	31.00	3.95
	39.00	3.07
	47.00	2.50
	53.00	1.54
	Cell count (cell/ml)	7.25E+07

Table D.25: Individual Data Set (E11-10a).

E11-10a	Time (min)	[As(III)] (μM)
	0.00	10.81
	12.00	8.89
	22.00	7.89
	33.00	7.70
	43.00	6.64
	53.00	5.83
	64.00	5.50
	73.00	4.62
	Cell count (cell/ml)	7.25E+07

Table D.26: Individual Data Set (E13-12b).

E13-12b	Time (min)	[As(III)] (μM)
	0.00	12.45
	20.00	8.52
	33.00	3.29
	45.00	2.36
	56.00	3.55
	67.00	2.80
	78.00	1.31
	91.00	0.47
	Cell count (cell/ml)	1.75E+08

Table D.27: Individual Data Set (E13-12a).

E13-12a	Time (min)	[As(III)] (μM)
	0.00	12.65
	21.00	7.98
	35.00	5.86
	46.00	4.55
	58.00	3.11
	68.00	2.29
	79.00	1.60
	92.00	0.31
	Cell count (cell/ml)	1.75E+08

Table D.28: Individual Data Set (E13-13b).

E13-13b	Time (min)	[As(III)] (μM)
	0.00	12.99
	19.00	10.06
	32.00	8.56
	43.00	5.84
	55.00	4.17
	65.00	2.75
	77.00	1.35
	Cell count (cell/ml)	1.75E+08

Table D.29: Individual Data Set (E13-13a).

E13-13a	Time (min)	[As(III)] (μM)
	0.00	13.05
	19.00	10.03
	32.00	7.95
	43.00	6.02
	55.00	4.69
	66.00	3.21
	77.00	1.56
	90.00	0.63
	Cell count (cell/ml)	1.75E+08

Table D.30: Individual Data Set (E11-20a).

E11-20a	Time (min)	[As(III)] (μM)
	0.00	19.26
	10.00	20.10
	21.00	16.80
	31.00	17.97
	42.00	17.44
	52.00	14.97
	62.00	13.81
	72.00	12.58
	Cell count (cell/ml)	7.25E+07

Table D.31: Individual Data Set (E11-20b).

E11-20b	Time (min)	[As(III)] (μM)
	0.00	20.56
	10.00	19.36
	21.00	17.10
	31.00	16.76
	41.00	16.20
	51.00	15.57
	61.00	13.68
	72.00	11.83
	Cell count (cell/ml)	7.25E+07

Table D.32: Individual Data Set (E11-25b).

E11-25b	Time (min)	[As(III)] (μM)
	0.00	21.26
	19.00	22.15
	33.00	18.80
	55.00	15.86
	73.00	22.54
	89.00	11.87
	106.00	10.34
	120.00	9.14
	Cell count (cell/ml)	7.25E+07

Table D.33: Individual Data Set (E11-25a).

E11-25a	Time (min)	[As(III)] (μM)
	0.00	24.76
	19.00	21.10
	34.00	20.79
	54.00	16.74
	73.00	15.13
	89.00	12.45
	106.00	11.73
	120.00	9.26
	Cell count (cell/ml)	7.25E+07

Table D.34: Individual Data Set (E11-50b).

E11-50b	Time (min)	[As(III)] (μM)
	0.00	47.83
	18.00	43.97
	33.00	39.85
	54.00	42.29
	72.00	36.28
	88.00	35.61
	105.00	31.63
	118.00	31.30
	Cell count (cell/ml)	7.25E+07

Table D.35: Individual Data Set (E9-100a).

E9-100a	Time (min)	[As(III)] (μM)
	0.00	98.70
	67.00	62.11
	110.00	2.38
	141.00	23.28
	185.00	12.05
	213.00	4.29
	251.00	1.50
	Cell count (cell/ml)	3.25E+08

Table D.36: Individual Data Set (E9-100b).

E9-100b	Time (min)	[As(III)] (μM)
	0.00	101.31
	66.00	62.56
	108.00	37.33
	140.00	24.51
	183.00	10.34
	212.00	9.82
	250.00	9.30
	Cell count (cell/ml)	3.25E+08

Table D.37: Individual Data Set (E9-150b).

E9-150b	Time (min)	[As(III)] (μM)
	0.00	149.77
	64.00	148.55
	106.00	91.79
	138.00	105.71
	182.00	53.28
	209.00	39.11
	247.00	23.21
	291.00	10.27
	Cell count (cell/ml)	3.25E+08

Table D.38: Individual Data Set (E9-150a).

E9-150a	Time (min)	[As(III)] (μM)
	0.00	150.52
	65.00	113.05
	108.00	90.09
	139.00	117.09
	184.00	49.95
	211.00	30.87
	249.00	26.08
	293.00	6.31
	Cell count (cell/ml)	3.25E+08

Table D.39: Individual Data Set (E9-200a).

E9-200a	Time (min)	[As(III)] (μM)
	0.00	219.70
	64.00	166.74
	104.00	139.09
	136.00	122.50
	180.00	112.28
	207.00	80.89
	245.00	61.15
	289.00	37.23
	Cell count (cell/ml)	7.25E+07

Table D.40: Individual Data Set (E9-200b).

E9-200b	Time (min)	[As(III)] (μM)
	0.00	227.48
	62.00	179.11
	103.00	157.50
	134.00	123.40
	179.00	108.89
	205.00	81.40
	244.00	61.64
	288.00	40.39
	Cell count (cell/ml)	3.25E+08

Table D.41: Individual Data Set (E9-250a).

E9-250a	Time (min)	[As(III)] (μM)
	0.00	269.64
	61.00	207.02
	102.00	182.90
	134.00	161.63
	177.00	124.27
	204.00	116.08
	244.00	93.55
	288.00	74.94
	Cell count (cell/ml)	3.25E+08

Table D.42: Individual Data Set (E9-250b).

E9-250b	Time (min)	[As(III)] (μM)
	0.00	269.71
	60.00	236.76
	101.00	199.12
	133.00	188.30
	176.00	140.09
	203.00	134.50
	242.00	109.26
	286.00	85.02
	Cell count (cell/ml)	3.25E+08

Table D.43: Individual Data Set (E9-300b).

E9-300b	Time (min)	[As(III)] (μM)
	0.00	289.19
	42.00	267.25
	99.00	233.85
	130.00	213.61
	173.00	193.17
	201.00	188.66
	241.00	166.22
	284.00	137.45
	Cell count (cell/ml)	3.25E+08

Table D.44: Individual Data Set (E9-350a).

E9-350a	Time (min)	[As(III)] (μM)
	0.00	315.99
	54.00	294.61
	97.00	265.89
	129.00	246.09
	172.00	239.93
	200.00	222.52
	242.00	194.34
	283.00	163.14
	Cell count (cell/ml)	3.25E+08

Table D.45: Individual Data Set (E9-300a).

E9-300a	Time (min)	[As(III)] (μM)
	0.00	323.63
	41.00	287.49
	100.00	263.54
	132.00	250.82
	174.00	204.96
	202.00	181.98
	242.00	163.08
	286.00	136.63
	Cell count (cell/ml)	3.25E+08

Table D.46: Individual Data Set (E9-350b).

E9-350b	Time (min)	[As(III)] (μM)
	0.00	346.82
	52.00	281.51
	96.00	259.68
	127.00	273.09
	171.00	242.60
	198.00	231.57
	240.00	194.45
	282.00	181.82
	Cell count (cell/ml)	3.25E+08

Table D.47: Individual Data Set (E9-400a).

E9-400a	Time (min)	[As(III)] (μM)
	0.00	374.86
	50.00	348.12
	93.00	358.35
	124.00	376.72
	168.00	298.47
	196.00	301.35
	238.00	262.48
	280.00	227.15
	Cell count (cell/ml)	3.25E+08

Table D.48: Individual Data Set (E9-400b).

E9-400b	Time (min)	[As(III)] (μM)
	0.00	397.59
	49.00	339.05
	92.00	370.25
	123.00	336.37
	166.00	294.28
	194.00	291.24
	237.00	264.43
	279.00	237.49
	Cell count (cell/ml)	3.25E+08

Appendix E

KINETIC DATA - 2

The data presented in this appendix are a subset of the whole-cell kinetic studies with AOL15. The data here are for those experiments conducted with cells harvested during different stages in the growth cycle: 12 hours (exponential phase), 24 hours (late exponential/early stationary phase), 40 hours (late stationary phase). The experiments were conducted at two different initial arsenite concentrations (3 μM: near K_s; 50 μM: at V_{max}).

Table E.1: Individual Data Set for cells harvested during exponential growth (12 hours of growth) with initial arsenite concentration near the K_s value.

T12-3a	Time (min)	[As(III)] (μM)
	0.00	3.65
	11.00	3.10
	18.00	2.77
	29.00	2.39
	36.00	2.09
	46.00	1.68
	59.00	1.39
	66.00	1.18
	79.00	0.89
	89.00	0.71
	102.00	0.49
	116.00	0.37
	Cell count (cell/ml)	3.34E+07

Table E.2: Individual Data Set for cells harvested during exponential growth (12 hours of growth) with initial arsenite concentration near the K_s value.

T12-3b	Time (min)	[As(III)] (μM)
	0.00	3.70
	11.00	3.34
	18.00	3.16
	29.00	2.54
	36.00	2.25
	46.00	1.83
	59.00	1.41
	65.00	1.20
	78.00	0.91
	88.00	0.68
	102.00	0.48
	116.00	0.32
	Cell count (cell/ml)	3.34E+07

Table E.3: Individual Data Set for cells harvested during exponential growth (12 hours of growth) with initial arsenite concentration above the K_s value in the V_{max} range.

T12-50a	Time (min)	[As(III)] (μM)
	0.00	56.69
	6.00	55.53
	16.00	55.43
	25.00	56.17
	41.00	54.97
	54.00	55.25
	76.00	50.08
	97.00	52.84
	114.00	51.70
	133.00	50.09
	145.00	49.22
	168.00	46.25
	Cell count (cell/ml)	3.34E+07

Table E.4: Individual Data Set for cells harvested during exponential growth (12 hours of growth) with initial arsenite concentration above the K_s value in the V_{max} range.

T12-50b	Time (min)	[As(III)] (μM)
	0.00	55.00
	11.00	53.05
	21.00	52.80
	30.00	51.42
	46.00	49.61
	59.00	50.36
	81.00	47.37
	102.00	47.18
	139.00	43.38
	150.00	42.89
	172.00	41.45
	Cell count (cell/ml)	3.34E+07

Table E.5: Individual Data Set for cells harvested during late exponential/early stationary growth (24 hours of growth) with initial arsenite concentration near the K_s value. These data were excluded from all analyses because of anomalous results.

T24-3a	Time (min)	[As(III)] (μM)
	0.00	3.48
	8.00	1.31
	24.00	0.31
	34.00	0.08
	43.00	0.05
	57.00	0.17
	68.00	0.05
	79.00	0.05
	Cell count (cell/ml)	5.25E+07

Table E.6: Individual Data Set for cells harvested during late exponential/early stationary growth (24 hours of growth) with initial arsenite concentration near the K_s value. These data were excluded from all analyses because of anomalous results.

T24-3b	Time (min)	[As(III)] (μM)
	0.00	3.48
	9.00	1.40
	25.00	0.24
	35.00	0.07
	44.00	0.06
	Cell count (cell/ml)	5.25E+07

Table E.7: Individual Data Set for cells harvested during late exponential/early stationary growth (24 hours of growth) with initial arsenite concentration above the K_s value in the V_{max} range. These data were excluded from all analyses because of anomalous results.

T24-50a	Time (min)	[As(III)] (μM)
	0.00	49.80
	5.00	47.25
	21.00	38.52
	35.00	30.09
	54.00	19.41
	76.00	8.74
	91.00	3.60
	106.00	0.82
	116.00	0.46
	125.00	0.43
	Cell count (cell/ml)	5.25E+07

Table E.8: Individual Data Set for cells harvested during late exponential/early stationary growth (24 hours of growth) with initial arsenite concentration above the K_s value in the V_{max} range. These data were excluded from all analyses because of anomalous results.

T24-50b	Time (min)	[As(III)] (μM)
	0.00	51.44
	9.00	46.55
	24.00	34.92
	38.00	26.51
	57.00	17.66
	80.00	7.08
	94.00	2.33
	110.00	0.41
	119.00	0.19
	Cell count (cell/ml)	5.25E+07

Table E.9: Individual Data Set for cells harvested during late stationary growth (40 hours of growth) with initial arsenite concentration near the K_s value.

T40-3a	Time (min)	[As(III)] (μM)
	0.00	3.44
	15.00	2.08
	24.00	1.47
	33.00	0.97
	41.00	0.70
	49.00	0.47
	54.00	0.34
	65.00	0.20
	73.00	0.12
	86.00	0.08
	96.00	0.06
	108.00	0.04
	Cell count (cell/ml)	8.75E+07

Table E.10: Individual Data Set for cells harvested during late stationary growth (40 hours of growth) with initial arsenite concentration near the K_s value.

T40-3b	Time (min)	[As(III)] (μM)
	0.00	3.51
	15.00	2.47
	24.00	1.45
	33.00	0.96
	41.00	0.63
	49.00	0.41
	54.00	0.33
	66.00	0.17
	74.00	0.11
	86.00	0.07
	96.00	0.05
	108.00	0.03
	Cell count (cell/ml)	8.75E+07

Table E.11: Individual Data Set for cells harvested during late stationary growth (40 hours of growth) with initial arsenite concentration above the K_s value in the V_{max} range.

T40-50a	Time (min)	[As(III)] (μM)
	0.00	52.60
	11.00	49.49
	22.00	47.40
	30.00	46.97
	45.00	43.60
	62.00	40.24
	82.00	36.83
	92.00	33.08
	105.00	27.56
	115.00	23.53
	125.00	19.32
	132.00	16.74
	Cell count (cell/ml)	8.75E+07

Table E.12: Individual Data Set for cells harvested during late stationary growth (40 hours of growth) with initial arsenite concentration above the K_s value in the V_{max} range.

T40-50b	Time (min)	[As(III)] (μM)
	0.00	54.22
	10.00	49.60
	21.00	47.66
	29.00	48.49
	45.00	44.43
	61.00	41.66
	82.00	37.09
	92.00	34.36
	104.00	29.18
	114.00	25.71
	125.00	21.94
	131.00	19.89
	Cell count (cell/ml)	8.75E+07

Appendix F

RFLP ANALYSIS

Gel images from RFLP analysis. In Figures F.1-F.5, boxed and numbered lanes are for clones that were sequenced. Of the remaining gels, the diversity was not studied. For the AOL15 primer gel (Figure F.7), one clone with identical pattern to AOL15 was sequenced but identified as a *Sphingomonas adhaesive* species.

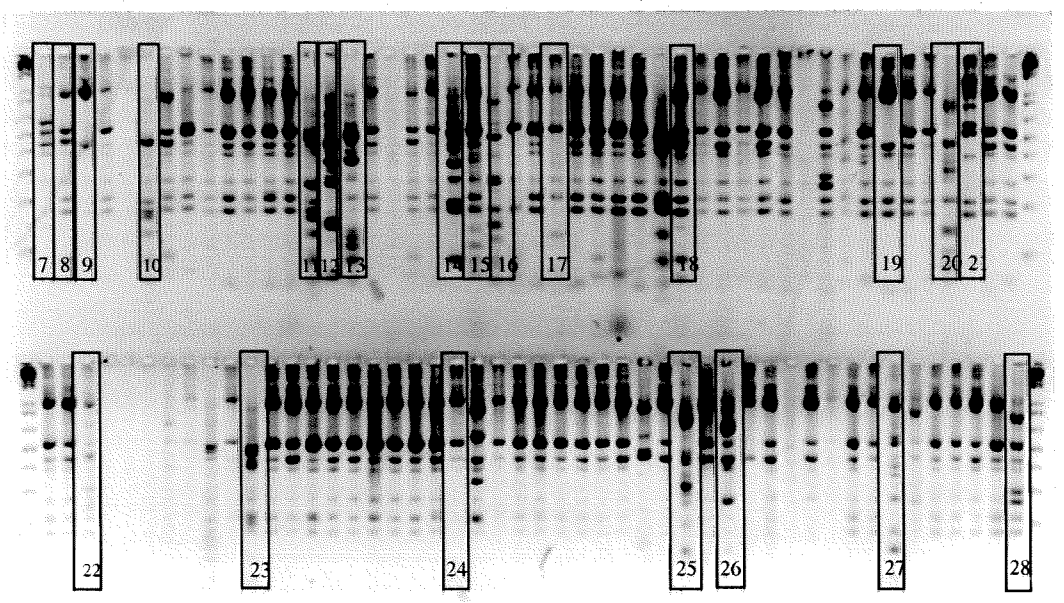

Figure F.1: (from 070900). PBS sample PCR product using bacterial primers 8F and 1492R digested with HinPII and MspI. The clones represented by the RFLP patterns that were selected for sequencing are outlined by a black box.

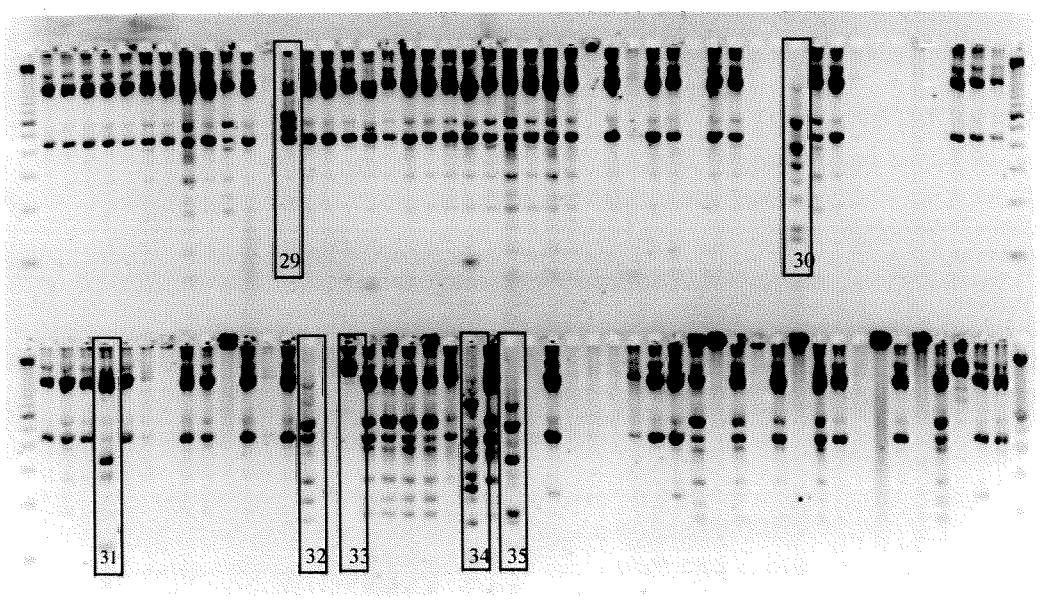

Figure F.2: (from 071600). EtOH sample PCR product using bacterial primers 8F and 1492R digested with HinPII and MspI. The clones represented by the RFLP patterns that were selected for sequencing are outlined by a black box.

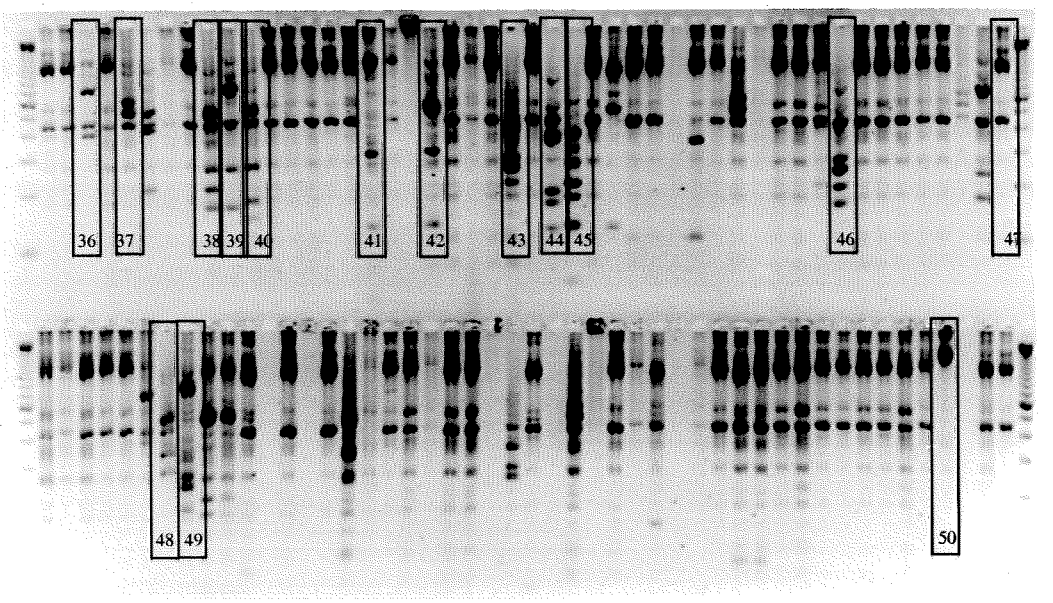

Figure F.3: (from 071600). PBS sample PCR product using bacterial primers 8F and 1492R digested with HinPII and MspI. The clones represented by the RFLP patterns that were selected for sequencing are outlined by a black box.

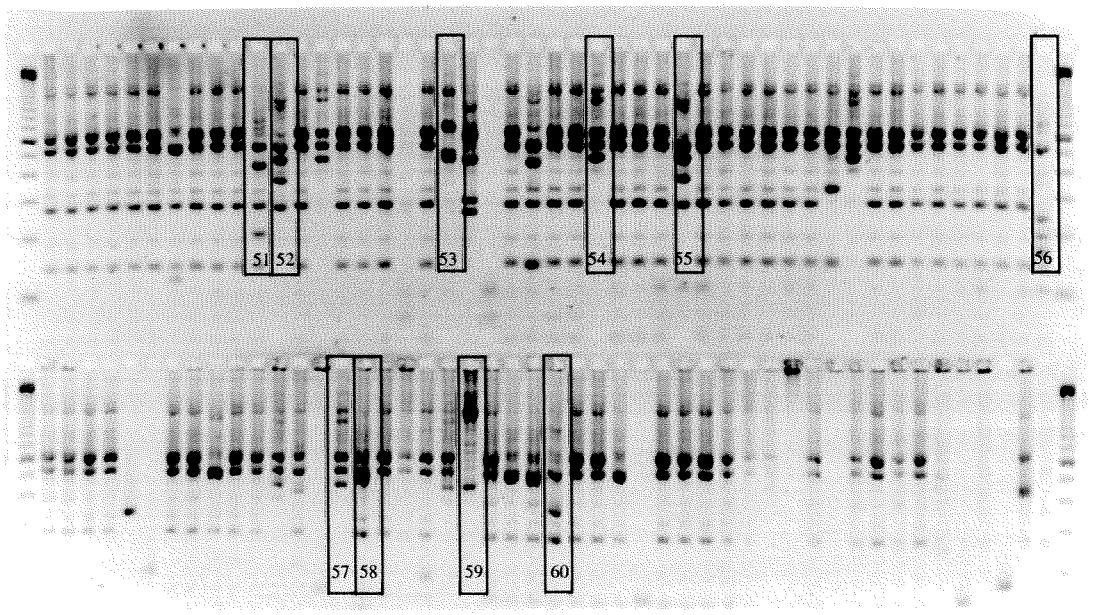

Figure F.4: (from 071700). PBS sample PCR product using bacterial primers 8F and 1492R digested with HinPII and MspI. The clones represented by the RFLP patterns that were selected for sequencing are outlined by a black box.

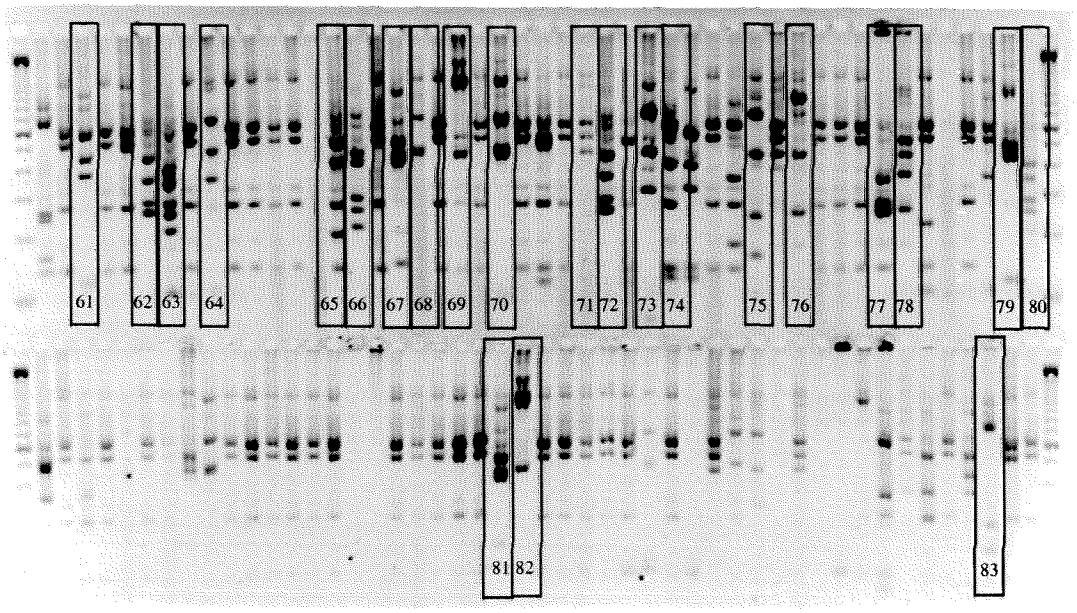

Figure F.5: (from 071700). PBS sample PCR product using bacterial primers 8F and 1492R digested with HinPII and MspI. The clones represented by the RFLP patterns that were selected for sequencing are outlined by a black box.

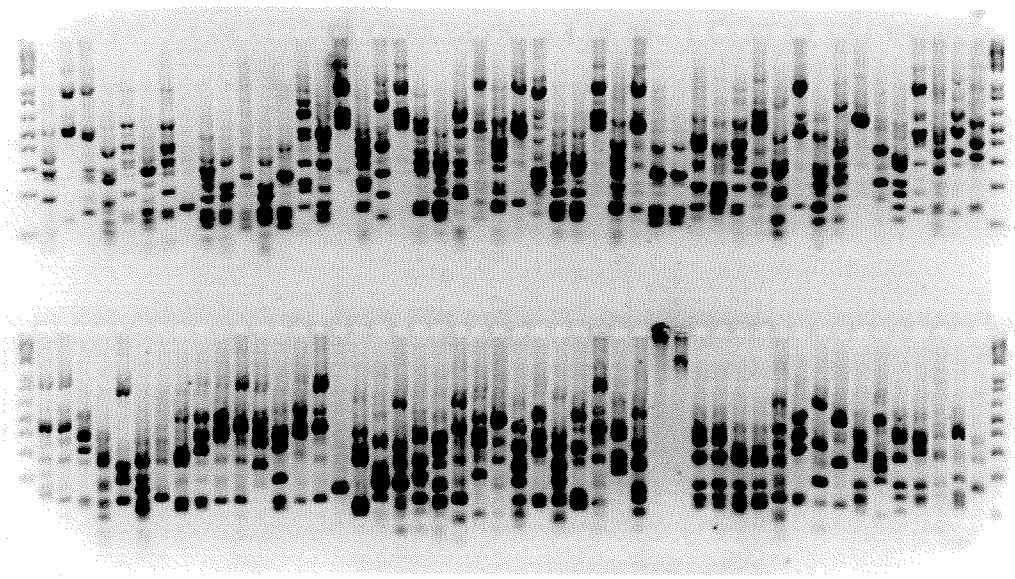

Figure F.6: (072700) EtOH and PBS samples. Representative gel with Alpha primer with 1492R digested with HinPII and MspI. Not analyzed for diversity.

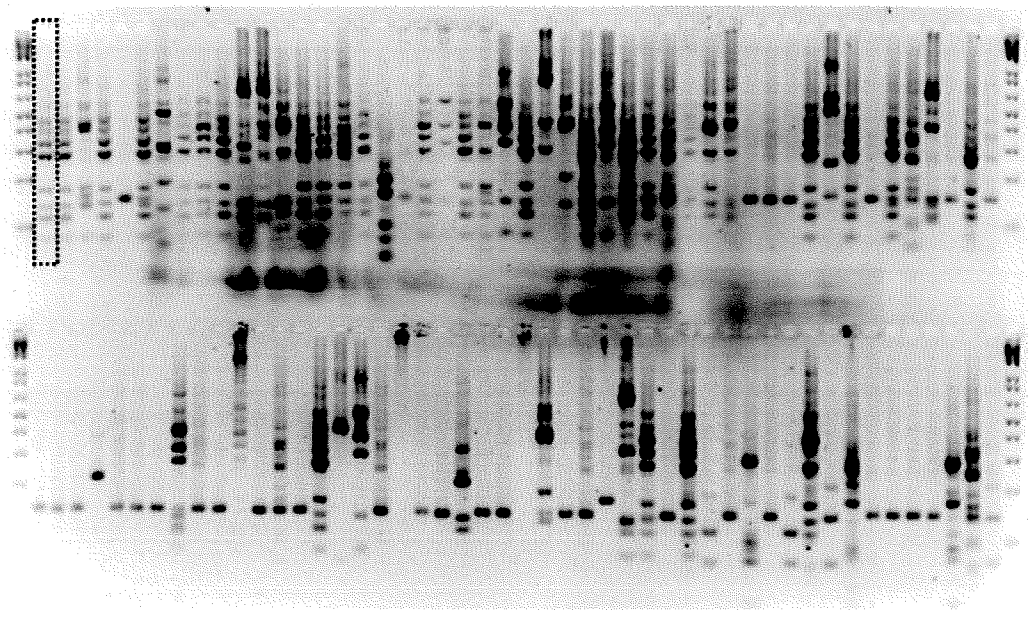

Figure F.7: (072700) EtOH and PBS samples. Representative gel with Alpha primer with 1492R digested with HinPII and MspI. Hatched box for AOL15 RFLP pattern. This pattern is observed in the gel; however sequencing of one of these clones did not result in AOL15.

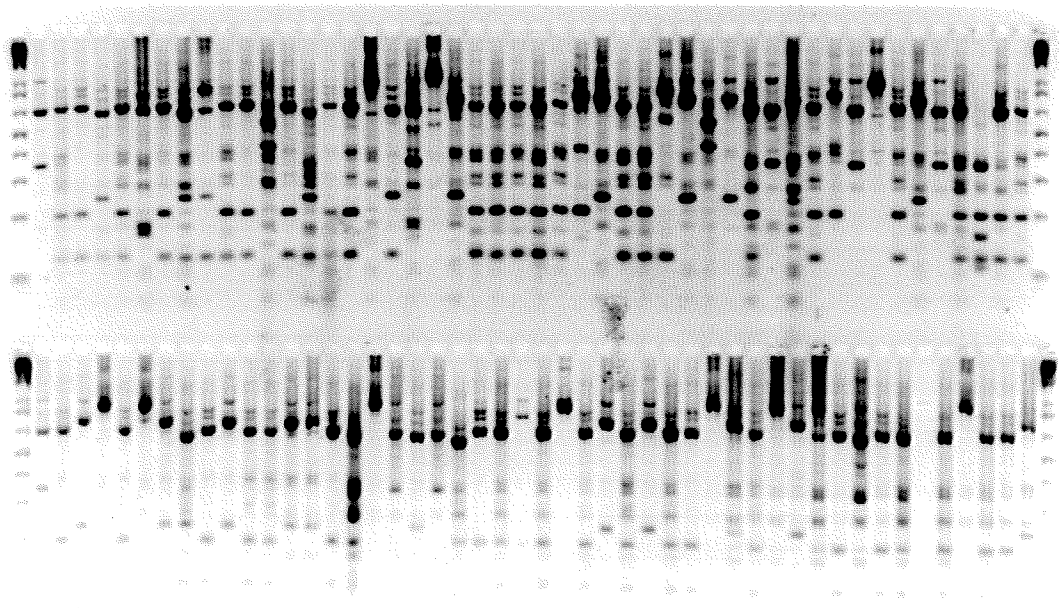

Figure F.8: 071500RFLP. EtOH sample PCR product using bacterial primers 515F and 1195R digested with HinPII and MspI.

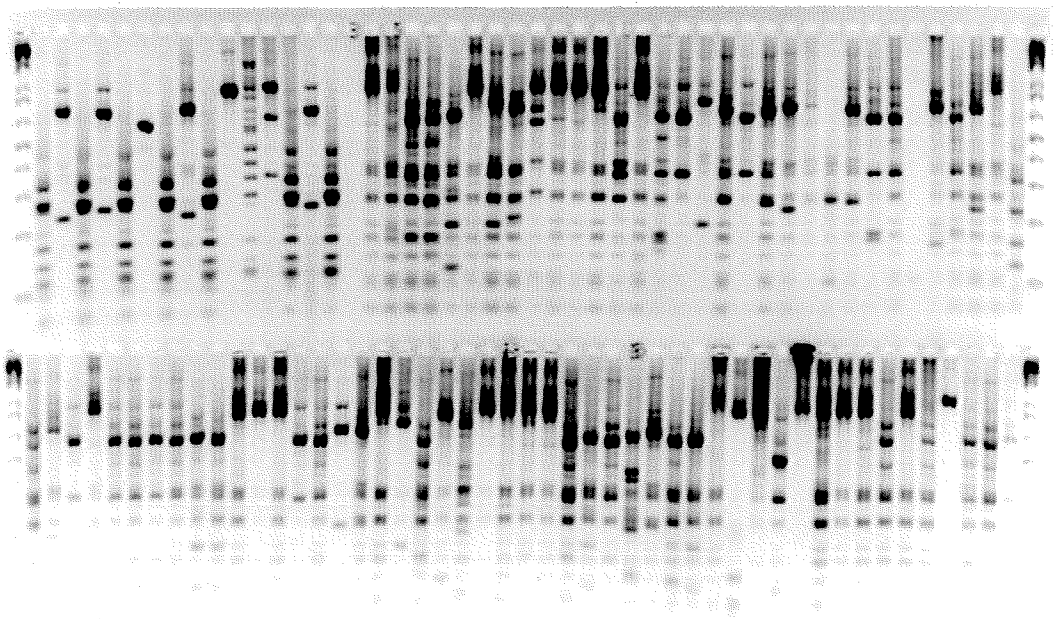

Figure F.9: 071500RFLP. PBS sample PCR product using bacterial primers 515F and 1195R digested with HinPII and MspI.

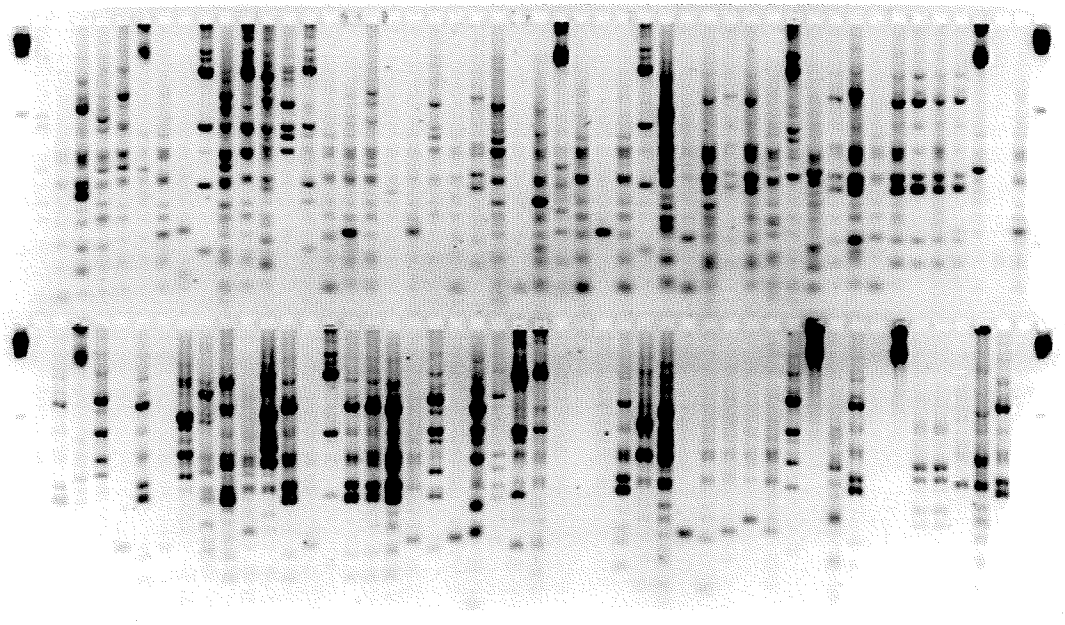

Figure F.10: 071500RFLP. EtOH sample PCR product using bacterial primers 4F and 1492R digested with HinPII and MspI.

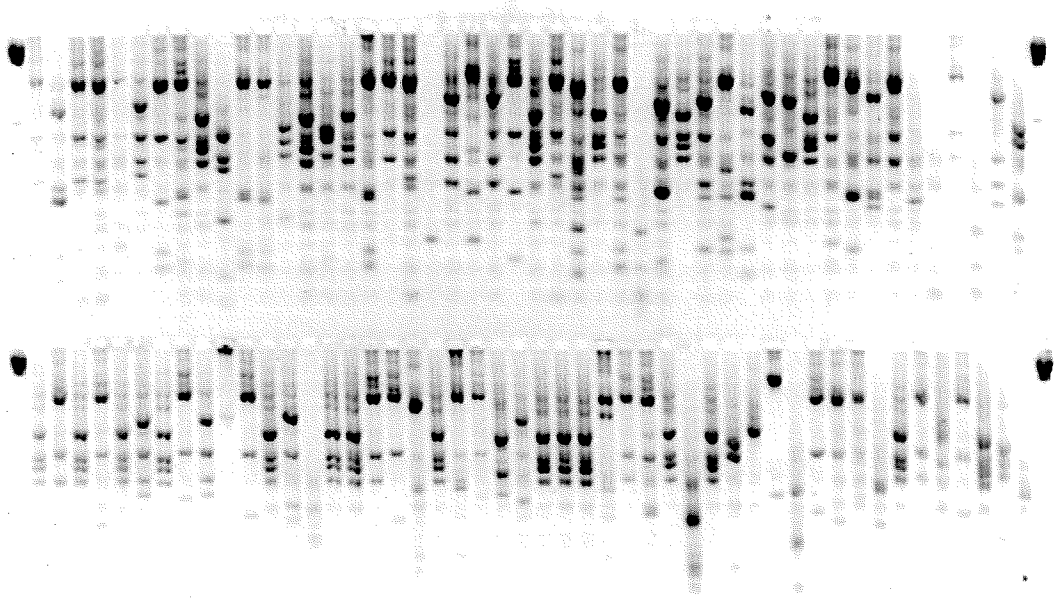

Figure F.11: 071500RFLP. PBS sample PCR product using bacterial primers 4F and 1492R digested with HinPII and MspI.

Appendix G

SEQUENCE ANALYSIS

Phylogenetic tress and similarity matrices for environmental clones.

Table G.1: Appendix G Summary.

Clone Name	Phylogenetic Tree	Similarity Matrix	
Clone #1	Figure G.1	Table G.2	
Clone #2	Figure G.2 Figure G.11	Table G.3 Table G.12	
Clone #3	Figure G.3 Figure G.6	Table G.4 Table G.7	
Clone #7 (partial)	Figure G.4	Table G.5	Cropped
Clone #8	Figure G.5	Table G.6	
Clone #10	Figure G.6	Table G.7	
Clone #11	Figure G.6 Figure G.7	Table G.7 Table G.8	
Clone #12	-	-	Chimeric
Clone #20	Figure G.8	Table G.9	
Clone #23	Figure G.6 Figure G.7	Table G.7 Table G.8	
Clone #25a (partial)	Figure G.9	Table G.10	Cropped
Clone #25b (partial)	Figure G.10	Table G.11	Cropped
Clone #27 (partial)	Figure G.11	Table G.12	Cropped
Clone #29	Figure G.6 Figure G.7	Table G.7 Table G.8	-
Clone #30	Figure G.10	Table G.11	
Clone #31	Figure G.12	Table G.13	-
Clone #32	Figure G.6 Figure G.13	Table G.7 Table G.14	
Clone #33	Figure G.14	Table G.15	
Clone #35	Figure G.15	Table G.16	
Clone #37 (partial)	Figure G.4	Table G.5	Cropped
Clone #38	Figure G.6 Figure G.7	Table G.7 Table G.8	

Clone #39	Figure G.6 Figure G.13	Table G.7 Table G.14	
Clone #42 (partial)	Figure G.5	Table G.6	Cropped
Clone #44 (partial)	Figure G.16	Table G.17	Cropped
Clone #48 (partial)	Figure G.6	Table G.7	Cropped
Clone #49 (partial)	Figure G.17	Table G.18	Cropped
Clone #58	Figure G.18	Table G.19	
Clone #60	Figure G.18	Table G.19	
Clone #61	Figure G.19	Table G.20	
Clone #64 (partial)	Figure G.6	Table G.7	Cropped
Clone #66	Figure G.20	Table G.21	
Clone #80	-	-	Chimeric
Clone #83	Figure G.2 Figure G.11	Table G.3 Table G.12	

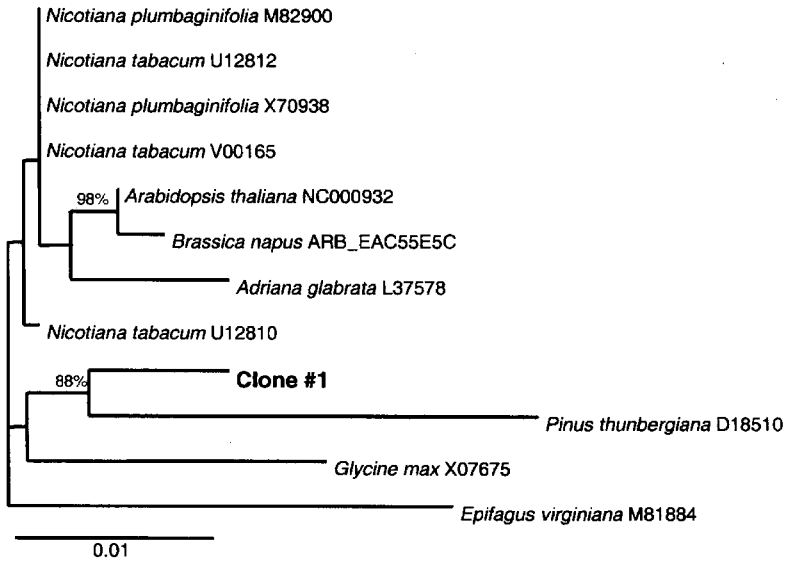

Figure G.1: Phylogenetic tree for Clone #1 by maximum likelihood algorithm in ARB program. A 1272 base mask was applied. The topology of this tree was also supported by a parsimony and distance based tree. Numbers at branch points are bootstrap values that support the tree topology by parsimony. Only bootstrap values greater than 70% are reported in the tree. The accession numbers for the species are shown in the figure.

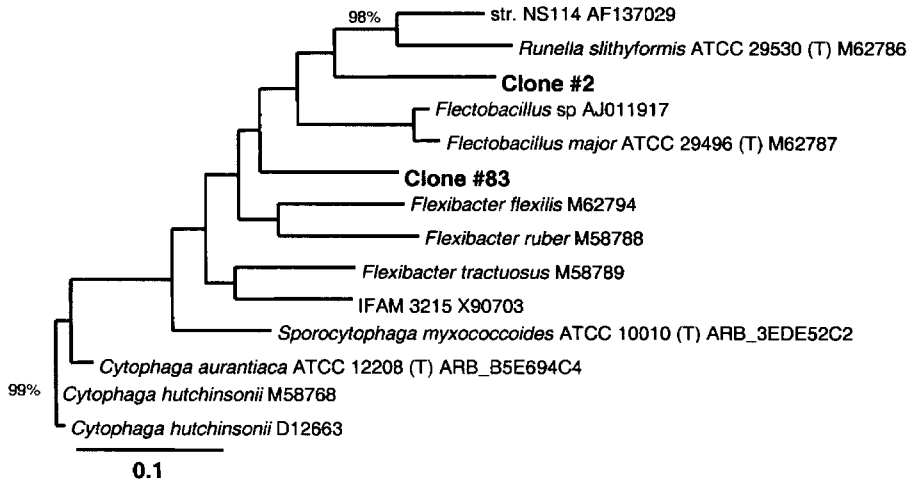

Figure G.2: Phylogenetic tree for Clones #2 and #83 by maximum likelihood algorithm in ARB program. A 1367 base mask was applied. The topology of this tree was also supported by a parsimony and distance based tree. Numbers at branch points are bootstrap values that support the tree topology by parsimony. Only bootstrap values greater than 70% are reported in the tree. The accession numbers for the species are shown in the figure.

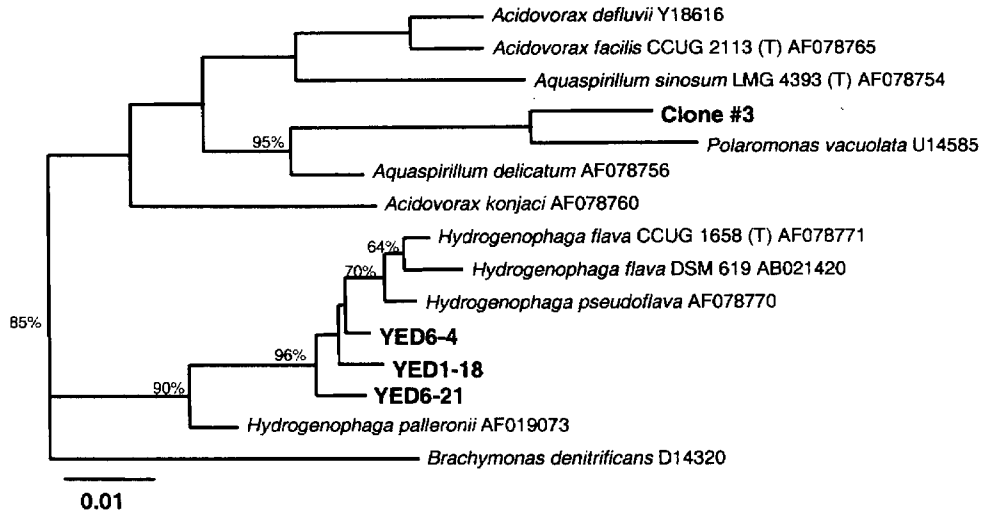

Figure G.3: Phylogenetic tree for Clone #3 by maximum likelihood algorithm in ARB program. A 1386 base mask was applied. The topology of this tree was also supported by a parsimony and distance based tree. Numbers at branch points are bootstrap values that support the tree topology by parsimony. Only bootstrap values greater than 64% are reported in the tree. The accession numbers for the species are shown in the figure.

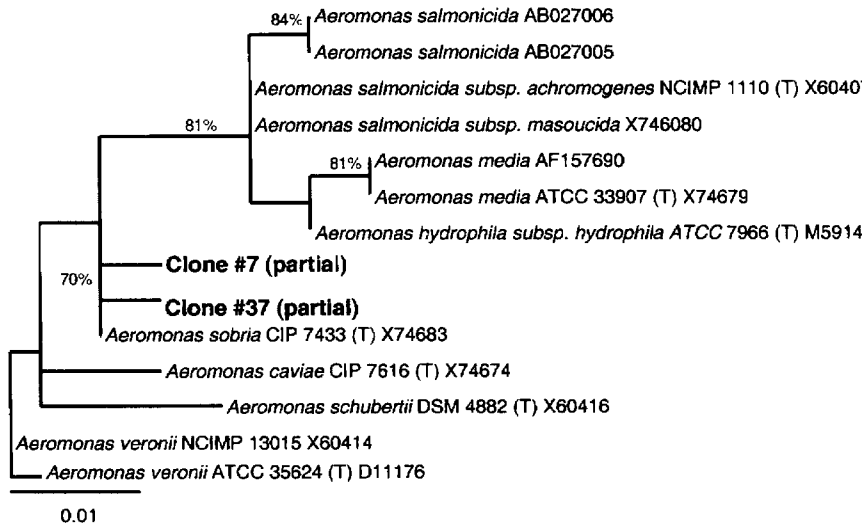

Figure G.4: Phylogenetic tree for Clones #7 (partial) and 37 (partial) by maximum likelihood algorithm in ARB program. A 429 base mask was applied. The topology of this tree was also supported by a parsimony and distance based tree. Numbers at branch points are bootstrap values that support the tree topology by parsimony. Only bootstrap values greater than 70% are reported in the tree. The accession numbers for the species are shown in the figure.

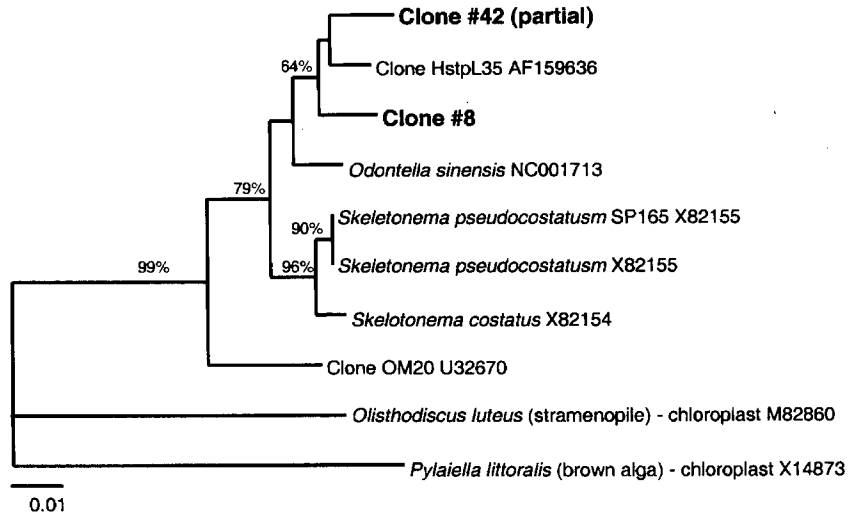

Figure G.5: Phylogenetic tree for Clones #8 and #42 (partial) by maximum likelihood algorithm in ARB program. A 888 base mask was applied. The topology of this tree was also supported by a parsimony and distance based tree. Numbers at branch points are bootstrap values that support the tree topology by parsimony. Only bootstrap values greater than 64% are reported in the tree. The accession numbers for the species are shown in the figure.

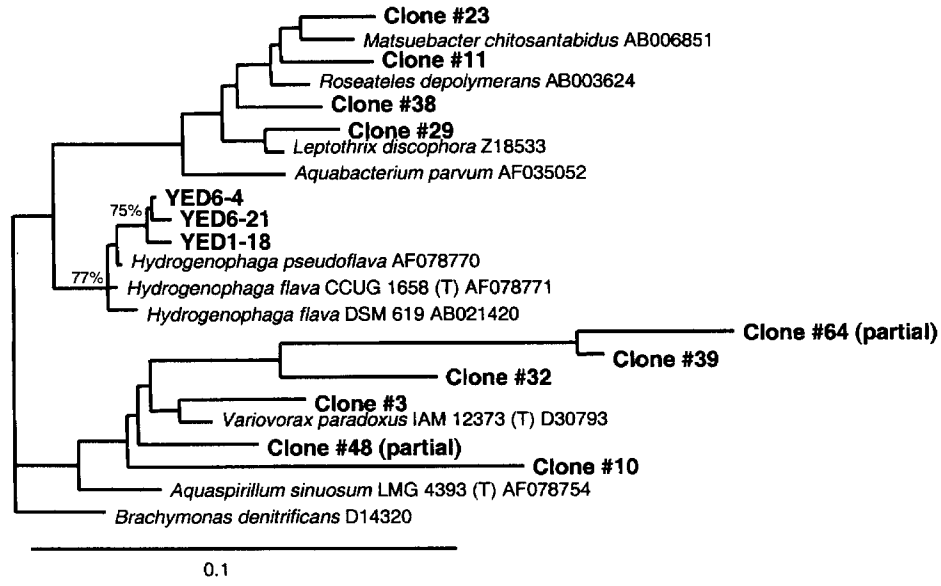

Figure G.6: Phylogenetic tree for Clone #3, #10, #11, #23, #29, #32, #38, #48 (partial) and #64 (partial) by maximum likelihood algorithm in ARB program. A 878 base mask was applied. The topology of this tree was also supported by a parsimony and distance based tree. Numbers at branch points are bootstrap values that support the tree topology by parsimony. Only bootstrap values greater than 70% are reported in the tree. The accession numbers for the species are shown in the figure.

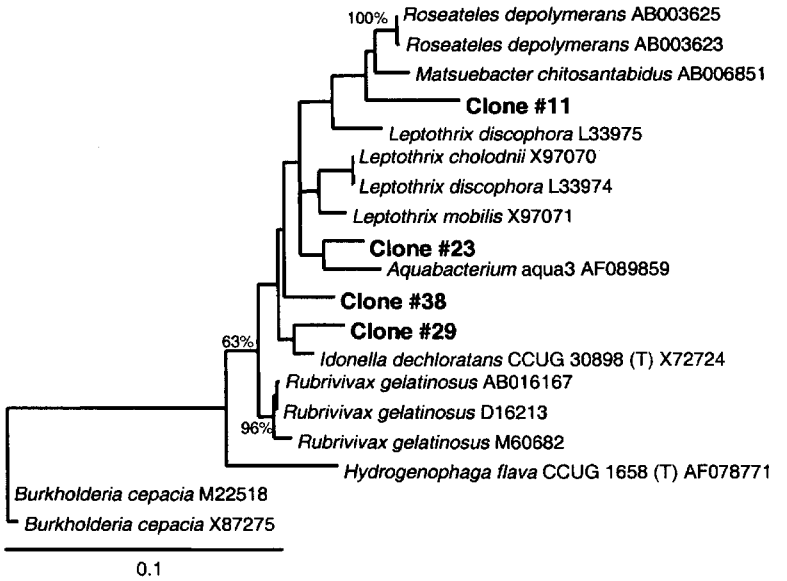

Figure G.7: Phylogenetic tree for Clones #11, #23, #29 and #38 by maximum likelihood algorithm in ARB program. A 1100 base mask was applied. The topology of this tree was also supported by a parsimony and distance based tree. Numbers at branch points are bootstrap values that support the tree topology by parsimony. Only bootstrap values greater than 63% are reported in the tree. The accession numbers for the species are shown in the figure.

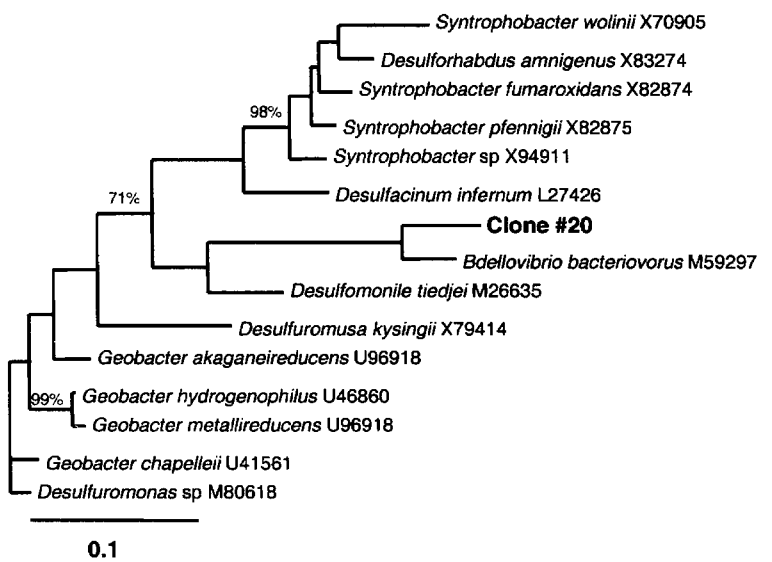

Figure G.8: Phylogenetic tree for Clone #20 by maximum likelihood algorithm in ARB program. A 1382 base mask was applied. The topology of this tree was also supported by a parsimony and distance based tree. Numbers at branch points are bootstrap values that support the tree topology by parsimony. Only bootstrap values greater than 70% are reported in the tree. The accession numbers for the species are shown in the figure.

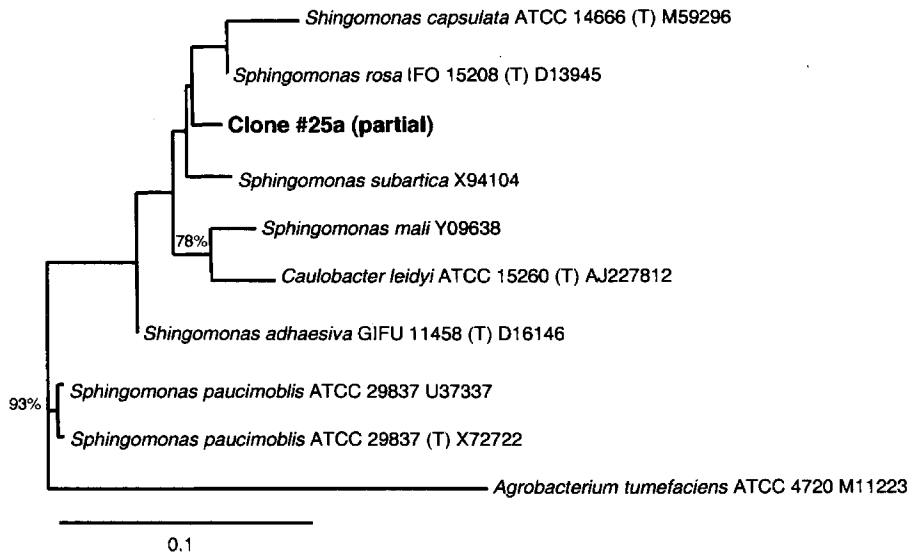

Figure G.9: Phylogenetic tree for Clone #25a (partial) by maximum likelihood algorithm in ARB program. A 396 base mask was applied. The topology of this tree was also supported by a parsimony and distance based tree. Numbers at branch points are bootstrap values that support the tree topology by parsimony. Only bootstrap values greater than 70% are reported in the tree. The accession numbers for the species are shown in the figure.

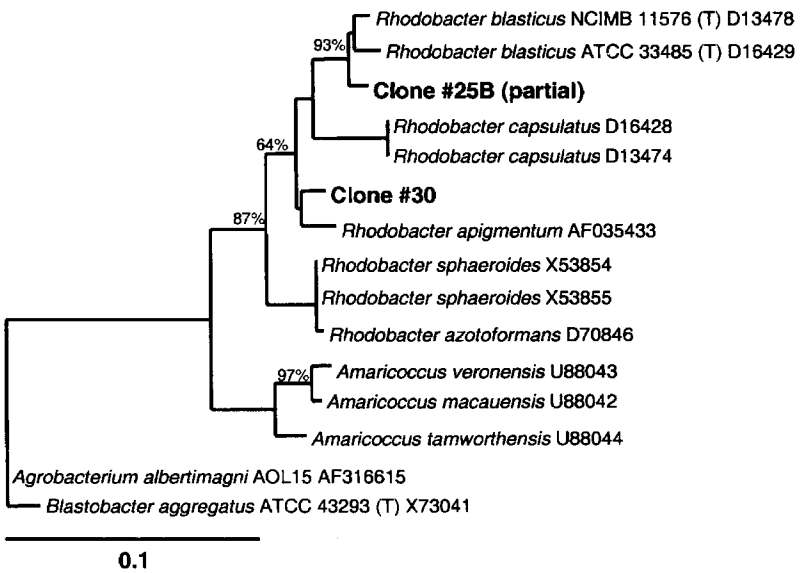

Figure G.10: Phylogenetic tree for Clones #30 and 25b (partial) by maximum likelihood algorithm in ARB program. A 704 base mask was applied. The topology of this tree was also supported by a parsimony and distance based tree. Numbers at branch points are bootstrap values that support the tree topology by parsimony. Only bootstrap values greater than 64% are reported in the tree. The accession numbers for the species are shown in the figure.

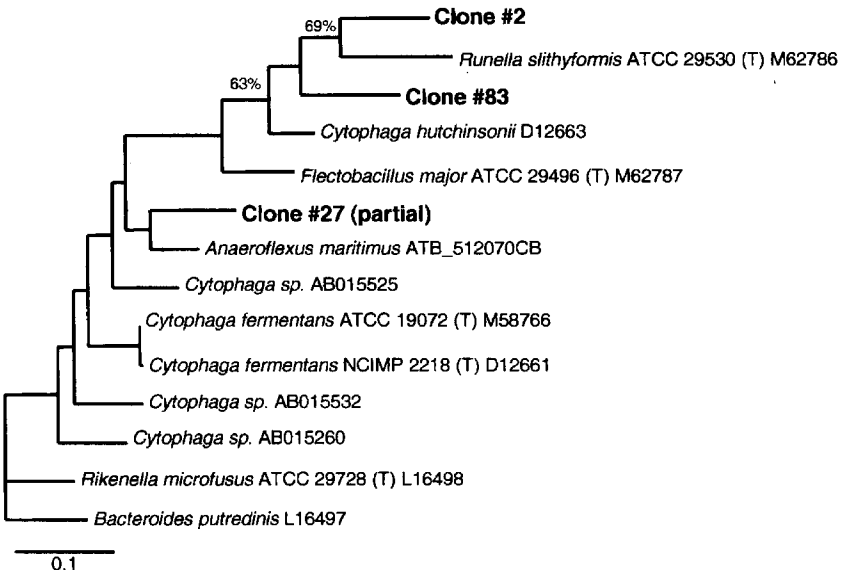

Figure G.11: Phylogenetic tree for Clones #2, #27b (partial) and #83 by maximum likelihood algorithm in ARB program. A 1014 base mask was applied. The topology of this tree was also supported by a parsimony and distance based tree. Numbers at branch points are bootstrap values that support the tree topology by parsimony. Only bootstrap values greater than 63% are reported in the tree. The accession numbers for the species are shown in the figure.

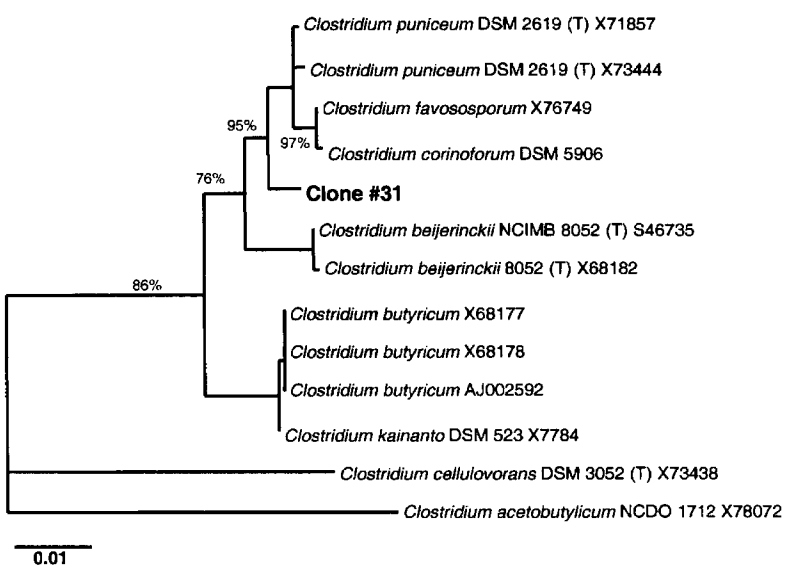

Figure G.12: Phylogenetic tree for Clone #31 by maximum likelihood algorithm in ARB program. A 1317 base mask was applied. The topology of this tree was also supported by a parsimony and distance based tree. Numbers at branch points are bootstrap values that support the tree topology by parsimony. Only bootstrap values greater than 70% are reported in the tree. The accession numbers for the species are shown in the figure.

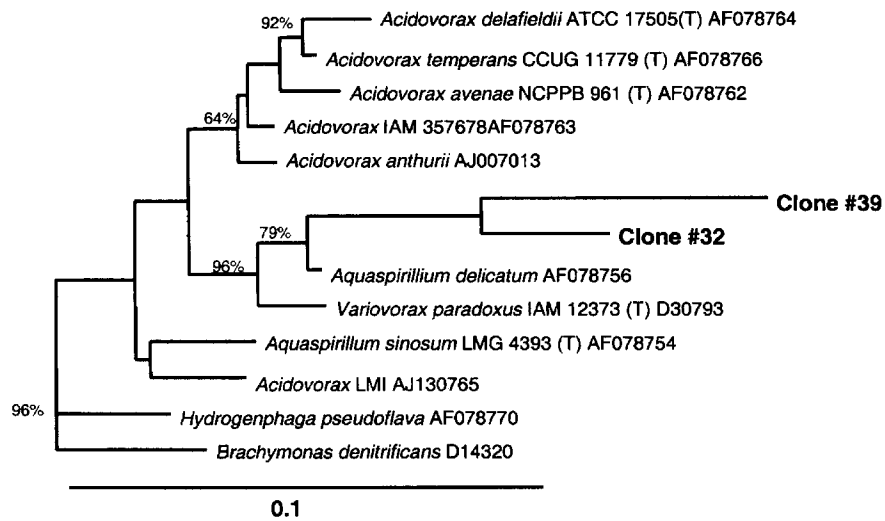

Figure G.13: Phylogenetic tree for Clones #32 and #39 by maximum likelihood algorithm in ARB program. A 1325 base mask was applied. The topology of this tree was also supported by a parsimony and distance based tree. Numbers at branch points are bootstrap values that support the tree topology by parsimony. Only bootstrap values greater than 64% are reported in the tree. The accession numbers for the species are shown in the figure.

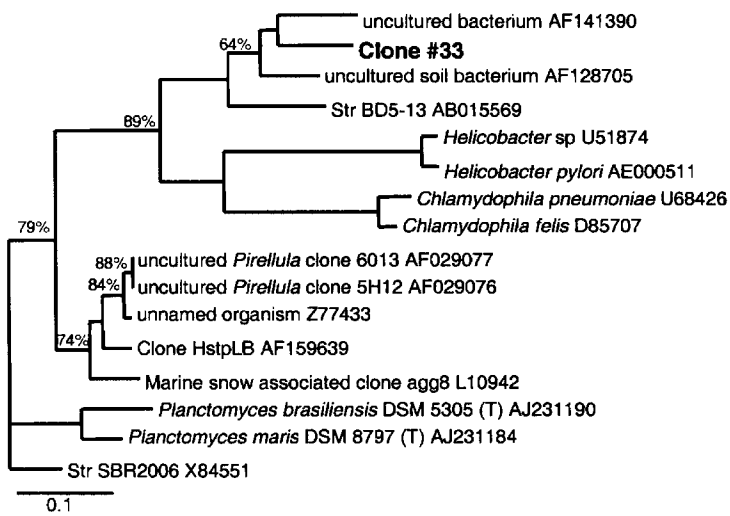

Figure G.14: Phylogenetic tree for Clone #33 by maximum likelihood algorithm in ARB program. A 272 base mask was applied. The topology of this tree was also supported by a parsimony and distance based tree. Numbers at branch points are bootstrap values that support the tree topology by parsimony. Only bootstrap values greater than 64% are reported in the tree. The accession numbers for the species are shown in the figure.

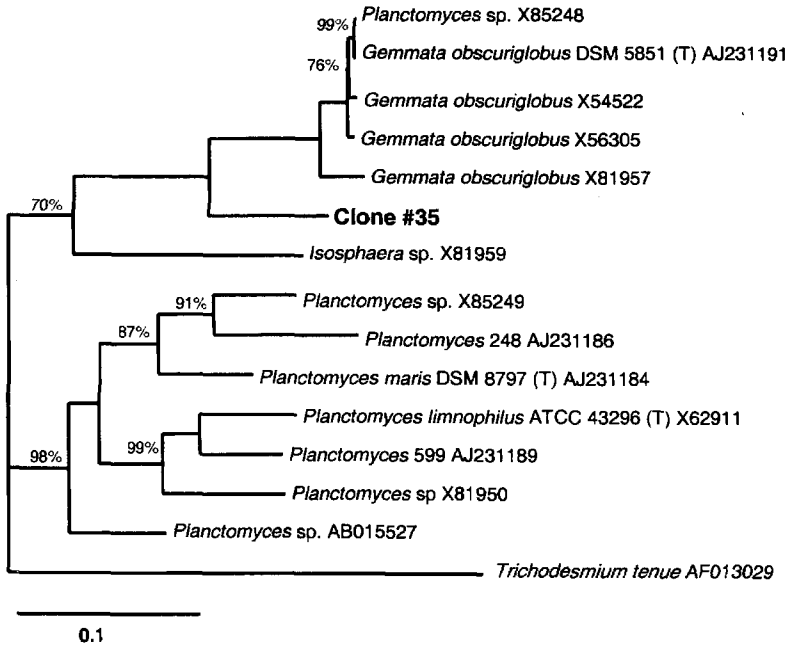

Figure G.15: Phylogenetic tree for Clone #35 by maximum likelihood algorithm in ARB program. A 1347 base mask was applied. The topology of this tree was also supported by a parsimony and distance based tree. Numbers at branch points are bootstrap values that support the tree topology by parsimony. Only bootstrap values greater than 70% are reported in the tree. The accession numbers for the species are shown in the figure.

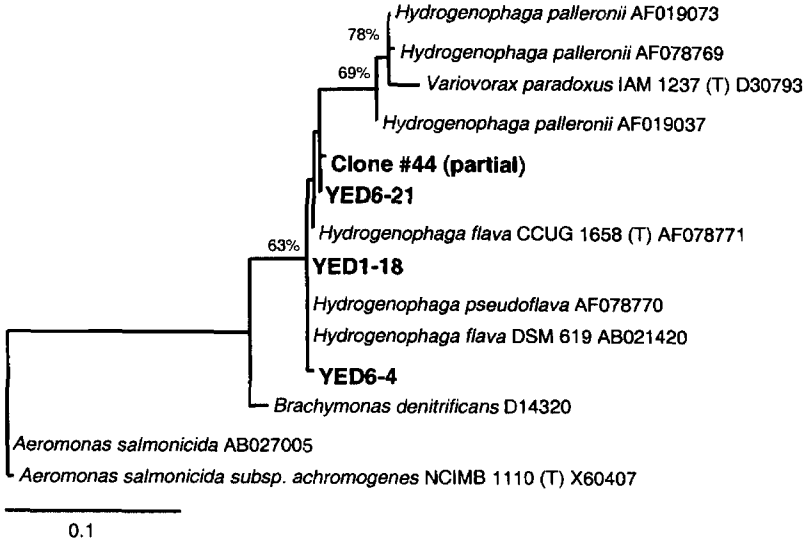

Figure G.16: Phylogenetic tree for Clone #44 (partial) by maximum likelihood algorithm in ARB program. A 286 base mask was applied. The topology of this tree was also supported by a parsimony and distance based tree. Numbers at branch points are bootstrap values that support the tree topology by parsimony. Only bootstrap values greater than 63% are reported in the tree. The accession numbers for the species are shown in the figure.

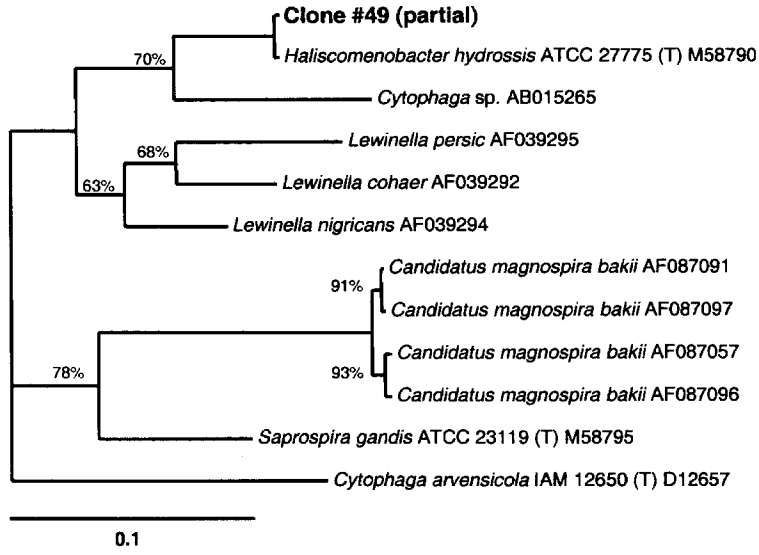

Figure G.17: Phylogenetic tree for Clone #49 (partial) by maximum likelihood algorithm in ARB program. A 1114 base mask was applied. The topology of this tree was also supported by a parsimony and distance based tree. Numbers at branch points are bootstrap values that support the tree topology by parsimony. Only bootstrap values greater than 63% are reported in the tree. The accession numbers for the species are shown in the figure.

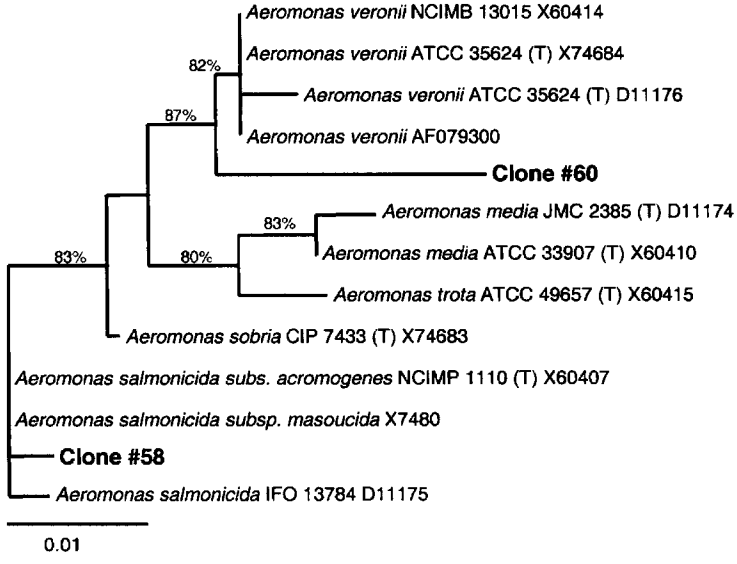

Figure G.18: Phylogenetic tree for Clone #60 and #58 by maximum likelihood algorithm in ARB program. A 429 base mask was applied. The topology of this tree was also supported by a parsimony and distance based tree. Numbers at branch points are bootstrap values that support the tree topology by parsimony. Only bootstrap values greater than 70% are reported in the tree. The accession numbers for the species are shown in the figure.

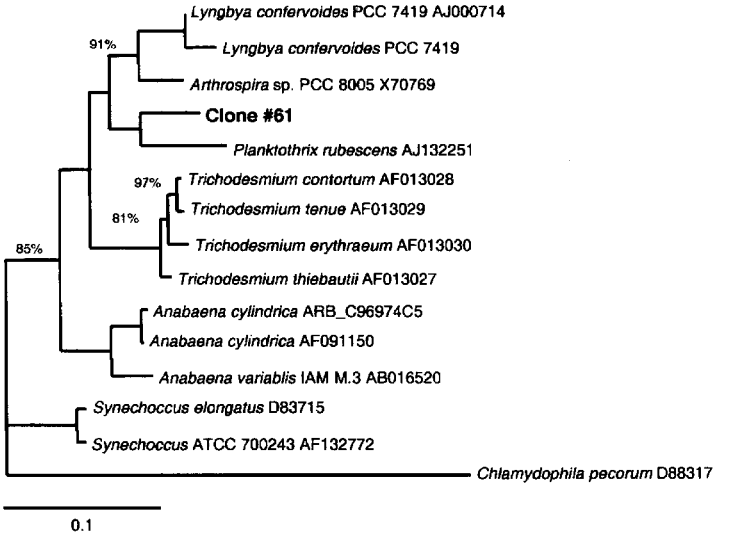

Figure G.19: Phylogenetic tree for Clone #61 by maximum likelihood algorithm in ARB program. A 1082 base mask was applied. The topology of this tree was also supported by a parsimony and distance based tree. Numbers at branch points are bootstrap values that support the tree topology by parsimony. Only bootstrap values greater than 70% are reported in the tree. The accession numbers for the species are shown in the figure.

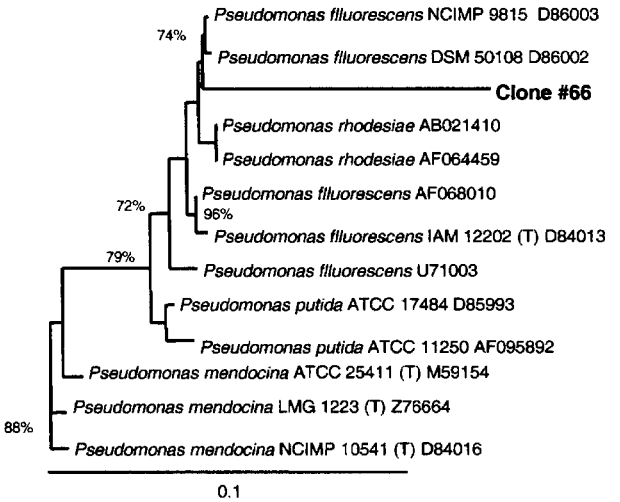

Figure G.20: Phylogenetic tree for Clone #66 by maximum likelihood algorithm in ARB program. A 1204 base mask was applied. The topology of this tree was also supported by a parsimony and distance based tree. Numbers at branch points are bootstrap values that support the tree topology by parsimony. Only bootstrap values greater than 70% are reported in the tree. The accession numbers for the species are shown in the figure.

Table G.2: Similarity matrix for Clone #1 comparing the 16S rDNA genes. Matrix generated using the maximum likelihood algorithm from the ARB program.

		1	2	3	4	5	6	7	8	9	10	11	12
1	*Epifagus virginiana chloroplast M81884*	100.0	-	-	-	-	-	-	-	-	-	-	-
2	*Nicotiana tabacum chloroplast U12810*	97.6	100.0	-	-	-	-	-	-	-	-	-	-
3	*Nicotiana tabacum chloroplast V00165*	97.6	99.8	100.0	-	-	-	-	-	-	-	-	-
4	*Pinus thunbergiana D17510*	95.0	97.2	97.2	100.0	-	-	-	-	-	-	-	-
5	*Nicotiana tabacum chloroplast U12812*	97.6	99.8	100.0	97.2	100.0	-	-	-	-	-	-	-
6	*Adriana glabrata L37578*	96.6	98.9	99.0	96.2	99.0	100.0	-	-	-	-	-	-
7	*Nicotiana plumbaginifolia M82900*	97.6	99.8	100.0	97.2	100.0	99.0	100.0	-	-	-	-	-
8	*Brassica napus ARB_EAC55E5C*	96.9	99.2	99.4	96.6	99.4	98.7	99.4	100.0	-	-	-	-
9	*Glycine max X07657*	96.1	98.2	98.2	96.1	98.2	97.7	98.2	98.1	100.0	-	-	-
10	*Nicotiana plumbaginifolia X70938*	97.6	99.8	100.0	97.2	100.0	99.0	100.0	99.4	98.2	100.0	-	-
11	**Clone #1**	96.6	98.7	**98.9**	97.0	**98.9**	98.1	**98.9**	98.6	97.7	**98.9**	100.0	-
12	*Arabidopsis thaliana NC000932*	97.2	99.5	99.6	96.9	99.6	99.0	99.6	99.8	98.2	99.6	98.7	100.0

Table G.3: Similarity matrix for Clones #2 and #83 comparing the 16S rDNA genes. Matrix generated using the maximum likelihood algorithm from the ARB program.

		1.0	2.0	3.0	4.0	5.0	6.0	7.0	8.0	9.0	10.0	11.0	12.0	13.0	14.0
1	*Cytophaga hutchinsonii D12663*	100.0	-	-	-	-	-	-	-	-	-	-	-	-	-
2	*Cytophaga hutchinsonii M58768*	99.4	100.0	-	-	-	-	-	-	-	-	-	-	-	-
3	*Cytophaga aurantiaca ATCC 12208 (T) ARB_B5E694C4*	96.8	97.5	100.0	-	-	-	-	-	-	-	-	-	-	-
4	*Flectobacillus major ATCC 29496 (T) M62787*	83.4	83.4	82.0	100.0	-	-	-	-	-	-	-	-	-	-
5	*Flectobacillus sp AJ011917*	82.8	83.0	82.2	97.2	100.0	-	-	-	-	-	-	-	-	-
6	*Runella slithyformis ATCC 29530 (T) M62786*	79.0	78.8	79.6	78.9	79.2	100.0	-	-	-	-	-	-	-	-
7	*str. NS114 AF137029*	80.6	80.0	80.3	82.4	83.2	86.4	100.0	-	-	-	-	-	-	-
8	*Flexibacter ruber M58788*	80.0	80.3	80.1	80.4	80.7	78.5	79.1	100.0	-	-	-	-	-	-
9	*Flexibacter flexilis M62794*	82.6	83.6	82.4	83.0	82.6	76.9	79.1	82.3	100.0	-	-	-	-	-
10	*Sporocytophaga myxococcoides ATCC 10010 (T) ARB_3EDE52C2*	86.5	86.0	85.7	81.5	81.1	78.3	80.4	81.9	81.2	100.0	-	-	-	-
11	*IFAM 3215 X90703*	82.4	82.7	82.9	81.3	80.9	78.8	79.4	80.8	82.1	83.2	100.0	-	-	-
12	*Flexivbacter tractuosus M58789*	82.9	82.2	81.7	79.5	80.2	75.7	79.1	80.4	80.1	85.2	84.2	100.0	-	-
13	**Clone #2**	81.2	81.0	80.6	79.8	80.9	80.5	79.5	79.6	78.3	80.6	79.3	76.8	100.0	-
14	**Clone #83**	84.5	84.6	84.6	80.4	80.4	79.6	80.1	80.3	83.4	82.4	83.5	78.8	79.6	100.0

Table G.4: Similarity matrix for Clone #3 comparing the 16S rDNA genes. Matrix generated using the maximum likelihood algorithm from the ARB program.

		1	2	3	4	5	6	7	8	9	10	11	12	13	14	15
1	*Bradymonas denitrificans D14320*	100.0	-	-	-	-	-	-	-	-	-	-	-	-	-	-
2	*Hydrogenophaga flava CCUG 1658 (T) AF078771*	94.3	100.0	-	-	-	-	-	-	-	-	-	-	-	-	-
3	*Hydrogenophaga flava DSM 619 AB021420*	94.3	99.1	100.0	-	-	-	-	-	-	-	-	-	-	-	-
4	*Hydrogenophaga pseudoflava (AF078770)*	94.4	99.1	98.8	100.0	-	-	-	-	-	-	-	-	-	-	-
5	*Hydrogenophaga palleronii AF029073*	94.1	97.3	97.2	96.9	100.0	-	-	-	-	-	-	-	-	-	-
6	*Aquaspirillum delicatum AF078756*	93.1	94.5	94.4	94.2	95.6	100.0	-	-	-	-	-	-	-	-	-
7	*Polaromonas vaculota U14585*	90.7	92.0	91.6	91.8	92.9	94.9	100.0	-	-	-	-	-	-	-	-
8	*Acidovorax facilis CCUG2113 (T) AF078765*	92.3	92.5	92.3	92.2	93.3	95.2	93.4	100.0	-	-	-	-	-	-	-
9	*Acidovorax defluvii Y18616*	92.6	93.1	93.1	92.9	93.6	95.3	93.6	98.4	100.0	-	-	-	-	-	-
10	*Acidovorax konjaci AF078760*	92.8	93.9	93.8	93.9	94.6	95.0	92.3	95.5	95.1	100.0	-	-	-	-	-
11	*Aquaspirillum sinosum LMG 4393 (T) AF078754*	93.9	94.1	93.8	94.1	93.6	95.1	92.1	95.4	95.4	94.3	100.0	-	-	-	-
12	**Clone #3**	90.9	92.7	92.4	92.4	93.6	95.3	96.8	93.1	93.2	91.8	92.4	100.0	-	-	-
13	**YED1-18**	94.4	98.5	98.2	98.6	97.6	94.6	92.1	92.4	92.5	93.8	94.3	92.8	100.0	-	-
14	**YED6-21**	93.9	98.3	97.9	98.3	97.5	94.6	92.3	92.4	92.6	93.9	94.1	92.7	98.7	100.0	-
15	**YED6-4**	94.3	98.8	98.5	98.9	97.4	94.6	92.2	92.5	92.5	94.1	94.5	92.7	99.5	99.0	100.0

Table G.5: Similarity matrix for Clones #7(partial) and #37(partial) comparing the 16S rDNA genes. Matrix generated using the maximum likelihood algorithm from the ARB program.

		1	2	3	4	5	6	7	8	9	10	11	12	13	14
1	*Aeromonas salmonicida subsp. Masoucida X74680*	100.0	-	-	-	-	-	-	-	-	-	-	-	-	-
2	*Aeromonas veronii ATCC 35624 (T) D11176*	98.1	100.0	-	-	-	-	-	-	-	-	-	-	-	-
3	*Aeromonas sobria CIP 7433 (T) X74683*	98.8	99.1	100.0	-	-	-	-	-	-	-	-	-	-	-
4	*Aeromonas veronii NCIMP 13015 X60414*	98.4	99.8	99.3	100.0	-	-	-	-	-	-	-	-	-	-
5	*Aeromonas hydrophila subsp. Hydrophila ATCC 7966 (T) M59148*	99.5	98.3	98.4	98.3	100.0	-	-	-	-	-	-	-	-	-
6	*Aeromonas salmonicida subsp. Achromogenes NCIMP 1110 (T) X60407*	100.0	98.1	98.8	98.4	99.5	100.0	-	-	-	-	-	-	-	-
7	*Aeomonas salmonicida AB027005*	99.5	97.6	98.4	97.9	99.1	99.5	100.0	-	-	-	-	-	-	-
8	*Aeromonas salmonicida*	99.5	97.6	98.4	97.9	99.1	99.5	100.0	100.0	-	-	-	-	-	-
9	*Aeromonas schubertii DSM 4882 (T) X60416*	97.9	98.3	98.1	98.6	97.9	97.9	97.9	97.9	100.0	-	-	-	-	-
10	*Aeromonas caviae CIP 7616 (T) X74674*	97.4	98.6	98.6	98.8	97.4	97.4	96.9	96.9	97.6	100.0	-	-	-	-
11	*Aeromonas media ATCC 33907 (T) X74679*	99.1	98.1	98.4	98.4	99.5	99.1	98.6	98.6	97.9	97.4	100.0	-	-	-
12	*Aeromonas media AF157690*	99.1	98.1	98.4	98.4	99.5	99.1	98.6	98.6	97.9	97.4	100.0	100.0	-	-
13	**Clone #37 (partial)**	98.3	98.6	99.5	98.8	97.9	98.3	97.9	97.9	97.6	98.1	97.9	97.9	100.0	-
14	**Clone #7 (partial)**	98.3	98.5	99.5	98.8	97.8	98.3	97.8	97.8	97.6	98.1	97.8	97.8	99.0	100.0

Table G.6: Similarity matrix for Clones #8 and 42(partial) comparing the 16S rDNA genes. Matrix generated using the maximum likelihood algorithm from the ARB program.

		1	2	3	4	5	6	7	8	9	10
1	*Clone OM20 U32670*	100.0	95.6	95.1	95.5	88.2	87.4	95.9	95.6	95.8	95.6
2	*Skeletonema pseudocostatum X82155*	95.6	100.0	99.1	96.9	89.2	87.4	97.0	96.7	97.4	100.0
3	*Skeletonema costatus X82154*	95.1	99.1	100.0	96.8	89.0	87.1	96.6	96.6	97.1	99.1
4	*Clone HstpL35 AF159636*	95.5	96.9	96.8	100.0	88.5	87.0	97.8	97.9	98.0	96.9
5	*Olisthodiscus luteus (stramenopile) - chloroplast M82860*	88.2	89.2	89.0	88.5	100.0	86.3	88.6	88.7	89.8	89.2
6	*Pylaiella littoralis (brown alga) - chloroplast X14873*	87.4	87.4	87.1	87.0	86.3	100.0	87.7	87.0	87.4	87.4
7	**Clone #8**	95.9	97.0	96.6	97.8	88.6	87.7	100.0	97.6	97.3	97.0
8	**Clone #42 (partial)**	95.6	96.7	96.6	97.9	88.7	87.0	97.6	100.0	97.2	96.7
9	*Odontella sinensis NC001713*	95.8	97.4	97.1	98.0	89.8	87.4	97.3	97.2	100.0	97.4
10	*Skeletonema pseudocostatum SP16S X82155*	95.6	100.0	99.1	96.9	89.2	87.4	97.0	96.7	97.4	100.0

Table G.7: Similarity matrix for several clones comparing the 16S rDNA genes. Matrix generated using the maximum likelihood algorithm from the ARB program.

		1	2	3	4	5	6	7	8	9	10	11	12	13	14	15	16	17	18	19	20	21	22	23
1	*Brachymonas denitrificans D14320*	100.0	-	-	-	-	-	-	-	-	-	-	-	-	-	-	-	-	-	-	-	-	-	-
2	*Hydrogenophaga flava CCUG 1658 (T) AF078771*	95.6	100.0	-	-	-	-	-	-	-	-	-	-	-	-	-	-	-	-	-	-	-	-	-
3	*Hydrogenophaga flava DSM 619 AB021420*	95.7	99.1	100.0	-	-	-	-	-	-	-	-	-	-	-	-	-	-	-	-	-	-	-	-
4	*Hydrogenophaga pseudoflava AF078770*	95.6	99.4	99.0	100.0	-	-	-	-	-	-	-	-	-	-	-	-	-	-	-	-	-	-	-
5	*Variovorax paradoxus IAM 12373 (T) D30793*	93.8	94.5	94.3	94.6	100.0	-	-	-	-	-	-	-	-	-	-	-	-	-	-	-	-	-	-
6	*Aquaspirillum sinuosum LMG 4393 (T) AF078754*	94.9	94.8	94.4	94.9	95.5	100.0	-	-	-	-	-	-	-	-	-	-	-	-	-	-	-	-	-
7	*Matsuebacter chitosantoabidus AB006851*	93.6	92.9	93.2	93.0	92.7	92.6	100.0	-	-	-	-	-	-	-	-	-	-	-	-	-	-	-	-
8	*Aquabacterium parvum AF035052*	92.9	93.6	93.6	93.5	91.4	92.6	95.6	100.0	-	-	-	-	-	-	-	-	-	-	-	-	-	-	-
9	*Roseateles depolymerans AB003624*	92.2	92.9	93.0	93.0	91.8	91.8	97.4	95.8	100.0	-	-	-	-	-	-	-	-	-	-	-	-	-	-
10	*Leptothrix discophora Z18533*	93.6	93.5	93.5	93.4	92.0	92.2	96.4	95.5	96.6	100.0	-	-	-	-	-	-	-	-	-	-	-	-	-
11	**Clone #10**	87.6	89.2	89.3	89.3	88.9	87.4	84.8	83.5	83.1	83.2	100.0	-	-	-	-	-	-	-	-	-	-	-	-
12	**Clone #11**	91.8	92.1	91.9	92.0	91.3	91.8	96.4	94.6	96.8	96.5	83.4	100.0	-	-	-	-	-	-	-	-	-	-	-
13	**Clone #23**	92.9	93.4	93.1	93.8	92.8	92.3	97.3	95.1	96.9	96.1	83.6	96.0	100.0	-	-	-	-	-	-	-	-	-	-
14	**Clone #29**	93.1	93.0	93.1	92.8	91.8	92.2	95.5	95.0	96.2	97.8	84.0	96.8	95.7	100.0	-	-	-	-	-	-	-	-	-
15	**Clone #3**	92.6	93.2	93.0	93.4	96.2	93.1	93.1	91.8	91.8	91.4	87.4	91.0	92.5	91.2	100.0	-	-	-	-	-	-	-	-
16	**Clone #32**	90.6	91.0	90.8	91.3	92.5	92.3	90.1	89.5	89.4	89.1	84.6	88.0	89.9	88.6	91.0	100.0	-	-	-	-	-	-	-
17	**Clone #38**	93.2	93.5	93.4	93.9	92.2	91.5	95.8	95.1	96.5	96.5	84.5	96.0	95.6	96.6	92.0	89.4	100.0	-	-	-	-	-	-
18	**Clone #39**	86.2	87.3	86.7	87.2	88.8	89.2	86.8	86.7	86.1	86.5	80.1	86.7	86.3	87.1	87.3	89.1	85.7	100.0	-	-	-	-	-
19	**YED1-18**	95.5	98.3	97.8	98.6	94.5	94.9	92.5	93.4	92.1	92.8	89.7	91.1	93.2	92.4	93.6	90.8	93.6	86.5	100.0	-	-	-	-
20	**YED6-21**	95.3	98.3	97.9	98.6	95.1	95.0	92.7	93.6	92.5	93.3	89.3	91.9	93.6	92.7	93.8	90.8	93.6	86.9	98.9	100.0	-	-	-
21	**YED6-4**	95.5	98.6	98.1	99.0	95.0	95.2	92.6	93.6	92.5	93.3	89.6	91.8	93.6	92.8	93.6	91.1	93.7	87.2	99.7	99.4	100.0	-	-
22	**Clone #48 (partial)**	94.0	94.1	93.5	94.0	96.1	94.7	92.2	90.7	90.6	91.6	87.7	90.9	91.5	91.8	93.5	90.4	91.0	88.7	93.7	94.4	94.3	100.0	-
23	**Clone_#64 (partial)**	84.8	85.0	84.5	84.9	86.1	86.2	86.1	85.8	85.5	85.9	78.0	86.1	85.3	86.8	85.4	86.8	85.8	95.7	84.6	84.6	85.0	86.5	100.0

Table G.8: Similarity matrix for several comparing the 16S rDNA genes. Matrix generated using the maximum likelihood algorithm from the ARB program.

		1	2	3	4	5	6	7	8	9	10	11	12	13	14	15	16	17	18	19
1	*Hydrogenophaga flava CCUG 1658 (T) AF078771*	100.0	-	-	-	-	-	-	-	-	-	-	-	-	-	-	-	-	-	-
2	*Idonella dechloratans CCUG 30898 (T) X72724*	94.1	100.0	-	-	-	-	-	-	-	-	-	-	-	-	-	-	-	-	-
3	*Rubrivivax gelatinosus M60682*	94.2	97.2	100.0	-	-	-	-	-	-	-	-	-	-	-	-	-	-	-	-
4	*Rubrivivax gelatinosus D16213*	94.5	97.7	99.3	100.0	-	-	-	-	-	-	-	-	-	-	-	-	-	-	-
5	*Rubrivivax gelatinosus AB016167*	94.6	97.7	99.2	99.9	100.0	-	-	-	-	-	-	-	-	-	-	-	-	-	-
6	*Leptothrix mobilis X97071*	92.3	96.9	96.5	97.0	97.0	100.0	-	-	-	-	-	-	-	-	-	-	-	-	-
7	*Roseateles depolymerans AB003623*	92.3	95.8	95.4	95.7	95.7	95.5	100.0	-	-	-	-	-	-	-	-	-	-	-	-
8	*Roseateles depolymerans AB003625*	92.2	95.7	95.5	95.8	95.8	95.6	99.9	100.0	-	-	-	-	-	-	-	-	-	-	-
9	*Matsuebacter chitosanotabidus AB006851*	92.8	95.2	94.9	95.2	95.2	95.1	98.2	98.1	100.0	-	-	-	-	-	-	-	-	-	-
10	*Aquabacterium Aqua3 AF089859*	92.3	95.6	95.4	95.6	95.6	95.6	94.6	94.7	93.9	100.0	-	-	-	-	-	-	-	-	-
11	*Leptothrix discophora L33974*	92.4	96.2	96.2	96.6	96.6	97.8	96.1	96.2	95.1	97.2	100.0	-	-	-	-	-	-	-	-
12	*Leptothrix cholodnii X97070*	92.4	96.2	96.2	96.6	96.6	97.8	96.1	96.2	95.1	97.2	100.0	100.0	-	-	-	-	-	-	-
13	*Leptothrix discophora L33975*	93.8	96.2	96.5	96.7	96.7	97.0	95.9	96.0	95.9	94.8	96.6	96.6	100.0	-	-	-	-	-	-
14	*Burkholderia cepacia X87275*	87.7	89.8	89.3	89.8	89.7	90.5	88.6	88.5	88.0	88.4	89.4	89.4	88.4	100.0	-	-	-	-	-
15	*Burkholderia cepacia M22518*	88.0	90.2	89.7	90.2	90.1	90.7	89.3	89.2	88.3	88.9	89.9	89.9	88.9	99.6	100.0	-	-	-	-
16	**Clone #11**	91.1	93.6	93.9	94.2	94.2	93.4	95.6	95.7	95.3	91.9	93.0	93.0	94.2	85.7	85.9	100.0	-	-	-
17	**Clone #23**	93.1	97.0	96.2	96.6	96.5	96.5	95.6	95.7	95.6	96.5	96.5	96.5	94.9	89.6	89.9	93.0	100.0	-	-
18	**Clone #29**	92.5	97.4	96.1	96.5	96.4	96.2	95.1	95.2	94.4	94.9	95.8	95.8	95.5	89.8	90.2	93.0	96.6	100.0	-
19	**Clone #38**	92.7	97.2	96.6	97.1	97.1	97.1	95.4	95.3	95.0	95.7	96.6	96.6	95.9	90.1	90.3	93.0	96.1	96.0	100.0

Table G.9: Similarity matrix for Clone #20 comparing the 16S rDNA genes. Matrix generated using the maximum likelihood algorithm from the ARB program.

		1	2	3	4	5	6	7	8	9	10	11	12	13	14	15
1	*Desulfuromusa kysingii X79414*	100.0	-	-	-	-	-	-	-	-	-	-	-	-	-	-
2	*Desulfuromonas sp M80618*	88.4	100.0	-	-	-	-	-	-	-	-	-	-	-	-	-
3	*Geobacter chapelleii U41561*	86.2	96.8	100.0	-	-	-	-	-	-	-	-	-	-	-	-
4	*Geobacter metallireducens L07834*	87.7	96.4	93.9	100.0	-	-	-	-	-	-	-	-	-	-	-
5	*Geobacter hydrogenophilus U46860*	87.7	96.6	94.4	99.0	100.0	-	-	-	-	-	-	-	-	-	-
6	*Geobacter akaganeireducens U96918*	88.3	94.4	94.8	93.4	93.9	100.0	-	-	-	-	-	-	-	-	-
7	*Bdellovibrio bacteriovorus*	77.1	79.5	78.9	78.2	79.1	79.6	100.0	-	-	-	-	-	-	-	-
8	*Syntrophobacter wolinii X70905*	80.2	84.5	82.9	82.6	83.1	83.0	74.3	100.0	-	-	-	-	-	-	-
9	*Syntrophobacter fumaroxidans X82874*	81.5	86.3	82.9	83.5	83.9	83.3	73.8	92.6	100.0	-	-	-	-	-	-
10	*Syntrophobacter sp. X94911*	80.8	85.8	83.2	83.5	83.9	84.2	73.9	92.2	94.8	100.0	-	-	-	-	-
11	*Syntrophobacter pfennigii X82875*	81.7	85.8	83.8	84.1	84.4	83.9	74.7	92.9	96.3	95.3	100.0	-	-	-	-
12	*Desulforhabdus amnigenus X83274*	82.4	86.5	84.1	84.5	84.9	84.7	75.4	92.9	94.9	94.5	95.1	100.0	-	-	-
13	*Desulfacinum infernum L27426*	81.4	84.8	83.2	83.7	84.4	84.6	75.3	88.4	89.9	91.2	90.3	90.0	100.0	-	-
14	*Desulfomonile tiedjei M26635*	83.2	90.6	85.3	86.1	86.6	86.1	81.3	84.3	84.8	85.1	86.5	85.7	84.3	100.0	-
15	**Clone #20**	76.0	78.3	78.0	77.6	78.4	77.9	92.1	73.8	73.4	73.1	74.1	74.9	73.8	80.3	100.0

Table G.10: Similarity matrix for Clone # 25a(partial) comparing the 16S rDNA genes. Matrix generated using the maximum likelihood algorithm from the ARB program.

		1	2	3	4	5	6	7	8	9	10
1	*Agrobacterium tumefaciens ATCC 4720 M11223*	100.0	-	-	-	-	-	-	-	-	-
2	*Sphingomonas adhaesiva GIFU 11458 (T) D16146*	80.5	100.0	-	-	-	-	-	-	-	-
3	*Sphingomonas paucimoblis ATCC 29837 (T) X72722*	81.6	95.7	100.0	-	-	-	-	-	-	-
4	*Sphingomonas paucimoblis ATCC 29837 (T) U37337*	82.5	95.9	99.5	100.0	-	-	-	-	-	-
5	*Caulobacter leidyi ATCC 15260 (T) AJ227812*	80.2	95.0	91.2	91.6	100.0	-	-	-	-	-
6	*Shingomonas mali Y09638*	80.5	95.5	91.8	92.2	95.8	100.0	-	-	-	-
7	*Sphingomonas rosa !FO 15208 (T) D13945*	81.3	96.3	93.9	94.2	93.9	95.2	100.0	-	-	-
8	*Sphingomonas subartica X94104*	81.3	96.3	92.1	92.8	93.8	95.5	96.6	100.0	-	-
9	*Sphingomonas capsulata ATCC 14666 (T) M59296*	82.2	94.4	91.1	91.8	91.2	94.1	97.1	95.8	100.0	-
10	**Clone_#25a (partial)**	79.3	97.4	94.2	94.2	94.9	95.0	97.4	96.9	94.9	100.0

Table G.11: Similarity matrix for Clones #25b(partial) and #30 comparing the 16S rDNA genes. Matrix generated using the maximum likelihood algorithm from the ARB program.

		1	2	3	4	5	6	7	8	9	10	11	12	13	14	15
1	*Blastobacter aggregatus ATCC 43293 (T) X73041*	100.0	-	-	-	-	-	-	-	-	-	-	-	-	-	-
2	*Rhodobacter azotoformans D70846*	87.4	100.0	-	-	-	-	-	-	-	-	-	-	-	-	-
3	*Rhodobacter apigmentum AF035433*	85.8	95.7	100.0	-	-	-	-	-	-	-	-	-	-	-	-
4	*Rhodobacter sphaeroides X53855*	87.6	99.7	96.0	100.0	-	-	-	-	-	-	-	-	-	-	-
5	*Rhodobacter sphaeroides X53854*	87.6	99.7	96.0	100.0	100.0	-	-	-	-	-	-	-	-	-	-
6	*Rhodobacter blasticus ATCC 33485 (T) D16429*	86.6	94.6	95.6	94.5	94.5	100.0	-	-	-	-	-	-	-	-	-
7	*Rhodobacter blasticus NCIMB 11576 (T) D13478*	87.8	94.8	96.2	94.8	94.8	98.6	100.0	-	-	-	-	-	-	-	-
8	*Amaricoccus tamworthensis U88044*	87.5	92.7	92.7	92.9	92.9	93.0	93.1	100.0	-	-	-	-	-	-	-
9	*Amaricoccus macuensis U88042*	87.3	92.1	92.1	92.3	92.3	91.8	91.9	96.9	100.0	-	-	-	-	-	-
10	*Amaricoccus veronensis U88043*	87.1	91.9	91.9	91.8	91.8	91.9	92.0	96.6	98.9	100.0	-	-	-	-	-
11	*Rhodobacter capsulatus D13474*	88.2	94.3	95.0	94.3	94.3	95.3	95.0	92.7	91.7	92.2	100.0	-	-	-	-
12	*Rhodobacter capsulatus D16428*	86.7	94.5	95.0	94.5	94.5	95.0	95.0	91.9	91.1	91.5	100.0	100.0	-	-	-
13	**Clone #30**	87.4	95.6	97.6	96.0	96.0	95.8	96.7	92.2	91.6	91.4	95.7	95.6	100.0	-	-
14	**Clone #25b (partial)**	86.1	94.2	96.9	94.2	94.2	98.0	98.4	91.9	91.3	91.7	95.2	95.0	96.6	100.0	-
15	**AOL15**	98.7	89.0	87.5	89.2	89.2	88.3	89.4	89.1	88.9	88.5	89.8	88.3	88.9	87.8	100.0

Table G.12: Similarity matrix for Clones #2 and #83 and #27(partial) comparing the 16S rDNA genes. Matrix generated using the maximum likelihood algorithm from the ARB program.

		1	2	3	4	5	6	7	8	9	10	11	12	13	14
1	*Bacteroides putredinis L16497*	100.0	-	-	-	-	-	-	-	-	-	-	-	-	-
2	*Rikenella microfusus ATCC 29728 (T) L16498*	85.0	100.0	-	-	-	-	-	-	-	-	-	-	-	-
3	*Anaeroflexus maritimus ARB_512070CB*	81.4	82.6	100.0	-	-	-	-	-	-	-	-	-	-	-
4	*Cytophaga fermentans NCIMB 2218 (T) D12661*	81.3	84.9	85.5	100.0	-	-	-	-	-	-	-	-	-	-
5	*Cytophaga fermentans ATCC 19072 (T) M58766*	82.1	85.6	85.7	99.7	100.0	-	-	-	-	-	-	-	-	-
6	*Cytophaga sp. AB015525*	80.0	81.5	86.9	86.2	86.9	100.0	-	-	-	-	-	-	-	-
7	*Cytophaga sp. AB015532*	80.6	82.1	84.6	86.9	87.5	85.5	100.0	-	-	-	-	-	-	-
8	*Cytophaga AB015260*	82.5	82.0	85.3	85.9	86.5	83.3	85.4	100.0	-	-	-	-	-	-
9	*Cytophaga hutchinsonii D12663*	75.5	76.0	77.6	77.2	77.3	77.6	78.3	77.7	100.0	-	-	-	-	-
10	*Flectobacillus major ATCC 29496 (T) M62787*	73.5	73.1	78.1	76.8	77.3	77.0	75.8	77.2	84.1	100.0	-	-	-	-
11	*Runella slithyformis ATCC 29530 (T) M62786*	70.4	67.6	70.8	72.0	72.4	71.1	69.0	69.4	77.7	78.7	100.0	-	-	-
12	**Clone #2**	72.4	69.2	73.1	73.6	73.9	72.8	72.4	71.4	81.5	78.9	79.9	100.0	-	-
13	**Clone #83**	70.8	69.3	72.7	71.3	71.4	72.6	71.0	70.0	83.9	79.8	77.8	79.4	100.0	-
14	**Clone #27 (partial)**	78.2	80.9	87.0	82.9	83.5	84.6	81.6	80.7	76.7	77.4	72.0	73.1	75.9	100.0

Table G.13: Similarity matrix for Clone #31 comparing the 16S rDNA genes. Matrix generated using the maximum likelihood algorithm from the ARB program.

		1	2	3	4	5	6	7	8	9	10	11	12	13
1	*Clostridium acetobutylicum NCDO 1712 X78072*	100.0	-	-	-	-	-	-	-	-	-	-	-	-
2	*Clostridium cellulovorans DSM 3052 (T) X73438*	90.6	100.0	-	-	-	-	-	-	-	-	-	-	-
3	*Clostridium kainantoi DSM 523 X7784*	91.9	92.5	100.0	-	-	-	-	-	-	-	-	-	-
4	*Clostridium butyricum X68178*	91.7	92.4	99.9	100.0	-	-	-	-	-	-	-	-	-
5	*Clostridium butyricum AJ002592*	91.7	92.4	99.9	100.0	100.0	-	-	-	-	-	-	-	-
6	*Clostridium cornioforum DSM 5906*	92.1	92.5	97.8	97.7	97.7	100.0	-	-	-	-	-	-	-
7	*Clostridium butyricum X68177*	91.7	92.4	99.9	100.0	100.0	97.7	100.0	-	-	-	-	-	-
8	*Clostridium beijerinckii NCIMB 8052 (T) X68182*	91.2	92.7	97.7	97.7	97.7	98.3	97.7	100.0	-	-	-	-	-
9	*Clostridium favososporum X76749*	92.1	92.6	97.8	97.8	97.8	99.9	97.8	98.4	100.0	-	-	-	-
10	*Clostridium puniceum DSM 2619 (T) X73444*	91.7	92.6	97.7	97.8	97.7	99.5	97.8	98.4	99.6	100.0	-	-	-
11	*Clostridium beijerinckii NCIMB 8052 (T) S46735*	91.2	92.8	97.7	97.7	97.7	98.4	97.7	99.9	98.5	98.5	100.0	-	-
12	*Clostridium punecium DSM 2619 (T) X71857*	91.7	92.7	97.8	97.8	97.8	99.5	97.8	98.5	99.6	99.8	98.5	100.0	-
13	**Clone #31**	91.4	92.4	97.9	97.9	97.9	98.9	97.9	98.4	98.9	99.1	98.5	99.2	100.0

Table G.14: Similarity matrix for Clones #32 and #39 comparing the 16S rDNA genes. Matrix generated using the maximum likelihood algorithm from the ARB program.

		1	2	3	4	5	6	7	8	9	10	11	12	13
1	*Brachymonas denitrificans D14320*	100.0	-	-	-	-	-	-	-	-	-	-	-	-
2	*Hydrogenophaga pseudoflava AF078770*	94.5	100.0	-	-	-	-	-	-	-	-	-	-	-
3	*Aqualspirillum delicantum AF078770*	92.9	94.3	100.0	-	-	-	-	-	-	-	-	-	-
4	*Variovorazx paradoxus IAM 12373 (T) D30793*	91.5	93.8	97.2	100.0	-	-	-	-	-	-	-	-	-
5	*Acidovorax avenae NCPPB 961 (T) D30793*	93.2	93.4	95.2	95.7	100.0	-	-	-	-	-	-	-	-
6	*Acidovorax temperans CCUG 11779 (T) AF078766*	93.6	93.4	95.1	95.0	97.9	100.0	-	-	-	-	-	-	-
7	*Acidovorax IAM 357678 AF078763*	94.3	94.3	95.5	95.7	97.6	98.2	100.0	-	-	-	-	-	-
8	*Acidovorax LWI AJ130765*	93.6	94.4	94.7	94.4	96.0	95.9	96.4	100.0	-	-	-	-	-
9	*Acidovorax anthurii AJ007013*	93.3	94.3	95.6	95.7	97.3	97.8	98.4	96.0	100.0	-	-	-	-
10	*Acidovorax delafieldii ATCC 17505 (T) AF078764*	93.5	92.7	95.0	94.7	96.8	98.2	97.1	94.7	96.6	100.0	-	-	-
11	*Aquaspirillum sinuosum LMG 4393 (T) AF078754*	94.0	94.5	95.3	95.4	96.3	95.8	94.9	95.7	95.1	95.2	100.0	-	-
12	**Clone #32**	89.0	90.9	93.7	92.2	90.6	90.0	90.4	89.8	90.7	89.7	91.3	100.0	-
13	**Clone #39**	85.9	87.9	90.0	89.8	89.2	89.0	87.9	87.5	88.3	88.3	89.4	91.6	100.0

Table G.15: Similarity matrix for Clone #33 comparing the 16S rDNA genes. Matrix generated using the maximum likelihood algorithm from the ARB program.

		1	2	3	4	5	6	7	8	9	10	11	12	13	14	15	16
1	*marine snow associated clone agg8 L10942*	100.0	-	-	-	-	-	-	-	-	-	-	-	-	-	-	-
2	*clone HstpLBAF159639*	91.1	100.0	-	-	-	-	-	-	-	-	-	-	-	-	-	-
3	*unnamed organism Z77433*	91.1	94.4	100.0	-	-	-	-	-	-	-	-	-	-	-	-	-
4	*Pirellula uncultured Pirellula clone 5H12 AF029076*	90.7	93.8	98.4	100.0	-	-	-	-	-	-	-	-	-	-	-	-
5	*Pirellula uncultured Pirellula clone 6013 AF029077*	90.7	93.8	98.4	100.0	100.0	-	-	-	-	-	-	-	-	-	-	-
6	*str SBR2006 X84551*	84.3	84.4	86.8	85.9	85.9	100.0	-	-	-	-	-	-	-	-	-	-
7	*Planctomyces maris DSM 8797 (T) AJ231184*	78.1	80.8	82.5	79.6	79.6	83.1	100.0	-	-	-	-	-	-	-	-	-
8	*Planctomyes brasiliensis DSM 5305 (T) AJ231190*	73.2	77.2	79.2	77.6	77.6	82.6	88.2	100.0	-	-	-	-	-	-	-	-
9	*Chlamydophila felis D85707*	64.3	59.7	68.5	62.7	62.7	61.3	65.4	64.9	100.0	-	-	-	-	-	-	-
10	*Chlamydophila pneumoniae U68426*	63.7	64.5	70.1	64.5	64.5	60.9	65.2	66.1	94.7	100.0	-	-	-	-	-	-
11	*Helicobacter pylori AE000511*	60.1	55.6	59.1	57.8	57.8	61.2	48.5	54.2	60.0	56.8	100.0	-	-	-	-	-
12	*str. BD5-13 AB015569*	65.4	61.6	65.4	63.4	63.4	64.9	61.5	63.3	62.2	59.5	66.0	100.0	-	-	-	-
13	*Helicobacter sp U51874*	59.2	54.6	59.9	56.9	56.9	63.6	53.4	56.7	60.1	59.5	96.6	66.1	100.0	-	-	-
14	**Clone #33**	65.7	61.2	66.6	61.7	61.7	63.1	63.4	67.2	60.6	61.2	59.8	75.5	60.6	100.0	-	-
15	*unclutured bacterium AF141390*	69.4	65.0	67.2	65.2	65.2	67.6	60.9	63.0	65.3	65.9	59.4	78.6	62.1	83.7	100.0	-
16	*unclutured soil bacterium AF128705*	73.2	70.8	71.8	69.1	69.1	69.8	64.7	66.7	60.6	62.1	57.4	81.0	54.5	85.5	83.6	100.0

Table G.16: Similarity matrix for Clone #35 comparing the 16S rDNA genes. Matrix generated using the maximum likelihood algorithm from the ARB program.

		1	2	3	4	5	6	7	8	9	10	11	12	13	14	15
1	*Planctomyces 599 AJ231189*	100.0	-	-	-	-	-	-	-	-	-	-	-	-	-	-
2	*Planctomyces sp X81950*	88.1	100.0	-	-	-	-	-	-	-	-	-	-	-	-	-
3	*Planctomyces limnophilus ATCC 43296 (T) X62911*	90.2	87.4	100.0	-	-	-	-	-	-	-	-	-	-	-	-
4	*Planctomyces maris DSM 8797 (T) AJ231184*	84.2	84.6	84.2	100.0	-	-	-	-	-	-	-	-	-	-	-
5	*Planctomyces sp. 248 AJ231186*	80.8	80.6	81.8	85.3	100.0	-	-	-	-	-	-	-	-	-	-
6	*Planctomyces sp. X85249*	83.5	81.5	82.1	87.8	87.8	100.0	-	-	-	-	-	-	-	-	-
7	*Planctomyces sp. AB015527*	85.3	84.1	86.0	86.9	82.2	84.9	100.0	-	-	-	-	-	-	-	-
8	*Isosphaera sp X81959*	75.8	76.5	75.5	74.2	73.3	74.6	76.9	100.0	-	-	-	-	-	-	-
9	*Gemmata obscuriglobus X54522*	75.5	74.0	75.8	75.0	74.0	75.0	76.3	74.5	100.0	-	-	-	-	-	-
10	*Gemmata obscuriglobus DSM 5851 (T) AJ231191*	75.8	74.3	75.9	75.4	74.5	75.5	76.7	74.8	99.2	100.0	-	-	-	-	-
11	*Gemmata obscuriglobus ACM 2246 X85248*	75.9	74.5	76.0	75.5	74.6	75.6	76.8	74.9	99.3	99.9	100.0	-	-	-	-
12	*Gemmata obscuriglobus X56305*	75.5	73.9	75.6	74.9	74.5	75.1	76.2	74.5	99.1	99.2	99.3	100.0	-	-	-
13	*Gemmata obscuriglobus X81957*	75.4	73.8	75.2	74.9	74.9	74.4	76.3	75.3	95.6	95.6	95.7	95.8	100.0	-	-
14	*Trichodesmium tenue AF013029*	65.3	63.5	64.9	67.6	66.9	66.1	66.7	63.1	63.2	63.4	63.5	63.3	62.1	100.0	-
15	**Clone #35**	76.1	73.8	77.1	75.8	76.1	76.9	78.8	74.7	85.9	86.5	86.6	86.1	86.0	62.4	100.0

Table G.17: Similarity matrix for Clones #44(partial) comparing the 16S rDNA genes. Matrix generated using the maximum likelihood algorithm from the ARB program.

		1	2	3	4	5	6	7	8	9	10	11	12	13	14
1	*Brachymonas denitrificans D14320*	100.0	-	-	-	-	-	-	-	-	-	-	-	-	-
2	*Hydrogenophaga flava CCUG 1658 (T) AF078771*	95.2	100.0	-	-	-	-	-	-	-	-	-	-	-	-
3	*Hydrogenophaga flava DSM 619 AB021420*	95.6	99.7	100.0	-	-	-	-	-	-	-	-	-	-	-
4	*hydrogenophaga pseudoflava AF078770*	95.6	99.7	100.0	100.0	-	-	-	-	-	-	-	-	-	-
5	*Hydrogenophaga palleronii AF078769*	92.5	95.2	95.2	94.8	100.0	-	-	-	-	-	-	-	-	-
6	*Hydrogenophaga palleronii AF019073*	92.9	95.6	95.6	95.2	99.7	100.0	-	-	-	-	-	-	-	-
7	*Hydrogenophaga DSM 5680 AF019037*	92.0	96.4	96.4	96.0	98.9	99.3	100.0	-	-	-	-	-	-	-
8	*Variovorax paradoxus IAM 12373 (T) D30793*	92.4	94.5	94.4	94.1	97.9	98.2	97.5	100.0	-	-	-	-	-	-
9	*Aeromonas salmonicida subs achromogenes NCIMB 1110 (T) X60407*	84.5	83.0	82.9	82.6	83.1	83.6	82.6	84.4	100.0	-	-	-	-	-
10	*Aeromonas salmonicida AB027005*	85.0	83.5	83.4	83.0	83.5	84.0	83.0	84.9	99.7	100.0	-	-	-	-
11	**YED1-18**	95.6	99.7	100.0	100.0	94.8	95.2	96.0	94.1	82.6	83.0	100.0	-	-	-
12	**YED6-21**	94.9	99.7	99.7	99.3	95.6	96.0	96.7	94.8	83.5	83.9	99.3	100.0	-	-
13	**YED6-4**	95.2	99.3	99.7	99.7	94.5	94.9	95.6	93.7	82.6	83.0	99.7	99.0	100.0	-
14	**Clone #44 (partial)**	94.4	99.3	99.3	98.9	95.1	95.5	96.3	94.4	82.7	83.1	98.9	99.6	98.6	100.0

Table G.18: Similarity matrix for Clone #49(partial)comparing the 16S rDNA genes. Matrix generated using the maximum likelihood algorithm from the ARB program.

		1	2	3	4	5	6	7	8	9	10	11	12
1	*Cytophaga arvensicola IAM 12650 (T) D12657*	100.0	-	-	-	-	-	-	-	-	-	-	-
2	*Saprospira grandis ATCC 23119 (T) M58795*	78.6	100.0	-	-	-	-	-	-	-	-	-	-
3	*Candidatus magnospirai bakii AF087096*	75.2	82.4	100.0	-	-	-	-	-	-	-	-	-
4	*Candidatus magnospirai bakii AF087057*	75.0	82.5	99.5	100.0	-	-	-	-	-	-	-	-
5	*Haliscomenobacter hydrossis ATCC 2775 (T) M58790*	80.6	83.7	77.6	77.6	100.0	-	-	-	-	-	-	-
6	*Cytophaga sp AB015265*	78.8	82.3	80.6	80.6	88.3	100.0	-	-	-	-	-	-
7	*Lewinella nigricans AF039294*	81.3	84.1	81.0	80.9	87.2	84.3	100.0	-	-	-	-	-
8	*Lewinella cohaerens AF039295*	80.0	83.7	78.7	78.7	87.0	83.2	90.5	100.0	-	-	-	-
9	*Lewinella persica AF039295*	78.4	81.8	79.6	79.6	84.1	82.5	88.6	89.1	100.0	-	-	-
10	*Candidatus magnospirai bakii AF087097*	75.5	82.7	98.8	98.6	77.0	80.2	80.9	79.1	80.0	100.0	-	-
11	*Candidatus magnospirai bakii AF087091*	75.9	82.8	98.7	98.7	77.3	80.4	81.1	79.3	80.1	99.7	100.0	-
12	**Clone #49 (partial)**	81.2	83.7	77.6	77.6	99.6	88.1	87.3	87.1	84.3	77.2	77.4	100.0

Table G.19: Similarity matrix for Clones #58 and #60 comparing the 16S rDNA genes. Matrix generated using the maximum likelihood algorithm from the ARB program.

		1	2	3	4	5	6	7	8	9	10	11	12	13
1	*Aeromonas media ATCC 33907 (T) X60410*	100.0	-	-	-	-	-	-	-	-	-	-	-	-
2	*Aeromonas media JCM 2385 (T) D11174*	99.6	100.0	-	-	-	-	-	-	-	-	-	-	-
3	*Aeromonas salmonicida subsp. Masoucida X7480*	98.7	98.3	100.0	-	-	-	-	-	-	-	-	-	-
4	*Aeromonas veronii ATCC 35624 (T) X74684*	98.3	98.1	98.4	100.0	-	-	-	-	-	-	-	-	-
5	*Aeromonas veronii AF079300*	96.1	95.8	96.9	100.0	100.0	-	-	-	-	-	-	-	-
6	*Aeromonas veronii ATCC 35624 (T) D11176*	98.2	98.3	97.7	99.6	99.5	100.0	-	-	-	-	-	-	-
7	*Aeromonas trota ATCC 49657 (T) X60415*	98.8	96.8	98.0	98.3	96.7	98.2	100.0	-	-	-	-	-	-
8	*Aeromonas sobira CIP 7433 (T) X74683*	98.4	98.1	99.2	99.0	97.7	99.0	98.3	100.0	-	-	-	-	-
9	*Aeromonas veronii NCIMB 13015 X60414*	98.3	98.1	98.4	100.0	100.0	99.6	98.3	99.0	100.0	-	-	-	-
10	*Aeromonas salmonicida subsp. Achromogenes NCIMP 1110 (T) X60407*	98.7	98.3	100.0	98.4	96.9	97.7	98.0	99.2	98.4	100.0	-	-	-
11	*Aeromonas salmonicida IFP 13784 D11175*	98.0	98.0	99.7	97.1	94.2	97.4	95.6	97.7	97.1	99.7	100.0	-	-
12	**Clone #58**	98.4	98.1	99.7	98.1	96.9	97.5	97.7	98.9	98.1	99.7	99.4	100.0	-
13	**Clone #60**	96.3	95.9	96.8	97.9	98.8	96.9	96.3	97.5	97.9	96.8	95.3	97.2	100.0

Table G.20: Similarity matrix for Clone #61 comparing the 16S rDNA genes. Matrix generated using the maximum likelihood algorithm from the ARB program.

		1	2	3	4	5	6	7	8	9	10	11	12	13	14	15
1	*Chlamydophila pecorum D88317*	100.0	-	-	-	-	-	-	-	-	-	-	-	-	-	-
2	*Trichodesmium erythraeum AF013030*	64.8	100.0	-	-	-	-	-	-	-	-	-	-	-	-	-
3	*Trichodesmium tenue AF013029*	64.5	97.7	100.0	-	-	-	-	-	-	-	-	-	-	-	-
4	*Trichodesmium contortum AF013028*	64.4	97.8	99.3	100.0	-	-	-	-	-	-	-	-	-	-	-
5	*Trichodesmium thiebautiiAF013027*	63.9	97.6	97.8	97.9	100.0	-	-	-	-	-	-	-	-	-	-
6	*Lyngbya conferroides PCC 7419*	61.9	88.1	88.7	88.8	89.1	100.0	-	-	-	-	-	-	-	-	-
7	*Arthrospira sp PCC 8005 X70769*	63.4	89.6	90.0	89.9	89.9	92.5	100.0	-	-	-	-	-	-	-	-
8	*Synechoccus ATCC 700243 AF132772*	66.2	84.8	85.5	85.8	85.1	85.5	87.7	100.0	-	-	-	-	-	-	-
9	*Synechoccus elongatus D83715*	66.4	85.1	85.7	85.8	85.6	85.9	87.7	98.8	100.0	-	-	-	-	-	-
10	*Lyngbya confervoides PCC 7419 AJ000714*	64.0	90.0	90.6	90.5	90.9	98.0	94.2	87.0	87.4	100.0	-	-	-	-	-
11	*Planktothrix rubescens AJ132251*	65.7	86.9	86.9	86.8	87.2	87.4	90.0	85.8	85.4	89.2	100.0	-	-	-	-
12	*Anabaena variablis IAM M.3 AB016520*	65.6	88.4	88.6	88.4	88.2	86.5	88.8	87.0	86.7	88.3	88.7	100.0	-	-	-
13	*Anabaena cylindrica AF091150*	65.4	88.3	88.8	88.6	88.6	87.0	89.0	86.9	86.9	88.9	88.8	95.5	100.0	-	-
14	*Anabaena cylindrica ARB_C96974C5*	65.5	88.4	88.8	88.7	88.7	88.2	89.1	87.4	87.4	89.3	88.6	95.5	99.5	100.0	-
15	**Clone #61**	64.8	89.5	90.3	90.6	90.3	89.2	90.1	86.7	86.6	90.9	90.7	87.9	88.1	88.0	100.0

Table G.21: Similarity matrix for Clone #66 comparing the 16S rDNA genes. Matrix generated using the maximum likelihood algorithm from the ARB program.

		1	2	3	4	5	6	7	8	9	10	11	12	13
1	*Pseudomonas mendocina ATCC 25411 (T) M59154*	100.0	-	-	-	-	-	-	-	-	-	-	-	-
2	*Pseudomonas mendocina NCIMP 10541 (T) D84016*	98.7	100.0	-	-	-	-	-	-	-	-	-	-	-
3	*Pseudomonas mendocina LMG 1223 (T) Z76664*	98.7	99.2	100.0	-	-	-	-	-	-	-	-	-	-
4	*Pseudomonas putida ATCC 11250AF095892*	96.3	96.1	96.1	100.0	-	-	-	-	-	-	-	-	-
5	*Pseudomonas fluorescens U71003*	96.1	95.6	96.2	97.5	100.0	-	-	-	-	-	-	-	-
6	*Pseudomonas fluorescens IAM 12022 (T) D84013*	95.7	95.2	95.8	97.3	98.1	100.0	-	-	-	-	-	-	-
7	*Pseudomonas fluorescens AF068010*	96.1	95.5	96.1	97.6	98.5	99.7	100.0	-	-	-	-	-	-
8	*Pseudomonas putudia ATCC 17484 D85993*	96.7	96.4	96.4	99.0	98.0	98.0	98.3	100.0	-	-	-	-	-
9	*Pseudomonas fluorescens DSM 50108 D86002*	96.4	95.7	96.0	97.5	98.2	98.7	99.1	98.2	100.0	-	-	-	-
10	*Pseudomonas fluorescens NCIMB 9815 D86003*	96.3	95.5	95.9	97.6	98.3	98.8	99.2	98.2	99.8	100.0	-	-	-
11	*Pseudomonas rhodesiae AF064459*	96.3	95.5	96.0	97.6	97.9	98.7	99.0	98.1	99.2	99.2	100.0	-	-
12	*Pseudomonas rhodesiae AB021410*	96.3	95.5	95.9	97.6	98.1	98.7	99.0	98.1	99.2	99.2	100.0	100.0	-
13	**Clone #66**	89.4	88.7	89.1	90.3	90.7	91.1	91.3	92.0	92.7	92.7	91.4	91.4	100.0

Appendix H

MOLECULAR ANALYSIS OF NEW ISOLATES

The following tables contain data for the similarity matrix the new arsenite oxidizers YED1-18, YED6-4, and YED6-21 comparing them with closed related bacteria based on 16S rDNA homology.

Table H.1: Similarity matrix for new isolated comparing the 16S rDNA genes. Matrix generated using the maximum likelihood algorithm from the ARB program.

		1	2	3	4	5	6	7	8	9	10	11	12	13	14	15
1	*Comamonas acidovorans IAM 12409 AB021417*	100.0	-	-	-	-	-	-	-	-	-	-	-	-	-	-
2	*Comamonas testosteroni M11224*	95.0	100.0	-	-	-	-	-	-	-	-	-	-	-	-	-
3	*Comamonas testosteroni AB007996*	95.0	100.0	100.0	-	-	-	-	-	-	-	-	-	-	-	-
4	*Brachymonas denitrificans D14320*	93.7	94.5	94.5	100.0	-	-	-	-	-	-	-	-	-	-	-
5	*Hydrogenophaga flava CCUG 1658 (T) AF078771*	94.0	94.1	94.1	94.3	100.0	-	-	-	-	-	-	-	-	-	-
6	*Hydrogenophaga flava DSM 619 AB021420*	94.2	94.2	94.2	94.4	99.0	100.0	-	-	-	-	-	-	-	-	-
7	*Hydrogenophaga pseudoflava AF078770*	93.8	94.1	94.1	94.4	99.0	98.7	100.0	-	-	-	-	-	-	-	-
8	*Hydrogenophaga taeniospiralis ATCC 49743 (T) AF078768*	92.7	93.8	93.8	93.1	97.1	96.7	96.9	100.0	-	-	-	-	-	-	-
9	*Hydrogenophaga palleronii AF078769*	92.6	93.5	93.5	93.8	97.0	96.8	96.6	98.3	100.0	-	-	-	-	-	-
10	*Hydrogenophaga palleronii AF019073*	93.1	93.9	93.9	94.2	97.2	97.2	96.9	98.6	99.6	100.0	-	-	-	-	-
11	*Pseudomonas spinosa ATCC 14606 AB021387*	93.0	93.5	93.5	93.4	96.6	96.3	96.6	97.4	97.1	97.5	100.0	-	-	-	-
12	*Hydrogenophaga DSM 5680 AF01937*	93.3	93.5	93.5	93.8	96.4	96.4	96.0	96.6	97.5	97.9	96.1	100.0	-	-	-
13	***YED1-18***	93.4	94.2	94.2	94.5	98.4	98.2	**98.6**	97.5	97.2	97.6	97.2	96.5	100.0	-	-
14	***YED6-21***	93.4	94.2	94.2	94.0	**98.3**	97.9	**98.3**	98.1	97.2	97.6	97.2	96.4	98.7	100.0	-
15	***YED6-4***	93.4	94.3	94.3	94.4	98.7	98.5	**98.9**	97.7	97.1	97.4	97.1	96.6	99.5	99.0	100.0

Appendix I

GROWTH DATA FOR NEW ISOLATES

This appendix contains data for the growth of YED1-18, YED6-4, and YED6-21 and their oxidation of arsenite under growth conditions.

Table I.1: 03-21-01 Experiments. Growth vs. Oxidation Data for YED1-18 in YE Medium at pH 8 at 30° C.

Sample Name	Time (hours)	[As(III)] (μM)	Cell Count (cells/ml)
150 μM-A-I	0.0	151.0	1.4E+07
	3.9	160.6	1.4E+07
	7.0	159.8	-
	11.5	129.6	1.6E+07
	16.4	3.5	9.8E+07
	23.0	5.3	1.6E+09
	27.4	1.7	2.6E+09
	31.0	-	2.1E+09
150 μM-A-II	0.0	148.4	1.8E+07
	3.8	170.3	1.2E+07
	6.9	163.3	-
	11.5	109.6	4.0E+07
	16.4	2.4	9.8E+07
	23.0	3.6	1.4E+09
	27.4	1.8	2.4E+09
	31.0	-	2.4E+09
150 μM-B-I	0.0	156.8	5.3E+06
	3.7	154.9	6.5E+06
	6.8	169.5	-
	11.4	172.1	4.5E+06
	16.3	116.8	1.9E+07
	22.9	1.5	1.4E+08
	27.2	1.6	1.2E+09
	31.0	-	2.4E+09
150 μM-B-II	0.0	157.7	3.3E+06
	3.7	163.9	3.1E+06
	6.8	146.2	-
	11.4	169.6	1.0E+07
	16.3	137.7	1.5E+07
	22.9	1.4	1.4E+08
	27.2	1.6	1.5E+09
	31.0	-	1.9E+09

Table I.2: 03-21-01 Experiments. Growth vs. Oxidation Data for YED6-4 in YE Medium at pH 8 at 30° C.

Sample Name	Time (hours)	[As(III)] (μM)	Cell Count (cells/ml)
150 μM-A-I	0	136.7	1.1E+06
	5.6	128.7	7.8E+05
	11.7	132.3	-
	16.7	133.4	-
	23.2	110.3	7.0E+07
	27.5	1.6	2.0E+08
	31.2	2.7	7.0E+08
	40.3	-	1.8E+09
150 μM-A-II	0.0	146.8	6.0E+05
	5.6	154.3	1.6E+06
	11.7	147.1	-
	16.7	158.6	-
	23.2	125.3	1.1E+08
	27.6	1.6	2.2E+08
	31.2	2.2	8.0E+08
	40.3	-	1.1E+09
150 μM-B-I	0.0	152.8	8.5E+05
	5.6	150.4	9.0E+05
	11.7	153.1	-
	16.7	153.5	-
	23.1	100.5	1.4E+08
	27.6	5.0	2.9E+08
	31.2	1.9	5.8E+08
	40.3	-	1.2E+09
150 μM-B-II	0.0	152.5	5.3E+05
	5.6	150.5	1.7E+06
	11.7	153.9	-
	16.7	158.2	-
	23.1	113.5	1.5E+08
	27.6	2.4	2.1E+08
	31.2	1.8	9.0E+08
	40.3	-	6.8E+09

Table I.3: 03-21-01 Experiments. Growth vs. Oxidation Data for YED6-21 in YE Medium at pH 8 at 30° C.

Sample Name	Time (hours)	[As(III)] (μM)	Cell Count (cells/ml)
150 μM-A-I	0.0	154.8	2.7E+03
	5.5	149.8	2.7E+04
	11.7	147.7	-
	16.6	152.9	-
	23.1	12.0	2.9E+07
	27.5	2.2	8.3E+07
	31.2	2.2	2.5E+08
	40.3	-	2.8E+07
150 μM-A-II	0.0	157.6	3.1E+03
	5.6	150.9	5.5E+03
	11.7	149.3	-
	16.6	155.3	-
	23.1	107.3	1.8E+07
	27.5	2.1	5.3E+07
	31.2	2.4	1.9E+08
	40.3	-	3.1E+08

Table I.4: 03-21-01 Experiments. Control experiments in YE Medium at pH 8 at 30° C.

Sample Name	Time (hours)	[As(III)] (μM)
150 μM	0	152.5
	11.0	151.7
	26.9	164.5
	39.5	158.0
	52.0	154.7

Appendix J

MPN DATA

The MPN data are presented in this appendix. A sample calculation is presented on the final page. Positive results for growth are for absorbance readings near 0.2 at 630 nm. Positive results for oxidation are for pale pink colored solutions based on the $KMnO_4$ assay.

Table J.1: Individual MPN Data Set for plant sample A-I.

Dilution	A-I-1 Growth	A-I-2 Growth	A-I-3 Growth	A-I-1 Oxidation	A-I-2 Oxidation	A-I-3 Oxidation
None	+	+	+	+	+	+
1:10	+	+	+	+	+	+
$1:10^2$	+	+	+	+	+	+
$1:10^3$	+	+	+	+	+	+
$1:10^4$	+	+	+	+	+	+
$1:10^5$	+	+	+	+	+	-
$1:10^6$	-	-	-	-	-	-
$1:10^7$	-	-	-	-	-	-
$1:10^8$	-	-	-	-	-	-
$1:10^9$	-	-	-	-	-	-

Table J.2: Individual MPN Data Set for plant sample A-II.

Dilution	A-II-1 Growth	A-II-2 Growth	A-II-3 Growth	A-II-1 Oxidation	A-II-2 Oxidation	A-II-3 Oxidation
None	+	+	+	+	+	+
1:10	+	+	+	+	+	+
$1:10^2$	+	+	+	+	+	+
$1:10^3$	+	+	+	+	+	+
$1:10^4$	+	+	+	+	+	+
$1:10^5$	+	+	+	+	-	+
$1:10^6$	+	-	-	-	-	-
$1:10^7$	-	-	-	-	-	-
$1:10^8$	-	-	-	-	-	-
$1:10^9$	-	-	-	-	-	-

Table J.3: Individual MPN Data Set for plant sample A-III.

Dilution	A-III-1 Growth	A-III-2 Growth	A-III-3 Growth	A-III-1 Oxidation	A-III-2 Oxidation	A-III-3 Oxidation
None	+	+	+	+	+	+
1:10	+	+	+	+	+	+
$1:10^2$	+	+	+	+	+	+
$1:10^3$	+	+	+	+	+	+
$1:10^4$	+	+	+	+	+	+
$1:10^5$	+	+	+	-	-	-
$1:10^6$	+	-	-	-	-	-
$1:10^7$	-	-	-	-	-	-
$1:10^8$	-	-	-	-	-	-
$1:10^9$	-	-	-	-	-	-

Table J.4: Individual MPN Data Set for plant sample B-I.

Dilution	B-I-1 Growth	B-I-2 Growth	B-I-3 Growth	B-I-1 Oxidation	B-I-2 Oxidation	B-I-3 Oxidation
None	+	+	+	+	+	+
1:10	+	+	+	+	+	+
$1:10^2$	+	+	+	+	+	+
$1:10^3$	+	+	+	+	+	+
$1:10^4$	+	+	+	-	+	+
$1:10^5$	+	+	+	-	-	+
$1:10^6$	+	-	-	-	-	-
$1:10^7$	-	-	-	-	-	-
$1:10^8$	-	-	-	-	-	-
$1:10^9$	-	-	-	-	-	-

Table J.5: Individual MPN Data Set for plant sample B-II.

Dilution	B-II-1 Growth	B-II-2 Growth	B-II-3 Growth	B-II-1 Oxidation	B-II-2 Oxidation	B-II-3 Oxidation
None	+	+	+	+	+	+
1:10	+	+	+	+	+	+
$1:10^2$	+	+	+	+	+	+
$1:10^3$	+	+	+	+	+	+
$1:10^4$	+	+	+	+	+	+
$1:10^5$	+	+	+	+	+	+
$1:10^6$	-	+	+	-	-	-
$1:10^7$	-	-	-	-	-	-
$1:10^8$	-	-	-	-	-	-
$1:10^9$	-	-	-	-	-	-

Table J.6: Individual MPN Data Set for plant sample B-III.

Dilution	B-III-1 Growth	B-III-2 Growth	B-III-3 Growth	B-III-1 Oxidation	B-III-2 Oxidation	B-III-3 Oxidation
None	+	+	+	+	+	+
1:10	+	+	+	+	+	+
$1:10^2$	+	+	+	+	+	+
$1:10^3$	+	+	+	+	+	+
$1:10^4$	+	+	+	+	+	+
$1:10^5$	+	+	+	+	+	+
$1:10^6$	-	-	+	-	-	-
$1:10^7$	-	-	-	-	-	-
$1:10^8$	-	-	-	-	-	-
$1:10^9$	-	-	-	-	-	-

Table J.7: Individual MPN Data Set for plant sample C-I.

Dilution	C-I-1 Growth	C-I-2 Growth	C-I-3 Growth	C-I-1 Oxidation	C-I-2 Oxidation	C-I-3 Oxidation
None	+	+	+	+	+	+
1:10	+	+	+	+	+	+
$1:10^2$	+	+	+	+	+	+
$1:10^3$	+	+	+	+	+	+
$1:10^4$	+	+	+	+	+	+
$1:10^5$	+	+	+	+	+	+
$1:10^6$	-	+	+	-	+	-
$1:10^7$	-	-	-	-	-	-
$1:10^8$	-	-	-	-	-	-
$1:10^9$	-	-	-	-	-	-

Table J.8: Individual MPN Data Set for plant sample C-II.

Dilution	C-II-1 Growth	C-II-2 Growth	C-II-3 Growth	C-II-1 Oxidation	C-II-2 Oxidation	C-II-3 Oxidation
None	+	+	+	+	+	+
1:10	+	+	+	+	+	+
$1:10^2$	+	+	+	+	+	+
$1:10^3$	+	+	+	+	+	+
$1:10^4$	+	+	+	+	+	+
$1:10^5$	+	+	+	+	-	+
$1:10^6$	+	-	-	+	-	-
$1:10^7$	-	-	-	-	-	-
$1:10^8$	-	-	-	-	-	-
$1:10^9$	-	-	-	-	-	-

Table J.9: Individual MPN Data Set for plant sample C-III.

Dilution	C-III-1 Growth	C-III-2 Growth	C-III-3 Growth	C-III-1 Oxidation	C-III-2 Oxidation	C-III-3 Oxidation
None	+	+	+	+	+	+
1:10	+	+	+	+	+	+
$1:10^2$	+	+	+	+	+	+
$1:10^3$	+	+	+	+	+	+
$1:10^4$	+	+	+	+	+	+
$1:10^5$	+	+	+	-	+	+
$1:10^6$	+	+	-	-	+	-
$1:10^7$	-	-	-	-	-	-
$1:10^8$	-	-	-	-	-	-
$1:10^9$	-	-	-	-	-	-

Sample calculations using the growth and oxidation data of Table J.9:

The positive and negative results for the C-III tubes are compiled in Table J.10

Table J.10: Sample MPN calculation.

Dilution	None	1:10	$1:10^2$	$1:10^3$	$1:10^4$	$1:10^5$	$1:10^6$	$1:10^7$	$1:10^8$	$1:10^9$
For Growth	3	3	3	3	3	***3***	***2***	***0***	0	0
For Oxidation	3	3	3	3	3	***2***	***1***	***0***	0	0

For the growth experiments, the three tubes that show dilution to extinction are the $1:10^5$, the $1:10^6$ and the $1:10^7$ dilutions (with a pattern of 3, 2, 0, italicized and bolded in Table J.10). One then refers to an MPN table and uses the obtained pattern to determine the cell concentration for the middle dilution. In this case, the 3, 2, 0 pattern yields a count of 0.93 bacterial cells in the $1:10^6$ tube inoculum of 90 μl (all other tubes were inoculated with 75 μl). From these results we have

$$MPN = \left(\frac{0.93\, cells}{90\ \mu l} \right) \cdot 10^6\,(dilution) = \mathbf{1.0 \times 10^7\ total\ cells/ml}$$

Similarly, for the oxidation we have the pattern (2, 1, 0) that corresponds to a value of 0.15 from the MPN tables yielding

$$MPN = \left(\frac{0.15\, cells}{90\ \mu l} \right) \cdot 10^6\,(dilution) = \mathbf{1.7 \times 10^6\ oxidizer\ cells/ml}$$

Appendix K

OXIDATION EXPERIMENTS

WITH BIOFILM COMMUNITY

This appendix contains data for oxidation experiments conducted with materials shaken off aquatic macrophytes at Hot Creek.

Table K.1: Batch oxidation experiments with 2 μM initial arsenite. Note that "t=0" samples were collected immediately after spiking with As(III) and mixing; filtration of these samples was completed within five seconds. Total arsenic concentrations were not determined for field studies.

Sample Name	Time (min)	[As(III)] (μM)	[As (total)] (μM)
2-lab-I	0	1.50	7.95
	2	0.75	8.28
	4	0.35	8.32
	6	0.10	8.17
2-lab-II	0	2.03	7.68
	4	0.85	7.83
	5	0.40	7.91
	7	0.14	7.84
2-field-I	0	2.03	-
	1	0.98	-
	2.5	0.50	-
	3.5	0.22	-
	4.5	0.08	-
	5.5	0.02	-
	6.25	0.01	-
2-field-II	0	2.03	-
	1.25	0.73	-
	2.25	0.16	-
	3.05	0.05	-
	4	0.03	-
	5	0.02	-
2-filtered-I	0	2.45	7.51
	25	2.46	7.69
	87	2.45	7.53
	99	2.36	7.70
2- filtered -II	0	2.52	7.84
	16	2.57	7.81
	76	2.51	7.82
	88	2.48	7.82

Table K.2: Batch oxidation experiments with 50 μM initial arsenite. Note that "t=0" samples were collected immediately after spiking with As(III) and mixing; filtration of these samples was completed within five seconds. Total arsenic concentrations were not determined for field studies.

Sample Name	Time (min)	[As(III)] (μM)	[As (total)] (μM)
50-lab-I	0	54.38	69.18
	11	43.75	69.25
	27	27.49	68.81
50-lab-II	0	55.68	71.88
	11	44.57	71.17
	27	32.10	72.30
50-lab-48hr-I	0	52.94	63.56
	9	50.68	62.28
	19	46.44	62.04
	30	43.68	62.53
	39	40.95	61.70
	49	30.44	54.49
	59	29.07	58.72
	67	25.34	57.43
	79	26.56	62.19
	88	23.15	62.13
	96	19.47	60.51
50-lab-48hr-II	0	57.19	61.89
	9	53.26	64.79
	19	49.71	64.57
	29	44.43	61.47
	39	43.79	64.19
	49	33.77	65.15
	60	33.10	59.44
	67	34.48	63.90
	79	29.96	64.78
	88	27.38	63.58
	96	24.92	65.13
50-field-I	0	55.11	-
	4	50.26	-
	8	42.86	-
	15	29.53	-
	20	19.73	-
	28	5.98	-
	34	0.24	-
50-field-II	0	57.59	-
	4	54.47	-
	8	37.95	-
	15	31.28	-
	20	22.61	-
	28	10.14	-
	34	0.84	-

Table K.3: Batch oxidation experiments filtered controls for 50 μM initial arsenite. Note that "t=0" samples were collected immediately after spiking with As(III) and mixing; filtration of these samples was completed within five seconds.

Sample Name	Time (min)	[As(III)] (μM)	[As (total)] (μM)
50- filtered -I	0	66.06	72.88
	25	65.67	73.90
	89	63.50	72.05
	102	66.20	74.10
	142	67.70	74.73
50- filtered -II	0	63.22	71.89
	23	63.11	71.88
	87	63.13	71.99
	100	64.17	69.27
	141	63.53	72.18
50- filtered -III	0	56.41	61.91
	9	56.09	61.58
	19	54.96	62.11
	59	54.39	87.57
	87	55.65	61.38

References

Ahmann D., A.L. Roberts, Lee R. Krumholz, and Francois M.M. Morel. (1994) Microbe grows by reducing arsenic. *Nature* **371**, 750.

Altschul S. F., W. Gish, W. Miller, E.W. Myers, and D.J.Lipman. (1990) Basic local alignment search tool. *Journal of Molecular Biology* **215**, 403-410.

Amann R. (2000) Who is out there? Microbial aspects of biodiversity. *Systematic and Applied Microbiology* **23**, 1-8.

Amann R., J. Snaidr, M. Wagner, W. Ludwig, and Schleifer K.-H. (1996) In situ visulaization of high genetic diversity in a natural microbial community. *Journal of Bacteriology* **178**(12), 3496-3500.

Amann R. and Ludwig W. (2000) Ribosomal RNA-targeted nucleic acid probes for studies in microbial ecology. *FEMS Microbiology Reviews* **24**(555-565).

Amann R. I. (1995) Fluorescently labelled, rRNA-targeted oligonucleotide probes in the study of microbial ecology. *Molecular Ecology* **4**, 543-554.

Amann R. I., Wolfgang Ludwig, and Schleifer K.-H. (1995) Phylogenetic identification and in situ detection of individual microbial cells without cultivation. *Microbial Reviews* **59**(1), 143-169.

Anderson G. L., Jeffrey Williams, and Hille R. (1992) The purification and characterization of arsenite oxidase from *Alcaligenes faecalis*, a molybdenum-containing hydroxylase. *The Journal of Biological Chemistry* **267**(33), 23674-23682.

Aragno M. and Schlegel H. G. (1999) The Mesophilic Hydrogen-Oxidizing (Knallgas) Bacteria. In *The Prokaryotes An Evolving Electronic Resource for the Microbiological Community* (ed. M. Dworkin). Springer-Verlag.

Ausubel F. M., Roger Brent, Robert E. Kingston, David D. Moore, J.G. Seidman, John A. Smith, and Struhl K. (1992) Short Protocols in Molecular Biology. John Wiley & Sons.

Blum J. S., Allana Burns Bindi, Joy Buzzelli, John F. Stolz, and Oremland R. S. (1998) *Bacillus arsenicoselantis*, sp. nov., and *Bacillus selenitireducens*, sp. nov.: two haloalkaliphiles from Mono Lake, California that respire oxyanions of selenium and arsenic. *Arch Microbiol* **171**, 19-30.

Cervantes C., Guangyong Ji, Jose Luis Ramirez, and Silver S. (1994) Resistance to arsenic compounds in microorganisms. *FEMS Microbiology Reviews* **15**, 355-367.

Chen H.-W., Michelle M. Frey, Dennis Clifford, Laurie S. McNeill, and Edwards M. (1999) Arsenic treatment considerations. *Journal of American Water Works Association* **91**(3), 74-85.

Cullen W. R. and Reimer K. J. (1989) Arsenic speciation in the environment. *Chem. Rev.* **89**, 713-764.

Dawson S. C. (2000) Evolutionary implications of uncultivated Eucarya and Archaea in anoix environments. University of California, Berkeley.

Dowdle P. R., Annuet M. Laverman, and Oremland R. S. (1996) Bacterial dissimilatory reduction of arsenic (V) to arsenic (III) in anoxic sediments. *Applied and Environmental Microbiology* **62**(5), 1664-1669.

DWR. (1967) Investigation of Geothermal Waters in the Long Valley, Mono County., pp. 141. California Department of Water Resources.

Eary L. E. and Schramke J. A. (1990) . In *Chemical Modeling of Aqueous Systmes II* (ed. Melchoir D.C. and R. L. Bassett), pp. 379-396. American Chemical Society.

Eccles L. (1976) Sources of Arsenic in Streams Tributary to Lake Crowley, CA. U.S. Geological Survey.

Ehrlich H. L. (1963) Bacterial action on orpiment. *Economic Geology* **58**, 991-994.

Ehrlich H. L. (1964) Bacterial oxidation of arsenopyrite and enargite. *Economic Geology* **59**, 1306-1312.

Ehrlich H. L. (1996) Geomicrobial interactions with arsenic and antimony. *Geomicrobiology*, pp. 276-294. Marcel Dekker, Inc.

EPA. (2001) http://www.epa.gov/safewater/arsenic.html.

Ezaki T., Yasuhiro Hashimoto, and Yabuuchi E. (1989) Fluorometric deoxyribonucleic acid-deoxyribonucleic acid hybridization in microdilution wells as an alternative to membrane filter hybridization in which radioisotopes are used to determine genetic relatedness among bacterial strains. *International Journal of Systematic Bacteriology* **39**(3), 224-229.

Ferguson J. F. and Gavis J. (1972) A review of the arsenic cycle in natural waters. *Water Research* **6**, 1259-1274.

Franson M. A. H. ed. (1981) Standard methods for the examination of water and wastewater, pp. 447-448. American Public Health Association.

Gerhardt P., R.G.E. Murray, Willis A. Wood, and Noel R. Krieg. (1994) Methods for General and Molecular Bacteriology. American Society for Microbiology.

Green H. H. (1918) Description of a bacterium that oxidizes arsenite to arsenate, and one which reduces arsenate to arsenite, isolated from a cattle-dipping tank. *South African Journal of Science* **14**, 465-467.

Head I. M., J.R. Saunders, and Pickup R. W. (1998) Microbial evolution, diversity, and ecology: a decade of ribosonal RNA analysis of uncultivated microoganisms. *Microbial Ecology* **35**, 1-21.

Hugenholtz P., Erko Stackebrandt, and Fuerst J. A. (1994) A phylogenetic analysis of the genus *Blastobacter* with a view to its future reclassification. *System. Appl. Microbiol.* **17**, 51-57.

Ilyaletdinov A. N. and Abdrashitova S. A. (1981) Autotrophic oxidation of arsenic by a culture of *Pseudomonas arsenitoxidans*. *Mikrobiologiya* **50**(2), 197-204.
Johnson D. L. and Pilson M. E. G. (1975) The oxidation of arsenite in seawater. *Environmental Letters* **8**(2), 157-171.

Kane M. D., L.K. Poulsen, and Stahl D. A. (1993) Monitoring the enrichment and isolation of sulfate-reducing bacteria by using oligonucleotide hybridization probes designed from environmentally derived 16S rRNA sequences. *Applied and Environmental Microbiology* **59**, 682-686.

Kepner R. L. J. and Pratt J. R. (1994) Use of fluorochromes for direct enumeration of total bacteria in environmental samples: past and present. *Microbiological Review* **58**(4), 603-615.

Kerr A. (1992) The genus *Agrobacterium*. *The Prokaryotes*, Vol. 3 (ed. A. Balows, Hans G. Truper, Martin Dworkin, Wim Harder, and K.-H. Schleifer), pp. 2214-2235. Springer-Verlag.

Kersters K. and Ley J. D. (1984) *Agrobacterium* Conn 1942. In *Bergey's manual of systematic bacteriology*, Vol. 1 (ed. N. R. K. a. J. G. Holt), pp. 244-254. Williams & Wilkins.

Legge J. W. (1954) Bacterial oxidation of arsenite. IV. some properties of bacterial cytochromes. *Australian Journal of Biological Science* **7**, 504-514.

Legge J. W. and Turner A. W. (1954) Bacterial oxidation of arsenite. III. cell-free arsenite dehydrogenase. *Australian Journal of Biological Science* **7**, 496-503.

Ludwig W. and Schleifer K.-H. (1999) Phylogeny of bacteria beyond the 16S rRNA standard. *ASM News* **65**(11), 752-757.

Maeda S. (1994) Biotransformation of arsenic in the freshwater environment. *Arsenic in the Environment. Part I: Cycling and Characterization* (ed. J. O. Nriagu), pp. 155-187. John Wiley & Sons.

Maidak B. L., J.R. Cole, T.G. Lilburn, C.T. Parker, P.R. Saxman, J.M. Stredwich, G.M. Garrity, B. Li, G.J. Olsen, S. Pramanik, T.M. Schmidt, and Tiedje J. M. (2000) The RDP (Ribosomal Database Project) continues. *Nucleic Acids Research* **28**, 173-174.

Mandl M., Pavlina Matulova, and Docekalova H. (1992) Migration of arsenic(III) during bacterial oxidation of arsenopyrite in chalcopyrite concentrate by *Thiobacillus ferrooxidans. Applied Microbiology and Biotechnology* **38**, 429-431.

Mandl M. and Vyskovsky M. (1994) Kinetics of arsenic(III) oxidation by iron(III) catalyzed by pyrite in the presence of *Thiobacillus ferrooxidans. Biotechnology Letters* **16**(11), 1199-1204.

Manz W., R. Amann, W. Ludwig, M. Vancanneyt, and Schleifer K.-H. (1996) Application of a suite of 16S rRNA-specific oligonucleotide probes designed to investigate bacteria of the phylum cytophaga-flavobacter-bateroides in the natural environment. *Microbiology* **142**, 1097-1106.

Manz W., R. Amann, W. Ludwig, M. Wagner, and Schleifer K.-H. (1992) Phylogenetic oligodeoxynucleotide probes for the major subclass of proteobacteria: problems and solutions. *Systematic and Applied Microbiology* **15**, 593-600.

McNellis L. and Anderson G. L. (1998) Redox-state dependent chemical inactivation of arsenite oxidase. *Journal of Inorganic Biochemistry* **69**, 253-257.

Morel F. M. M. and Hering J. G. (1993) *Principles and Applications of Aquatic Chemistry*. John Wiley & Sons, Inc.

Muyzer G. and Ramsing N. B. (1996) Molecular methods to study the organization of microbial communities. *Water Science Technology* **32**, 1-9.

Newman D. K., Beveridge T. J., and Morel F. M. M. (1997) Precipitation of arsenic trisulfide by *Desulfotomaculum auripigmentum. Applied and Environmental Microbiology* **63**(5), 2022-2028.

Newman D. K., Dianne Ahmann, and Morel F. M. M. (1998) A brief review of microbial arsenate respiration. *Geomicrobiology* **15**, 255-268.

Newman D. K., Kennedy E. K., Coates J. D., Ahmann D., Ellis D. J., Lovley D. R., and Morel F. M. M. (1997) Dissimilatory arsenate and sulfate reduction in *Desulfotomaculum auripigmentum* sp. nov. *Arch Microbiol* **168**, 380-388.

Ng W.-L., M. Schummer, F.D. Cirisano, R.L. Baldwin, and Karlan B. Y. (1996) High throughput plasmid mini preparations facilitated by micromixing. *Nucleic Acids Research* **24**, 5045-5047.

Osborne F. H. and Ehrlich H. L. (1976) Oxidation of arsenite by a soil isolate of *Alcaligenes*. *Journal of Applied Bacteriology* **41**, 295-305.

Oscarson D. W., P.M. Huang, C. Defosse, and Herbillon A. (1981) Oxidative power of Mn(IV) and Fe(III) oxides with respect to As(III) in terrestrial and aquatic environments. *Nature* **291**, 50-51.

Oscarson D. W., P.M. Huang, and Hammer U. T. (1983) Oxidation and sorption of arsenite by manganese dioxide as influenced by surface coatings of iron and aluminum oxides and calcium carbonare. *Water, Air, and Soil Pollution* **20**, 233-244.

Oscarson D. W., P.M. Huang, and Liaw W. K. (1981) Role of manganese in the oxidation of arsenite by freshwater sediments. *Clays and Clay Minerals* **29**(3), 219-225.

Oscarson D. W., P.M. Huang, W.K. Liaw, and Hammer U. T. (1983) Kinetics of oxidation of arsenite by various manganese dioxides. *Soil Sciences Society of America Journal* **47**, 644-648.

Page R. D. M. (1996) TREEVIEW: An application to display phylogentic trees on personal computers. *Computer Applications in the Biosciences* **12**, 357-358.

Pettine M., L. Camanella, and Millero F. J. (1999) Arsenite oxidation by H2O2 in aqueous solutions. *Geochimica et Cosmochimica Acta* **63**(18), 2727-2735.

Pettine M. and Millero F. J. (2000) Effects of metals on the oxidation of As(III) by H2O2. *Marine Chemistry* **70**, 223-234.

Phillips S. E. and Taylor M. L. (1976) Oxidation of arsenite to arsenate by *Alcaligenes faecalis*. *Applied and Environmental Microbiology* **32**(3), 392-399.

Pontius F. W., Kenneth G. Brown, and Chen C.-J. (1994) Health implications of arsenic in drinking water. *Journal of American Water Works Association*, 52-63.

Quastel J. H. and Scholefield P. G. (1953) Arsenite oxidation in soil. *Soil Science* **75**, 279-285.

Ringelberg D. B., G.T. Townsend, K.A. DeWeerd, J.M. Suflita, and White D. C. (1994) Detection of the anaerobic dechlorinating microorganism *Desulfomonile tiedjei* in environmental matrices by its signature lipopolysaccharide branched-long-chain hydroxy fatty acids. *FEMS Microbiol Ecology* **14**, 9-18.

Robinson D. G., U. Ehlers, R. Herken, B. Herrmann, F. Mayer, and Schurmann F. W. (1987) *Methods of Preparation for Electron Microscopy An Introduction for the Biomedical Sciences*. Springer-Verlag.

Rosen B. P. (1996) Bacterial resistance to heavy metals and metalloids. *Journal of Biological Inorganic Chemistry* **1**, 273-277.

Rosen B. P., Simon Silver, Tatuaba B G., Guangyong Ji, Kristine L. Oden, Suchitra Jagannathan, Weiping Shi, Yajing Chen, and Wu J. (1994) The arsenite oxyanion-translocating ATPase: Bioenergetics, functions, and regulation. In *Phosphate in Microorganisms, Cellular and Molecular Biology* (ed. A. Torriani-Gorini, Ezra Yagil, and S. Silver), pp. 97-108. ASM Press.

Ruimy R., V. Breittmayer, P. Elbaze, B. Lafay, O. Boussemart, M. Gauthier, and Christen R. (1994) Phylogenetic analysis and assessment of the genera Vibrio, Photobacterium, Aeromonas, and Plesiomonas deduced from small subunit rRNA sequences. *International Journal of Systematic Bacteriology* **44**, 416-426.

Santini J. M., Lindsay I. Sly, Roger D. Schnagl, and Macy J. M. (2000) A new chemolithoautotrophic arsenite-oxidizing bacterium isolated from a gold mine: phylogenetic, physiological and preliminary biochemical studies. *Applied and Environmental Microbiology* **66**(1), 92-97.

Satomi M., B. Kimura, M. Hayashi, M. Okuzumi, and Fujii T. (1998) *Marinospirillum* gen. nov., with descriptions of *Marinospirillum megaterium* sp. nov., isolated from kusaya gravym and transfer of *Oceanospirillium minutulum* to *Marinospirillum minutulum* copb. nov. *International Journal of Systematic Bacteriology* **48**, 1341-1348.

Satomi M., Bon Kimura, Michiko Mizoi, Tsuneo Sato, and Fujii T. (1997) *Tetragenococcus muriaticus* sp. nov., a New Moderately Halophilic Lactic Acid Bacterium Isolated from Fermented Squid Liver Sauce. *International Journal of Systematic Bacteriology* **47**(3), 832-836.

Scudlark J. R. and Johnson D. L. (1982) Biological oxidation of arsenite in seawater. *Estuarine, Coastal and Shelf Science* **14**, 693-706.

Sehlin H. M. and Lindstrom E. B. (1992) Oxidation and reduction of arsenic by *Sulfolobus acidocaldarius* strain BC. *FEMS Microbioloby Letters* **93**, 87-92.

Silver S. (1996) Bacterial resistances to toxic metal ions – a review. *Gene* **179**, 9-19.

Silver S. (1998) Genes for all metals – a bacterial view of the periodic table, the 1996 Thom Award Lecture. *Journal of Industrial Microbiology & Biotechnology* **20**, 1-12.

Silver S. and Phung L. T. (1996) Bacterial heavy metal resistance: new surprises. *Annual Reviews in Microbiology* **50**, 753-789.

Sohrin Y. and Matsui M. (1997) Arsenic biogeochemistry affected by eutrophication in Lake Biwa, Japan. *Environmental Science and Technology* **31**(10), 2712-2720.

Stolz J. F. and Oremland R. S. (1999) Bacterial respiration of arsenic and selenium. *FEMS Microbiology Reviews* **23**, 615-627.

Strunk O., O. Gross, B. Reichel, M. May, S. Hermann, N. Stuchmann, B. Nonhoff, M. Lenke, A. Ginhart, A. Vilbig, W. Ludwig, A. Bode, K.H. Schleifer, and Ludwig W. (1998) ARB: a software environment for sequence data. Department of Microbiolofy, Technische universitat Munchen.

Summers A. O. and Silver S. (1978) Microbial transformations of metals. *Annual Reviews in Microbiology* **32**, 637-672.

Tamaki S. and Frankenberger W. T. (1992) Environmental biochemistry of arsenic. *Review of Environmental Contamination and Toxicology* **124**, 79-110.

Theron J. and Cloete T. E. (2000) Molecular techniques for determining microbial diversity and community structure in natural environments. *Critical Reviews in Microbiology* **26**(1), 37-57.

Turner A. W. (1949) Bacterial oxidation of arsenite. *Nature* **164**, 76-77.

Turner A. W. (1954) Bacterial oxidation of arsenite. I. description of bacteria isolated from arsenical cattle-dipping fluids. *Australian Journal of Biological Science* **7**, 452-476.

Turner A. W. and Legge J. W. (1954) Bacterial oxidation of arsenite. II. the activity of washed suspensions. *Australian Journal of Biological Science* **7**, 452-476.

Vink B. W. (1996) Stability relations of antimony and arsenic compounds in the light of revised and extended Eh-pH diagrams. *Chemical Geology* **130**(1-2), 21-30.

Wakao N., Hiroyasu Koyatsu, Yumiko Komai, Hiroshi Shimokawara, Yonekichi Sakurai, and Shiota H. (1988) Microbial oxidation of arsenite and occurrence of arsenite-oxidizing bacteria in acid mine water from a sulfer-pyrite mine. *Geomicrobiology Journal* **6**, 11-24.

Wayne L. G., D.J. Brenner, R.R. Colwell, P.A.D. Grimont, O. Kandler, M.I. Krichevsky, L.H. Moore, W.E.C. Murry, E. Stackbrandt, M.P. Starr, and Truper H. G. (1987) Report of the Ad Hoc Committee on Reconciliation of Approaches to Bacterial Systematics. *International Journal of Systematic Bacteriology* **37**, 463-464.

Weeger W., Didier Lievremont, Magalie Perret, Florence Lagarde, Jean-Claude Hubert, Maurice Leroy, and Lett M.-C. (1999) Oxidation of arsenite to arsenate by a bacterium isolated from an aquatic environment. *BioMetals* **12**, 141-149.

Welch A. H., Michael S. Lico, and Hughes J. L. (1988) Arsenic in Ground Water of the Wester United States. *Ground Water* **26**(3), 333-347.

Wheeler A. E., Daniel B. Oerther, Niels Larsen, David Stahl, and Raskin L. (1996) The Oligonucleotide Probe Database. *Applied and Environmental Microbiology* **62**, 3557-3559.

Wilkie J. A. (1997) Processes Controlling Arsenic Mobility in Natural and Engineered Systems. University of California, Los Angeles.

Wilkie J. A. and Hering J. G. (1998) Rapid oxidation of geothermal arsenic (III) in streamwaters of the eastern Sierra Nevada. *Environmental Science and Technology* **32**, 657-662.

Wintzingerode F. v., U.B. Gobel, and Stackebrandt E. (1997) Determination of microbial diversity in environmental samples: pitfalls of PCR-based rRNA analysis. *FEMS Microbiology Reviews* **21**, 213-229.

Woomer P. L. (1994) Most Probable Number Counts. In *Methods of Soil Analysis: Part 2 - Microbiolgical and Biochemical Properties* (ed. R. W. Weaver, J.S. Angle, and P. S. Bottomley). Soil Science Society of America, Inc.

Xu C., Tongquing Zhou, Masayuki Kuroda, and Rosen B. P. (1998) Metalloid resistance mechanisms in prokaryotes. *Journal of Biochemistry* **123**, 16-23.